博士 論文 (要約)

Phosphoserine phosphatases and serine related metabolism of *Hydrogenobacter thermophilus* TK-6

(*Hydrogenobacter thermophilus* TK-6 の phosphoserine phosphatases とセリン関連代謝)

東京大学大学院

応用生命工学　専攻

平成２５年度博士課程 入学

氏　　名　　金 克泰

指導教員名　石井 正治

Contents

Contents 2
Preface and acknowledgements 1
General introduction 3
Motivation of this study 3
Thiol and intracellular oxygen 3
Overview of iPSPs 4
Overview of *H.thermophilus* TK-6 6
Chapter 1 Disulfide bond 8
1.1 Introduction 8
1.2 Detection of Intermolecular Disulfide Bonds 9
1.2.1 Introduction 9
1.2.2 Materials and Methods 9
1.2.3 Results 15
1.2.4 Discussion 25
1.3 Thermostability 29
1.3.1 Introduction 29
1.3.2 Materials and Methods 30
1.3.3 Results 32
1.3.4 Discussion 39
1.4 Thermal characteristics between A-A and A-B 46
1.4.1 Introduction 46
1.4.2 Materials and Methods 48
1.4.3 Results 50
1.4.4 Discussions 56

Chapter 2 Physiology of iPSPs 59
2.1 *pspA gene* deletion serine auxotroph 59
2.1.1 Introduction 59
2.1.2 Materials and methods 62
2.1.3 Discussion 67
2.2 Physiology of PspA 74
2.2.1 Introduction 74
2.2.2 Materials and Methods 75
2.2.3 Discussion 79
2.3 Physiology of PspB 84
2.3.1 Introduction 84
2.3.2 Materials and methods 85
2.3.3 Discussion 91
Conclusions and prospects 95
References 98

Preface and acknowledgements

This study has been carried out under the direction of Professor Masaharu Ishii in the Laboratory of Applied Microbiology, Department of Applied Biotechnology, The University of Tokyo.

First and foremost I would like to thank my supervisor, Professor Masaharu Ishii for knowing scientist way and for his trust and confidence over the past few years. Now I can open the eye for the consilience of scientist and engineer. My gratitude is also extended to retired Professor Yasuo Igarashi for this opportunity and Assistant Professor Hiroyuki Arai for his invaluable advice for my genetic experiments.

I am grateful for all the helping hands of Makoto Ato, Yoko Chiba, and all who have contributed immensely toward my thesis. I would like to thank my other lab members Yumi Yonezawa, Yasufumi Igarashi, Erika Yamaguchi, Kazumasa Ogura, Mami Kato, Masaru Ishizaki, Osamu Amano, Yoshiaki Sakai, Kazuhiro Okuda, Tatsuya Inoue, Shinta Watanabe, Cheseung Lim, Kei Tatara, Mirei Machida, Ryo Arai, Reiko Kido, Gaku Kono, and Nguyen Huu Tri for companionship. My thanks to Dr. Hirano for his helping for biochemical experiments.

Finally, I would like to thank my parents, JongIk Kim & KeumSim Choi, whose courage have been deeply inspirational and my family, Sol & InHae & my wife for all their love, and support for 3years

Abbreviations

A-A	iPSP1; PspA-PspA
A-B	iPSP2; PspA-PspBt
As-As	PspA C198S-PspA C198S mutant of iPSP1
As-Bs	PspA C198S-PspB C197S mutant of iPSP2
ΔA	pspA gene deletion serine auxotroph H.thermophilus
ΔB	pspB gene deletion H.thermophilus
CFE	Cell-free extract
CBB	Coomassie Brilliant Blue
CPM	7-diethylamino-3-(4'-maleimidylphenyl)-4-Methylcoumarin
DTT	Dithiothreitol
dPGM	cofactor(2,3-bisphosphoglycerate)-dependent phosphoglycerate mutase
GOGAT	glutamine: 2-oxoglutarate aminotransferase
H_2O_2	Hydrogen peroxide
IAA	Iodoacetamide
iPSPs	metal independent phosphoserine phosphatase
IPTG	isopropyl-β-thiogalactopyranoside
KEGG	Kyoto Encyclopedia of Genes and Genomes
LB	Luria-Bertani
PPI	Ptrotein-protein interaction
PGDH	3-phosphoglycerate dehydrogenase
PSAT	3-phosphoserine aminotransferase
RTCA cycle	Reductive tricarboxylic acid cycle
SHMT	serine hydroxymethyltransferase
THF	Tetrahydrofolate
TCEP	Tris(2-carboxyethyl)phosphine
Trx	Thioredoxin
WB	western blotting
WL pathway	Wood-Ljungdahl pathway
5, 10-CH_2-THF	5, 10-methylene-tetrahydrofolate

General introduction

Motivation of this study

The understanding of intracellular metabolic mechanism and its application have been giving an infinite amount of benefit to our real life. As the cells have intrinsically homeostasis characteristics, the cells show positive or negative feedback to survive when they are placed in an environmental stress situation. Some of these feedback frequently has been giving rise to enlighten our insight for its application for our real life. Thiols of amino acid, especially cysteine, have been known to be related with forming disulfide bond within cell and to do a special role in intracellular oxidative reduction situation. I focused on some special thiols in target proteins with an aim to know its physiology and application possibility. Investigation was performed using gene manipulation and biochemical analyses.

Thiol and intracellular oxygen

Of the twenty natural amino acids, only cysteine and methionine contain sulfur. Cysteine is a polar amino acid containing a thiol side chain, but methionine is a non-polar amino acid containing a thioether side chain (17). Unlike methionine, cysteine's sulfur atom can become ionized (18) and thiol of cysteine plays an important role in the biological system. Different types of proteins such as enzymes, antibodies, receptors, and hormones often contain one or more Cys residues which can be preserved as the formation of intra- and inter-molecular disulfide bonds or free thiols (19). Over the past few decades, thermostability using disulfide bond and other factors such as electrostatic interaction has been studied. This was because high temperature is usually required to enhance reaction rate, reactant solubility, and concurrently decrease the risk of microbial contamination in industrial field (20).

Intramolecular disulfide bonds has been known to contribute to protein thermal stability (21) and introduction of a disulfide bond by Cys mutation has been shown to improve the physical stability of some protein (22).

Furthermore, reactive thiol(s) of cysteine residues has been also studied because of their roles in cell signaling, redox switch, and so on, which is related to the intracellular redox regulation. The first evidence that cells may resist oxidative stress via protein thiolation was provided by Dominici and his coworkers (23).

This work addresses metal independent phosphoserine phosphatase, iPSPs, containing thiol. Focus is specially directed toward the intermolecular disulfide bond, thermostability, and physiology of iPSPs.

Overview of iPSPs

Phosphoserine phosphatase (PSP), also known as O-phosphoserine phosphohydrolase, takes part in both serine and glycine biosynthesis. It catalyzes the irreversible reaction (3-phospho-serine + $H_2O \rightarrow$ L-serine + phosphate), which is the last step in the biosynthesis of serine from glycolysis / gluconeogenesis (24). It acts as a homodimer, and requires Mg^{2+} as a cofactor (25). However, iPSPs are metal independent phosphoserine phosphatase, which was firstly identified from *H.thermophilus*. It was composed of iPSP1, homodimer of PspA subunit, or iPSP2, heterodimer of PspA and PspB subunits. Although both PspA and PspB subunits share 35% sequence identity, enzyme activity of PSP was detected only on PspA subunit (1).

Moreover, iPSPs are not homologous to any known PSP and only lack phosphoglycerate mutase activity even if iPSPs are classified as cofactor-dependent phosphoglycerate mutase (dPGM). Thus iPSPs was annotated as a novel-type PSPs (1).

Although genes coding for dPGM-like phosphatases have been detected in a broad range of organisms, it is difficult to predict the function of the corresponding protein using sequence information alone because of their various substrate preferences (26, 27). With the enzymatic characteristics, crystal structure of iPSP1 (PspA-PspA) showed that side chains of His^{85} and C-

terminal region characteristic of iPSP1 (PspA-PspA) are in charge of the PSP activity (Fig. 0-1A), which suggests that these two structural properties can be used as an indicators to identify dPGM-like proteins with high PSP activity (2). Furthermore, crystal structural analysis of iPSP1 (PspA-PspA) suggested the possibility of intermolecular disulfide bond of PspA-PspA linked via Cys 198 of both subunit. Multiple sequence alignment of PSPs showed that cysteine residue is conserved in PspB (Cys 197) of *H.thermophilus* (3).

Considering the glycine related metabolic pathway of *H.thermophilus*, the schema of metabolic pathway can be assumed as in Fig. 0-1B, which was based on the detected enzyme activity, homology search via protein BLAST, and KEGG pathway (http://www.genome.jp/keeg/). Here, the red arrow means detected the presence of enzyme activity within cell-free extract (CFE) of *H.thermophilus* (3, 28) and the blue and gray arrow means presence of homologous gene and absence of enzyme activity, respectively. Therefore, glycine and serine can be synthesized through several pathways, respectively.

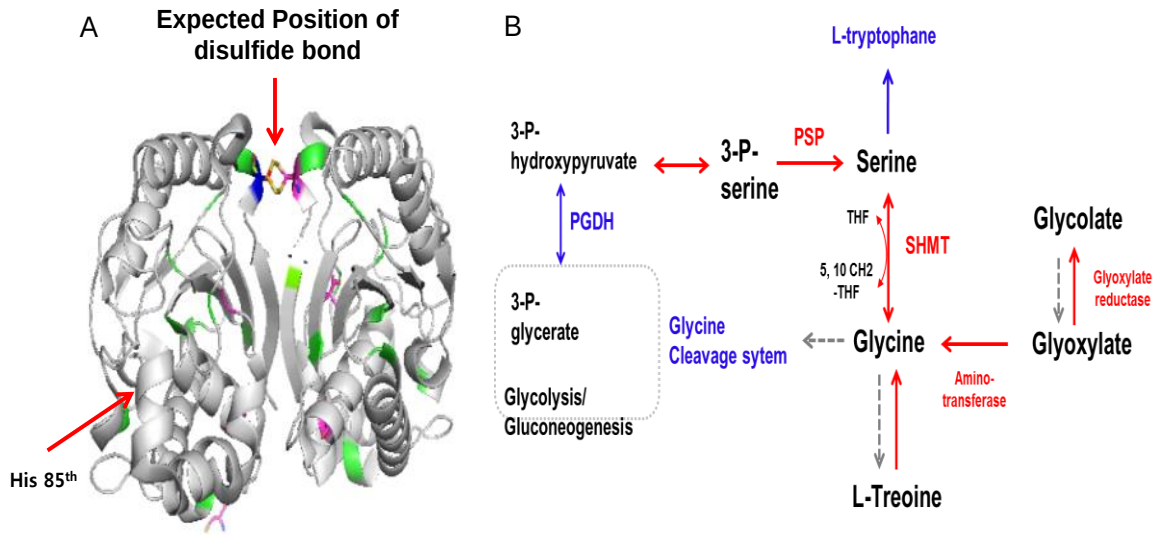

Fig. 0-1 Structure of iPSP1 (PspA-PspA) and Suspected glycine and serine metabolism from *H.thermophilus*

(A) Expected position of intermolecular disulfide bond from crystal structure of iPSP1 (PspA-PspA). Image was reconstructed using PyMOL via the raw data of Chiba *et al* (2).

(B) Scheme of serine related metabolic pathway. Here, the red, blue, and gray line indicated the detected enzyme activity, presence of homologous genes, and absence of enzymatic activity. Image was generated using previously detected enzyme activity(3), homology searching via protein BLAST, and KEGG pathway

Overview of *H.thermophilus* TK-6

Hydrogenobacter thermophilus (TK-6) is an obligately chemolithoautotrophic, extremely (and strictly) thermophilic hydrogen-oxidizing bacterium whose optimal growth temperature for autotrophic growth on H_2-O_2-CO_2 is between 70 and 75°C, which was isolated from a hot spring located in Izu, Japan in 1980. The neutral pH range was suitable for growth (Table 0-1).

It has been proposed that aerobic, thermophilic, hydrogen oxidizing, autotrophic bacteria played an important role in the primary production of organic matter on the early earth and that the ancestors of the *Bacteria* may have been thermophilic (29, 30). Subsequent phylogenetic analysis based on the 16S ribosomal DNA sequence indicates that the genus *Hydrogenobacter* is closely related to the genus *Aquifex*, and the the *Aquifex-Hydrogenobacter* complex is the deepest branching order in the *Bacteria* domain (31).

This bacterium assimilates carbon dioxide (CO_2) as the sole source for carbon via a reductive tricarboxylic acid (RTCA) cycle, which is a reverse metabolic pathway of well-known TCA cycle. Reverse reactions of the TCA cycle are used to form citrate from oxalacetate, $2CO_2$, and 8[H] (32). The RTCA pathway was verified to function as a CO_2 fixation pathway in *H.thermophilus* in 1985 (32). Four enzymes, 2-oxoglutarate : ferredoxin oxidoreductase, fumarate reductase, citryl-CoA synthetase (CCS), and citryl-CoA lyase (CCL) are proposed as the keys to determine the direction of carbon flow and the individual enzymes catalyzing the reaction of the RTCA cycle have been characterized in *H.thermophilus* (33-38) (Fig. 0-2). The key enzyme, citryl-CoA synthetase (CCS), catalyze the first step of the citrate cleavage reaction in *H.thermophilus*(34).

As several key enzymes of the RTCA cycle are highly sensitive to O_2, the cycle commonly functions in anaerobic and microaerobic organisms(39, 40). However, *H. thermophilus* preferentially grows under aerobic conditions, even at 30% O_2 concentrations as far. With systems of detoxifying reactive oxygen species (ROS), several genes predicted to encode peroxidases, such as ferriperoxin (Fpx), cytochrome c peroxidase (CcpR), thiol peroxidase (Tpx), bacterioferritin comigratory protein (BCP), and alkyl hydroperoxide reductase (AhpC), were found in the *H. thermophilus* genome (10). In addition, the function of Fpx, which is a novel

peroxidase found from *H. thermophilus*, was shown to be essential for aerobic growth with more than 10% oxygen. (41).

Table 0-1 Properties of *H.thermophilus*

Property	Description	
Cell shape [a]	Long straight rod, 2.0-3.0 × 0.3 μm	
Gram reaction [a]	Negative	
Motility [a]	Negative	
GC content (mol%) [b]	44.0 mol%	
Optimal growth temperature [c]	70-75°C	
Carbon source [a]	CO_2 (obligate autotroph)	
CO_2-fixation pathway	RTCA cycle	
Nitrogen source [c]	NH_4^+, NO_3^-	
Electron donor [a, d]	H_2, $Na_2S_2O_3$	
Terminal electron acceptor [a, d, e]	O_2, NO_3^-, Fe^{3+}, S	
Classification [f]	Domain	*Bacteria*
	Phylum	*Aquificae*
	Class	*Aquificae*
	Order	*Aquificales*
	Family	*Aquificaceae*
	Genus	*Hydrogenobacter*
	Species	*Hydrogenobacter thermophilus*

[a] (4), [b] (10), [c] (7), [d] (12), [e] (14), [f] (3)

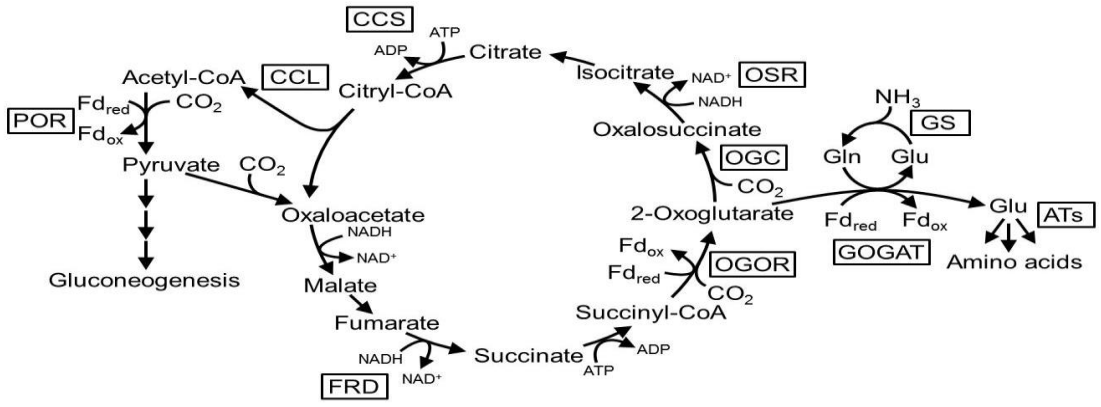

Fig. 0-2 **The RTCA cycle in *H. thermophilus***. CCS, citryl-CoA synthetase; CCL, citryl-CoA lyase; POR, pyruvate:ferredoxin oxidoreductase; FRD, fumarate reductase; OGOR, 2-oxoglutarate:ferredoxin oxidoreductase; OGC, 2-oxoglutarate carboxylase; OSR, oxalosuccinate reductase; GOGAT, glutamine:2-oxoglutarate amidotransferase; GS, glutamine synthetase; AT, aminotransferase; Fdred, reduced ferredoxin; Fdox, oxidized ferredoxin. This figure was adapted from Chiba *et al* (3).

Chapter 1 Disulfide bond

1.1 Introduction

The amino acid cysteine is prominent as a thiol functional group including a sulfur atom and a hydrogen atom. As the polarizable sulfur atom in a thiol group is electron-rich and quite nucleophilic, its reactivity is enhanced in the deprotonated form of the thiol (42). Two cysteines are oxidized to form a disulfide bond according to the redox potential of cysteine-cysteine depending on the topology, temperature, and pH (43). Intra- and inter-molecular disulfide bond is easily formed between the two cysteines under oxidative stress (19). Structural disulfide bonds are acting to stabilize a folded protein structure (44). It has been known that structural disulfide bonds are present almost in extracellular and compartmentalized proteins as the reducing environment of the cytosol makes disulfide bonds unstable (45), indicating that it is difficult for disulfide bond to be formed in cytoplasm. However, these usual notion start to be changed after the finding of protein disulfide bonds within the cytoplasm of certain mutants of *E.coli* utilizing thioredoxin as a disulfide exchange protein (46). Additionally, resent genomic evidence has implicated a critical role for disulfide bonds in the structural stabilization of intracellular proteins of thermophilic organisms (47).

As described in overview of iPSPs, intermolecular disulfide bond was suggested from the crystal structure of iPSP1 (PspA-PspA). However, it was difficult to agree with the presence of disulfide bond between the both PspA subunit. This is because the intracellular environment of *H.thermophilus* is a strongly reduced condition (< -300mV ORP) due to the RTCA cycle and the condition for making the crystal structure of A-A was under the aerobic condition.

Although the presence of disulfide bond was unfavorable, I found positive clues from *H.thermophilus* genome information. Thioredoxin and protein disulfide bond isomerase were detected from complete genome of *H.thermophilus* TK-6 (10), suggesting the possibility of iPSP1 (PspA-PspA) linked by disulfide bond in the cytoplasm of *H.thermophilus.*

Therefore, this study focused on the presence of disulfide bond *in vivo* and the function of disulfide bond in terms of thermostability and redox response.

1.2 Detection of Intermolecular Disulfide Bonds

1.2.1 Introduction

Previous study showed the possibility of S-S bond formation within iPSP1 (PspA-PspA) through crystal structural analysis. However, it was need to clarify the presence of S-S bond within iPSP1 since crystals were made under oxidative condition. This was because the intracellular environment of *H.thermophilus* is expected to be more reduced condition than other organism.

Furthermore, our previous study clarified the presence of heterodimeric iPSP2 (PspA-PspB) using size exclusion chromatography (1). However, what kind of interaction exists between PspA and PspB subunits was not known. Therefore, this chapter focused on the presence of intermolecular disulfide bond *in vitro* and *in vivo*.

1.2.2 Materials and Methods

Bacterial strain and growth condition

H. thermophilus TK-6 (IAM 12695, DSMZ 6534) was cultivated at 70°C under a gas phase of H_2:O_2:CO_2 (75:10:15, v/v) and in an inorganic medium as shown in (Table 1-1) (48). Cultivation was carried out with an aim to gain cell-free extract (CFE) or cell suspension by using 5L culture bottle containing 1L medium and gas mixtures. The culture bottle was cultivated at the shaking condition of 150 rpm for 48 hours. Cells were harvested after centrifugation at 6,000 × *g* for 15 min and washed with inorganic medium. Subsequently, harvested cells were stored at -80ºC until use.

Construction of expression plasmids for wild type and site-directed mutants

For heterologous expression, plasmids were constructed in our previous study as described below (1). The gene encoding *PspA* (YP_003431771, HTH0103) and *PspB* (YP_003431851, HTH0183) were amplified by PCR using the chromosomal DNA of *H.thermophilus* as a template

Table 1-1 Medium composition for the cultivation of *H. thermophilus*.

Composition	quantity
$(NH_4)_2SO_4$	3 g
KH_2PO_4	1 g
K_2HPO_4	2 g
$MgSO_4 \cdot 7H_2O$	0.5 g
NaCl	0.25 g
$CaCl_2$	0.03 g
$FeSO_4 \cdot 7H_2O$	0.014 g
Trace element solution*	0.5 mL
Deionized water	1.0 L

*Trace element solution

Composition	quantity
MoO_3	4 mg
$ZnSO_4 \cdot 7H_2O$	28 mg
$CuSO_4 \cdot 5H_2O$	2 mg
H_3BO_3	4 mg
$MnSO_4 \cdot 5H_2O$	4 mg
$CoCl_2 \cdot 6H_2O$	4 mg
Deionized water	1.0 L

with the following primers: HTH0103F – HTH0103R and HTH0183F-HTH0183R. The amplified fragments were first inserted into pUC19 plasmid using EcoRI and PstI or SalI restriction sites introduced in the primers (single-underlined sequences). After the sequences were confirmed, *pspA* and *pspB* were re-inserted into multi-cloning site 1 of pCDFDuet-1 or pET21c vector (Novagen) using NcoI and PstI or NdeI and XhoI (double-underlined sequences in the primers) restriction sites, respectively. The resultant plasmid sequence was reconfirmed by DNA sequencing with a view to overexpress and purify both iPSP1 (PspA-PspA) and iPSP2 (PspA-PspB) by the methods described below.

In order to construct plasmid for site-directed mutants, the genes encoding the PspA and PspB subunits of *H. thermophiles* TK-6 (IAM 12695, DSM 6534) were cloned into the expression vectors pCDFDuet-1 and pET21c (Novagen, Darmstadt, Germany) with the same method in wild-type, respectively. The constructed plasmids were then mutated for expressing C198S and C197S mutants of the PspA and PspB subunits in which Cystein198 and Cystein197 were converted to Serine, respectively. Site-directed mutagenesis was performed by following the instruction of the Prime STAR mutagenesis blast kit (TaKaRa Bio, Otsu, Japan) protocol.

Table 1-2 Primers used for wild-type and site-directed mutagenesis of pspA and pspB gene

Primer	Sequence
HTH0103F	5’-GTA*GAATTC*GGGCCATGGTAAAGC-3’
HTH0103R	5’-TAT*CTGCAG*AAATGAGGAAAAGCG -3’
HTH0183F	5’-AAA*GAATT*CATATGAAGCGTTTGTATTTGGTCAG-3’
HTH0183R	5’-ACA*GTCGAC*GCTCGAGAAAATCAGGTAAGC -3’
PspA C198S F	5’-ATAACCAGCCATCTGGGAGAGTTT-3’
PspA C198S R	5’-AGATGGCTGGTTATGTTAAGCTTTAG-3’
PspA C198A F	5’-ATAACCGCACATCTGGGAGAGTTT-3’
PspA C198A R	5’-AGATGTGCGGTTATGTTAAGCTTTAG-3’
PspB C197S F	5’-AAACTTTCCCACACAAGACAGCTTAC-3’
PspB C197S R	5’-TGTGTGGGAAAGTTTGTTTAGATAAACC-3’

Heterologous Protein Expression and Purification.

Recombinant iPSP1 (PspA-PspA: A-A), iPSP2 (PspA-PspB: A-B), and their mutants were expressed in *E.coli* BL21-Codon Plus (DE3)-RIL for the individual and co-expression of *pspA* and *pspB*. Hereafter, wild-type iPSP1 and iPSP2 are referred to as A-A and A-B, respectively, and the mutant forms of each recombinant protein are named as As-As and As-Bs, respectively because cysteine residues of A-A and A-B were changed to serine residues.

With the expression plasmids, the transformed hosts were cultivated aerobically in LB medium containing antibiotic(s) such as 50μg ml^{-1} streptomycin, 50μg ml^{-1} ampicillin, and 34 μg ml^{-1} chloramphenicol at 37ºC. When the optical density ($OD_{600\ nm}$) of the culture reached 0.6, 1mM of isopropyl thio-β-$_D$-galactopyranoside was added to the medium, followed by further cultivation for 3hr at 37ºC. Cells harvested at 10,000× g for 15min were resuspended in buffer containing 20 mM Tris-HCl [pH 8.0, 3ml per 1g of wet cells], and then disrupted by sonification using an Ultrasonic disruptor (TOMY, Nerima, Tokyo, Japan) at 100W using a 50% duty cycle

for 15min. The disrupted cells were centrifuged at 100,000× g for 1hr to obtain supernatants. The supernatant, cell-free extract (CFE), was transferred into a vial, which was then sealed with a rubber stopper and an aluminum cap, followed by head space gas changing to argon and stored at -80ºC until use.

CFE was applied to Q Sepharose fast-flow column (10 mm × 100 mm; GE Healthcare) equilibrated with bufferA (20 mM Tris, pH 8.0). After the elution of bound proteins with buffer B (1 M NaCl, 20 mM Tris, pH 8.0), ammonium sulfate was added to the obtained fractions to give 20% saturation, and then samples were applied to a Butyl-Toyopearl column (22 mm / 15 cm; Tosoh, Tokyo, Japan) equilibrated with buffer A supplemented with ammonium sulfate at 20% saturation. This and subsequent chromatography steps were performed using an ÄKTA purifier system (GE Healthcare) at room temperature. Proteins were eluted with a gradient of ammonium sulfate from 20 to 0% at a flow rate of 4 ml min^{-1}. The active fractions were dialyzed against buffer A and the active fractions were then applied to a MonoQ HR 5/5 column (bed volume, 1 ml; GE Healthcare) equilibrated with buffer A. Proteins were eluted with a gradient of NaCl from 0 to 1M at a flow rate of 0.5 ml min^{-1}.

Reductive and Non-reductive SDS-PAGE

Analysis of purified WT and mutant of PspA-PspA and PspA-PspB were performed using a method essentially similar to the method described by Laemmli (49). Reductive and non-reductive SDS-PAGE was conducted on a 5% stacking gel and a 10% separating gel with and without 3.5 mM DTT in the loading buffer, respectively.

Preparation cell suspension

The harvested *H. thermophilus* cell was prepared for western blotting. The cells were suspended in cultivation medium with 3 volumes of cells, disrupted by sonification, and centrifugated at 100,000 × *g* for 1h. The supernatant designated as cell-free extract (CFE) was stored at -80ºC until use for next step of experiment.

Western Blotting

The rabbit antisera for PspA and PspB were prepared using synthesized peptides (^{67}AEAKNLEVIKED^{78} for PspA and ^{83}MSFGEYEGKH^{92} for PspB) as the antigens by Eurofins Operon, Japan. After proteins on PAGE gel were transferred, PVDF membranes were blocked for at least 4 h using TBST buffer (50 mM Tris, 150 mM NaCl, pH 7.5, and 0.1% Tween 20) containing 5 % (w/v) skim milk at room temperature. Membranes were then probed overnight at 4°C with a PspA or PspB antiserum (1/1000 and 1/ 250 dilution, respectively) in TBST buffer with skim milk. The amount of purified iPSPs applied for western blotting was about 0.1 μg and 1 μg per well for anti-PspA and PspB- antibodies, respectively. The membranes were then washed three times in TBST buffer. The membrane was then probed with a Goat anti-rabbit lgG, pAb (HRP conjugate (Enjo)). After washing the membrane twice in TBST buffer, once in TBST without Tween 20, and once in distilled water, the immunopositive spots were visualized by using POD Immunostain Set (Wako) as directed by the manufacturer.

Protein Assay

Protein concentrations were measured using the Bradford protein assay (Bio-Rad) with bovine serum albumin as the standard.

Quantification

The protein amount from the results of SDS-PAGE and western blotting was quantified by Image J software as a densitometry values with arbitrary units.

Gel-filtration chromatogrphy

Native molecular weight was determined using gel-filtration column of Superdex^{TM} 75 (10/300). The protein was eluted with 100 mM NaCl, 20 mM Tris-HCl (pH 8.0) at a flow rate of 0.8 ml min^{-1}. Gel filtration standard (Bio-Rad) was used as a marker for calibration. Measurements for standards and samples were performed in triplicate and duplicate, respectively.

Fluorescent Labeling of Cysteines Involved in Disulfide Bonds

Heterologously expressed proteins (A-B & mutant) from *E.coli* and *H. thermophiles* TK-6 were treated identically throughout the procedure. Cell pellets having 650 μg protein were resuspended in 0.1ml of lysate buffer (20 mM Tris [pH 8.0], 10 mM NaCl, 1mM EDTA, 20 mM Iodoacetamide). After centrifugation at 20,000×g for 5 min, the cells were resuspended in 0.1 ml of lyasate buffer, disrupted on ice by sonification, and subjected to centrifugation at 20,000×g for 10 min to obtain supernatants. Following the sonification and centrifugation, the volume of supernatants was adjusted to 500μl with lysate buffer and SDS (Sodium dodecyl sulfate) to a final concentration of 1% SDS. Samples were denatured by heating to 95˚C (2 min for *E. coli*, 4 min for *H. thermophilus*), and then treated with 20 mM iodoacetamide (IAA) for 30 min. in the dark to block free cysteine thiols. After the alkylation with IAA, samples were washed by using lysate buffer with 0.1% SDS but without IAA for three times via viva spin (5,000 MWCO), Here, the final volume of washed samples were about 100μl and the dilution ratio of them was about 1,000 times). Samples were reduced with 10mM tris(2-carboxyethyl)phosphine (TCEP) for 30min in the dark at room temperature. Here, pH of TCEP was adjusted to 7.0 by careful addition of 5N NaOH. Following disulfide cleavage by reduction, samples were reacted with a 50μM of 7-diethylamino-3-(4'-maleimidylphenyl)-4-Methylcoumarin (CPM) in the dark at room temperature for 30 min for fluorescent labelling of free thiols. Two fraction of fully labelled sample was prepared. One fraction was followed the above-mentioned protocol. As a control, another fraction was followed the above-mentioned protocol with the exception of IAA and TCEP treatment. Both fractions were mixed with 6×sample loading buffer without reductant and run on a 12% acrylamide gel. Makrer (Precision Plus Protein^{TM} Dual color standards, Bio-Rad) was used to check the M.W.. CPM labeling of protein bands was analyzed by UV (365nm) excitation. After photo taking of CPM labeling, CBB staining of acrylamide gel was performed.

Modified Western Blotting for intermolecular disulfide bond detection.

Heterologously expressed, purified proteins (A-A & A-B) and *H. thermophilus* TK-6 cells were treated throughout the procedure. Purified A-A and A-B having 43.8 μg and 26.15 μg were washed by using lysate buffer (20 mM Tris [pH 8.0], 10 mM NaCl, 1mM EDTA, 20 mM

Iodoacetamide) for two times via viva spin (5,000 MWCO) and the volume of A-A and A-B was adjusted to 200μl with lysate buffer.

On the other hand, cell pellet of *H.thermophilus* having 650 μg protein was resuspended in 0.1ml of lysate buffer (20 mM Tris [pH 8.0], 10 mM NaCl, 1mM EDTA, 20 mM Iodoacetamide). After centrifugation at 20,000×g for 5 min, the cells were resuspended in 0.1 ml of lyasate buffer, disrupted on ice by sonification, and subjected to centrifugation at 20,000×g for 10 min to obtain supernatants. Following the sonification and centrifugation, the volume of supernatants was adjusted to 200μl with lysate buffer.

After measuring the protein concentration of A-A, A-B and *H.thermophilus* with 200μl, samples were treated with 20 mM iodoacetamide (IAA) for 30 min. in the dark to block free cysteine thiols. Following alkylation with IAA, western blotting was performed using A-A(0.03ug/well), A-B(0.054ug/well), and *H.thermophilus* lysate(17.4ug/well).

1.2.3 Results

Construction of mutant proteins and protein purification.

A-A, A-B, and their mutant proteins were constructed to confirm the presence of intermolecular disulfide bonds within A-A (iPSP1) and A-B (iPSP2). C198 of PspA and C197 of PspB were changed to serine, because serine effectively suppresses sulfur chemistry without influencing protein structure (50).

The wild-type and mutant proteins were heterologously expressed using the same procedure in *Escherichia coli*. The elution patterns of the mutants during the purification by column chromatography exhibited similar profiles as the respective wild-type proteins, suggesting that the overall structure did not changed by the mutations. Additional analysis of Far UV CD (circular dichroism) spectra showed that wild-types (A-A and A-B) and their mutants (As-As and As-Bs) had almost similar CD spectroscopic properties from 200nm to 250nm, indicating the identical structure between them (data not shown). The homogeneity of the purified proteins was also confirmed by SDS-PAGE and CBB staining (data not shown).

Interestingly, when I introduced PspA and PspB plasmids to *E.coli* (BL21) simultaneously to make recombinant protein and purify protein, what I gained was only A-B recombinant protein, indicating that PspA subunit was more inclined to link to PspB subunit than PspA subunit (data not shown).

Expression and purification of recombinant iPSPs

To examine the biochemical characteristics of iPSPs enzymes, recombinant A-A and A-B were expressed in *E.coli*. A-A and A-B recombinant proteins were purified under aerobic conditions at room temperature. Generally, two times more soluble A-A protein was gained than A-B protein from a bacterial culture (Table 1-3). The overall purification steps and yields of both recombinants are shown inTable 1-3.

Considering the protein purification step, heat-treatment has been used to purify recombinant proteins originated from *H.thermophilus* because proteins originated from *H.thermophilus* are more thermostable than proteins originated form *E.coli.* Previous study also used heat-treatment step to purify recombinant A-A and A-B protein (3). However, as this study focused on thermostability which will be described in next section, Q Sepharose fast-flow column (Q. F.F.) was used in place of heat-treatment step for purifying recombinant A-A, A-B, and their mutants.

Table 1-3 Purification of iPSPs from *E.*coli

Enzyme	Fraction	Activity (U)	Protein (mg)	Specific activity (U/mg)	Purification (fold)	Yiels (%)
A-A	CFE	28001	155.1	180.5	1.0	100
	Q.F.F	7440.6	42.5	175.2	1.0	26.6
	B.T.	3943.9	24.0	164.3	0.9	14.1
	MonoQ	1451.6	6.7	216.2	1.2	5.2
A-B	CFE	11515	207.3	58.2	1.0	100
	Q.F.F	1193	29.8	68.7	1.2	17
	B.T.	818	13.1	51.6	0.9	5.6
	MonoQ	1914	2.9	113.2	1.9	2.7

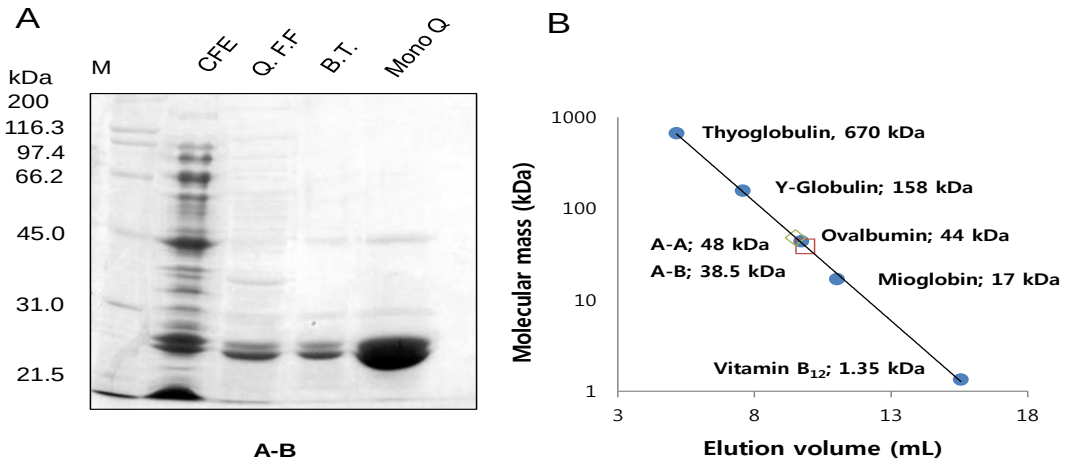

Fig. 1-1 Purity of protein purification step and gel-filtration chromatography of A-A or A-B. (A) SDS-PAGE of the CFE and active fraction from Q Sepharose fast-flow (Q.F.F), Butyl Toyopearl (B.T.), and Mono Q columns. (B) Size exclusion chromatography, elution volume of A-A and A-B gives the molecular mass of A-A and A-B, respectively.

The SDS-PAGE shows the protein purity (Fig. 1-1A), indicating protein purification scheme using Q Sepharose fast-flow column may available to this study.

Although the major protein bands of SDS-PAGE were corresponding to the molecular weights of PspA and PspB (24.6 and 23.5 kDa), respectively (Fig. 1-1A), the native molecular mass of A-A and A-B measured by using size-exclusion chromatography were 48 and 38.5kDa, respectively (Fig. 1-1B), indicating that A-A and A-B was composed of dimeric protein. These results was consistent with previous results using protein purification step containing heat-treatment (1).

Detection of intermolecular disulfide bond from recombinant iPSPs

To determine if intermolecular disulfide bonds are present not only in the crystal of A-A, but also in the soluble form of A-A and A-B, SDS-PAGE analysis of A-A, A-B, and the generated mutants were performed under non-reducing conditions (Fig. 1-2). This was because intermolecular disulfide bond is easily cleaved by reducing agent (DTT). Two distinct bands of 24.0 and 38.0 kDa were detected when A-A was subjected to non-reduced SDS-PAGE (Fig. 1-2A), whereas only the 24.0-kDa band, which was consistent with the predicted molecular weight of the PspA subunit (24.6 kDa), was detected from As-As. In contrast, a single major

protein band of 45.0 kDa was observed when A-B was subjected to non-reducing SDS-PAGE (Fig. 1-2A), whereas 23.5- and 24.5-kDa bands, corresponding to PspB and PspA, respectively, were detected when reduced A-B or non-reduced As-Bs were analyzed by SDS-PAGE (Fig. 1-2A, B). Additionally, molecular mass calculated from amino acid sequence of PspA and PspB were 24.6 and 23.5 kDa, respectively. Considering the native molecular mass of A-A (48 kDa) and A-B (38.5 kDa) mentioned in Fig. 1-1B, both dimeric protein A-A and A-B were revealed to be linked by intermolecular disulfide bond.

From the CBB-stained band intensities in the non-reduced SDS-PAGE gels, the ratio of proteins containing an intermolecular disulfide bond was estimated to be 35% for A-A and 97% for A-B by using Image J software **(**Fig. 1-2C), suggesting that cysteine of PspB may be more reactive than that of PspA.

To determine whether the intermolecular disulfide bonds between the PspA and PspB subunits also exist in A-A and A-B proteins obtained from *H. thermophilus* lysate, Western blotting (WB) was performed using anti-PspA or PspB antisera. The specificity of anti-PspA and PspB antisera to each subunit was confirmed using purified A-A and A-B (Fig. 1-3, lane A-A and A-B). When anti-PspA antiserum was reacted with reduced *H. thermophilus* lysate, a distinct band was

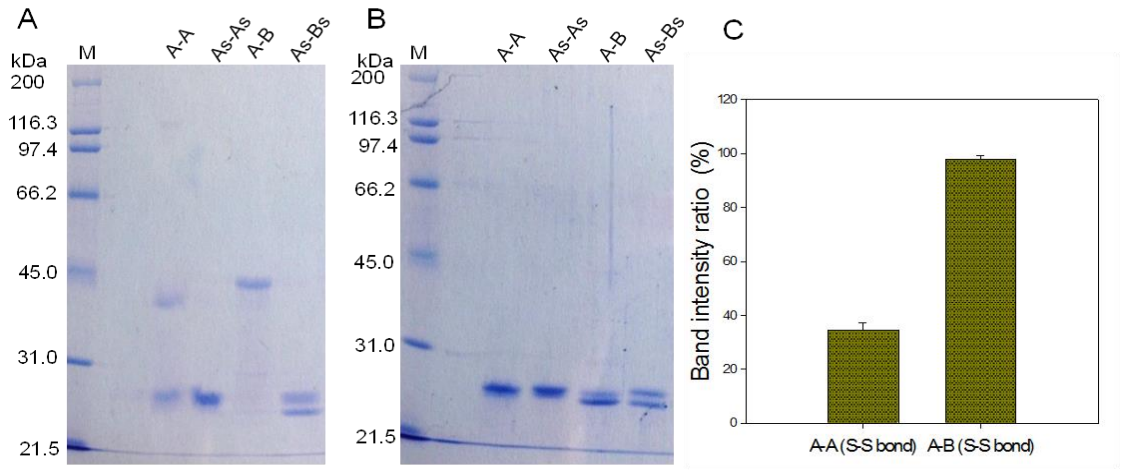

Fig. 1-2 Detection of monomeric and dimeric iPSPs by SDS-PAGE, and the ratio of S-S bond. Four μg of heterologously expressed and purified A-A, A-B, As-As, and As-Bs were subjected to 10% SDS-PAGE (A: without reduction, B: reduced with DTT), Densitometry values of the bands detected by A-A and A-B on SDS-PAGE without reduction (C). M: molecular marker.

observed at 24.5 kDa, confirming the presence of monomeric PspA subunits (A). However, when the anti-PspA antibody was reacted with non-reduced lysate, the intensity of 24.5-kDa band had been markedly reduced and additional bands of 38.0 and 43.0 kDa were also observed (A). These two bands most likely corresponded to A-A and A-B protein dimers that contained an intermolecular disulfide bonds. Although greater cross-reactivity with proteins in the *H. thermophilus* lysate was observed with the anti-PspB antiserum, a 23.5-kDa band corresponding to monomeric PspB was detected in reduced lysate Fig. 1-3B). Moreover, a 43.0-kDa band was present in the non-reduced lysate sample, also suggesting that PspB forms a heterodimer with PspA, and that the two subunits are interconnected by a disulfide bond. However, there is a doubt that it is the disulfide bond that was made afterwards since *H.themophilus lysate* (CFE) and purification steps of A-A and A-B were performed under aerobic condition. The formation of disulfide bond under redox condition will be described in the next section.

Two types of dimer within iPSP1 (A-A)

Two distinct bands of 24.0 kDa without S-S bond and 38.0 kDa with S-S bond were detected when A-A was subjected to non-reduced SDS-PAGE and western blotting as shown in previous

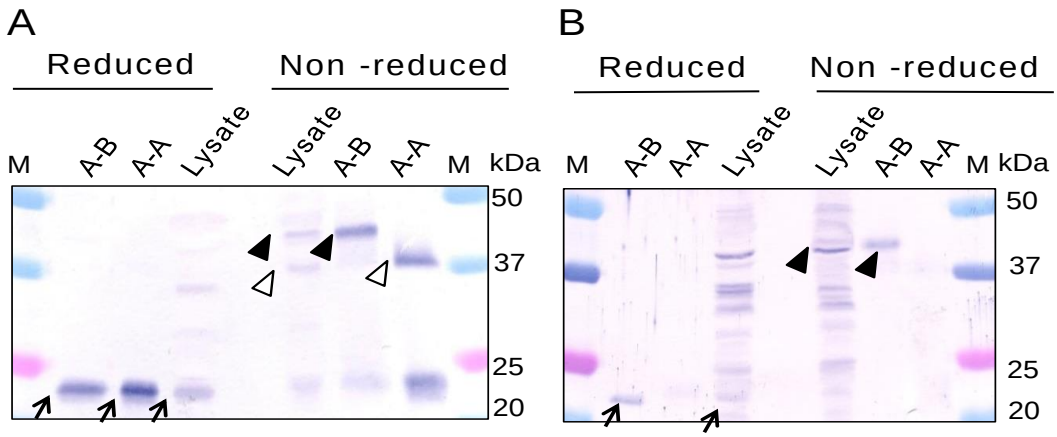

Fig. 1-3 Detection of disulfide bonds of iPSPs from *H. thermophilus* lysate (CFE) by Western blotting. (A) Antibody PspA : 1'st antibody (5ul / 5ml Skim milk), 5% Skim milk, A-A(0.06ug/well), A-B(0.095ug/well), Lysate(17.4ug/well). (B) Antibody PspB : 1'st antibody (20ul / 5ml Skim milk), 5% Skim milk, A-A(0.6ug/well), A-B(0.95ug/well), Lysate(35ug/well). Arrow, white arrowhead and black arrowhead point monomeric PspA or PspB, A-A and A-B, respectively**.** Here, A-B, A-A, and Lysate indicate purified A-B, purified A-A, and *H.thermophilus* CFE.

results (Fig. 1-2A). In contrast, only one distinct major band of A-A, A-B, and its mutants was detected from the Native-Page and size exclusion chromatography (Fig. 1-4A and C).

The experimental results showed two species of A-A under non-reducing SDS-PAGE and one species of A-A under Native-Page and gel-filtration chromatography, indicating that A-A existed as two types of dimeric protein composed of dimer with intermolecular disulfide bond and dimer without intermolecular disulfide bond. The ratio of A-A with disulfide bond and without disulfide bond was quantified by measuring the band intensity through image J and the result was 34% and 66%, respectively. I suspected that this ratio of 34% might change according to redox condition. In this context, reversible disulfide bond formation will be described in the next section.

The migration speed between A-A and As-As was same but As-Bs migrated faster than A-B under Native-Page (Fig. 1-4A), suggesting the side chains of serine residues caused different migration speed between A-B and As-Bs due to the charge of serine. In contrast, the migration speed of A-A and As-As was the same. This is probably because A-A has a compact structural characteristics, exchanging the cysteine residues with serine residues didn't give the charge effect of serine. The structural characteristic between A-A and A-B will be focused more detail in chapter 1.4.3.

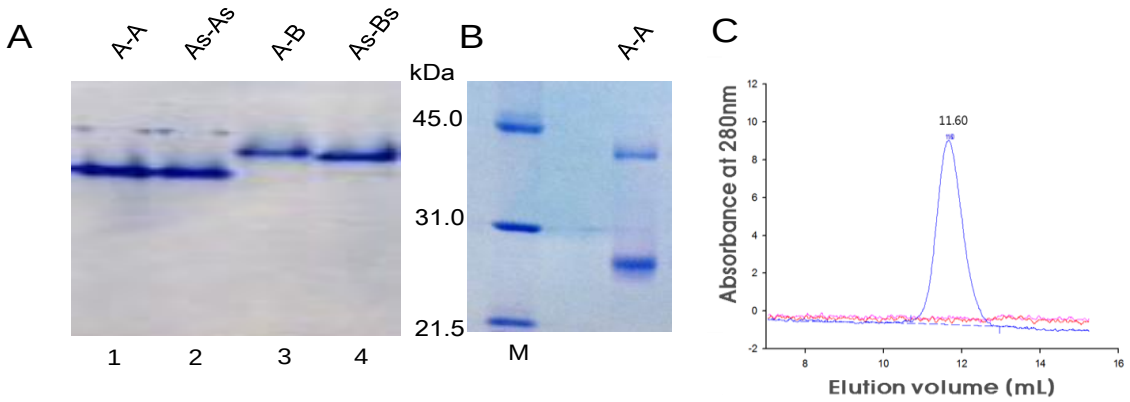

Fig. 1-4 12% of Native-Page analysis of iPSPs and its mutants A, 10% Non-reducing SDS-PAGE B, Size exclusion chromatography of A-A C. (A), lane1, 4ug of purified A-A (A-A); lane2, 4ug of purified As-As (mutants); lane3, 4ug of purified A-B; lane4, 4ug of purified As-Bs (mutants). (B), 4ug of purified A-A. (C), 4ug of purified A-A under size exclusion chromatography.

Detection of intracellular disulfide bond from *H.thermophilus*.

To determine whether the intermolecular disulfide bonds in A-A and A-B proteins were formed *in vivo* or not, thiols from disulfide bonds were labelled with the thiol-reactive fluorescent reagent CPM (16). For the analysis, free thiols were blocked before cell lysis by adding the alkylation reagent IAA (Iodoacetamide), disulfide bonds were then reduced by treatment with TCEP, and the cleaved thiols were labeled with CPM.

Firstly, the proper blocking of free thiol groups by IAA and thiol labeling by CPM were confirmed as a positive control by preparing control samples without addition of TCEP (Fig. 1-5A). As a control for fluorescent reagent CPM, control samples were not treated with IAA and as a control for blocking by IAA, control samples were treated with IAA. As can be seen **Fig. 1-5**A, lots of dense band were detected in all samples, indicating all samples have lots of thiol residues reacting with CPM. Whereas, protein bands were not detected when control samples were treated with IAA, indicating that IAA could block the thiols of protein properly (**Fig. 1-5**B).

In this context, purified A-B and As-Bs were also applied to positive and negative control for detecting intracellular disulfide bond. As can be detected in Fig. 1-6A, two monomeric bands corresponding to PspA and PspB were detected from the positive control sample, purified A-B, but not from the negative control, purified As-Bs, confirming that this assay system was able to detect intermolecular disulfide bonds.

In contrast, no additional bands were observed in whole cell lysates of *E. coli* cells expressing A-B compared with lysates from cells expressing As-Bs, indicating that the disulfide bond between PspA and PspB was not formed in *E. coli*. It was presumed that the intermolecular disulfide bond didn't exist between PspA and PspB in *E. coli* due to the strong reduced condition of *E.coli* and absence of making disulfide bond enzyme such as protein disulfide bond isomerase (PDI). In addition, the thiols of PspA 198C and PspB 197C may be blocked by IAA.

When the same amount of cell lysate from *H. thermophilus* and *E. coli* was analyzed, more bands were clearly observed in the cell lysate from *H. thermophilus* compared to *E. coli*, indicating that various proteins within *H. thermophilus* contain disulfide bonds. In addition, a relatively strong band was observed around 24.5 kDa, which is the same size as PspA, suggesting

that PspA in *H. thermophilus* has a disulfide bond. However, expected PspB band was not detected. This is probably because the total quantity of PspB was smaller than PspA, it was difficult to detect the PspB band *in H.thermophilus*.

Although lots of intracellular disulfide bonds were detected *in H.thermophilus*, it was not clear whether A-A or A-B linked by intermolecular disulfide bond exist in *H.thermophilus* or not.

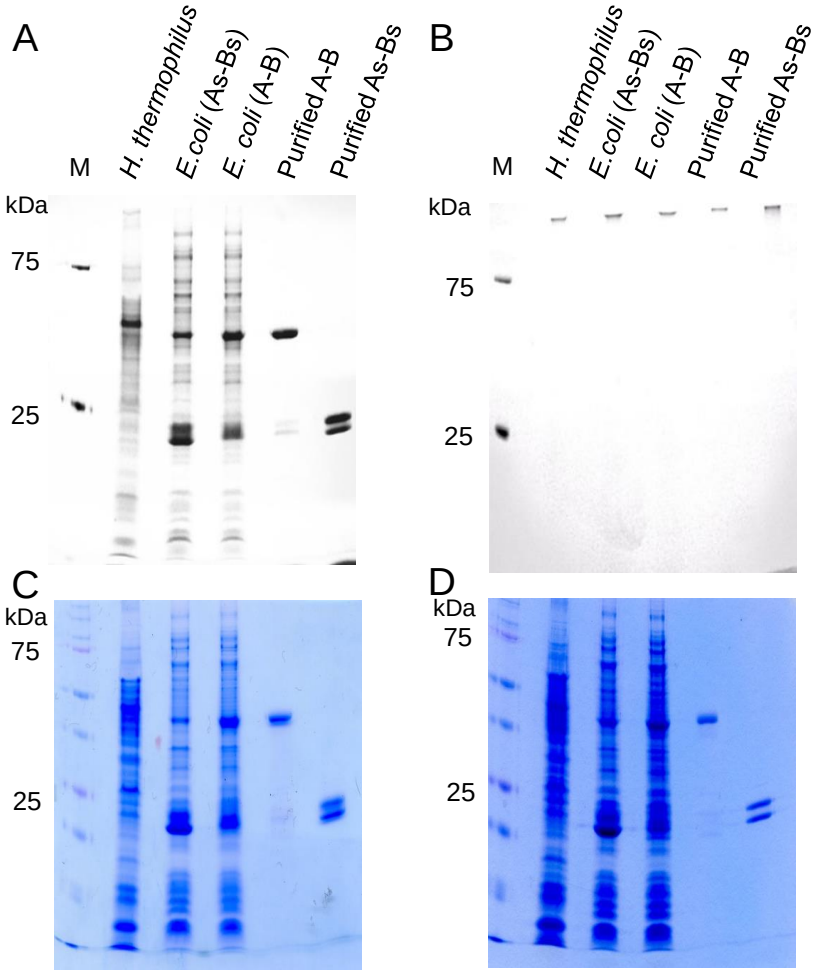

Fig. 1-5 Controls of CPM assay. (A) To confirm that the CPM labeling procedure was effective, the free thiols of cysteine residues were labeled with CPM by reacting cells and protein samples with CPM without blocking by IAA and reduction by TCEP. (B) To confirm that IAA blocked free thiols, CPM was added after alkylation without reducing disulfide bonds by TCEP. (C) and (D) are CBB-stained gels of (A) and (B), respectively.

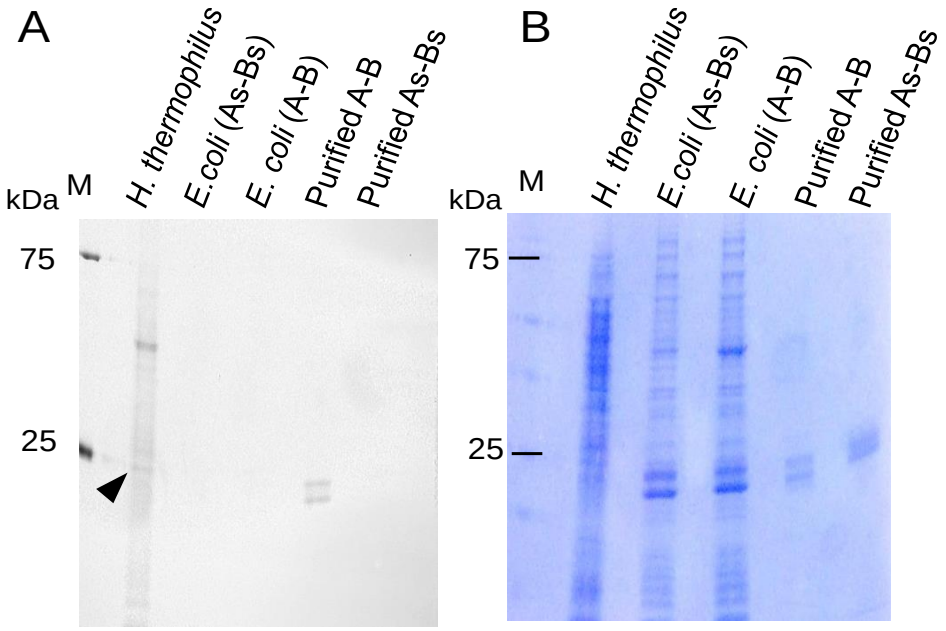

Fig. 1-6 Detection of intracellular proteins containing disulfide bonds. Thiols forming disulfide bonds were labeled with CPM, applied to 12% SDS-PAGE gels, and the label was then visualized by UV excitation at 365 nm (A). A black and white-converted picture is shown. The gel of (A) was stained with CBB (B). Arrowhead points the position of monomeric PspA.

Detection of A-A and A-B with S-S bond in vivo

Although lots of disulfide bonds were detected from *H.thermophilus* using Fluorescent Labeling analysis, there were no exact evidence that A-A and A-B with S-S bond is preserved in *H.thermophilus.* Therefore, Modified western blotting was carried out with a hypothesis as follows. IAA would block the free thiols of PspA and PspB subunit in *H.thermophilus,* indicating free thiols of both subunit couldn't form intermolecular disulfide bond. If intermolecular disulfide bonds, however, exist *in H.themophilu,* IAA could not influence on disulfide bond. Subsequent western blotting using non reducing SDS-PAGE and antiserum for PspA or PspB may clarify the presence of intermolecular disulfide bond of A-A or A-B. With this hypothesis modified western blotting was performed.

Dimeric iPSPs, but absence of multimeric iPSPs

Cysteine residues of PspA and PspB linked by intermolecular disulfide bond was investigated with an aim to find the position of cysteine residues with S-S bond and check the possibility of multimer of A-A and A-B.

Structure of PspA-PspA from the previous study (2) was regenerated by using PYMOL. As can be seen Fig. 1-7A, Cys158 and Cys173 of pspA and Cys157 of PspB was seemed to be buried inside of protein. In contrast, Cys198 of PspA and Cys197 of PspB seemed to be located in the surface area of protein and linked by intermolecular disulfide bond. In addition, when mutated AsB and ABs was prepared in *E. coli* and the cells were applied to Non-Reducing SDS-PAGE, AsB and ABs were not detected in dimeric position (Fig. 1-7B).

These results clearly indicats that heterologously expressed and purified A-A and A-B have intermolecular disulfide bonds between C198 of both of PspA subunits and between C198 of PspA and C197 of PspB, respectively in the soluble form.

Multimer of A-A or A-B was not detected (Fig. 1-7 C). This is because buried cysteine residues may not form intermolecular disulfide bond.

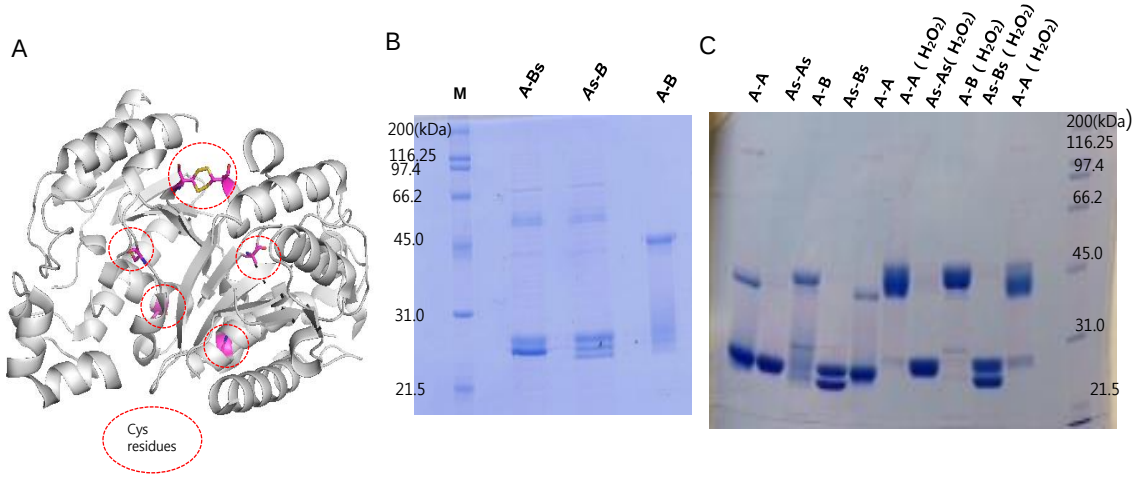

Fig. 1-7 The structure of PspA-PspA (A), 10% of Non reducing SDS-PAGE of recombinant A-B mutnats (B), 10% Non reducing SDS-PAGE of purified A-A and A-B (C). (A) The six cysteine residues are indicated in red. Red dotted circle show the position of cysteine residues. (B) Cell lysate of *E.coli* heat-treated at 70°C and purified A-B was applied to Non-reducing SDS-PAGE. (C) Purified A-A, A-B, and its mutant treated by H_2O_2 or not treated was applied to Non-reducing SDS-PAGE

1.2.4 Discussion

Crystal structure of A-A showed the possibility of intermolecular disulfide bond (2). However, recombinant purified A-A and the process for making crystal structure was not performed under anaerobic condition. Furthermore, intracellular environment of *H.thermophilus* was expected to be a strong reduced condition.

Due to the reducing environment of the cytosol, disulfide bonds are not usually found in cytosolic proteins. In eukaryotes, disulfide bonds are formed in the lumen of the endoplasmic reticulum in reactions catalyzed by protein disulfide isomerase (51). As the intracellular redox potential of *E. coli*, a mesophilic prokaryote, is around -200 to -300 mV, recombinant proteins with disulfide bonds may not fold properly (52, 53). Therefore, I examined whether the disulfide bonds found in iPSPs, which was heterologously expressed and purified, and also exist *in vivo*.

The soluble forms of heterologously expressed and purified A-A, a homodimer of PspA, and A-B, a heterodimer of PspA and PspB, were shown to be connected by a disulfide bond formed between the 198th cysteine residues of both PspA and 198th cysteine and 197th cysteine residues of PspA and PspB, respectively. Both of A-A and A-B could form dimers linked by intermolecular disulfide bond. On the other hand, it seemed that A-A and A-B couldn't form the multimeric protein. This was because other cysteine residues, 158th and 173th cysteine residues of pspA and 157th cysteine residue of PspB were buried inside the protein. A deeply buried Cys may behave as a hydrophobic reside due to the hydrophobic nature of amino acid packing inside the protein (54). And, nearly 100% of A-B dimers, and 35% of A-A dimers were connected by a disulfide bond *in vitro*.

Interestingly, A-A was composed of two types of dimer. One was dimer linked by intermolecular disulfide bond, another was dimer without intermolecular disulfide bond. It was assumed that redox condition might decide the dimeric state. Therefore, analysis of reversible disulfide bond formation was checked and the results showed that the status of intermolecular disulfide bond changed under redox condition, implying that reactive thiol of A-A or A-B might have some role in *H.thermophilus*. It has been known that the rate of the interchange reactions

varies with the microenvironment of the reacting thiols (55). Therefore, transcriptome analysis related thiol will be described in chapter 2.

Monomeric position A-A was changed into dimeric position with intermolecular disulfide bond when the reduced condition (-21 mV ORP) was changed into oxidative condition (59 mV ORP). Enzyme activity of A-A and As-As also decreased from this point. However, enzyme activity might not be related with disulfide bond formation directly due to the far distant position between activity site and disulfide bond formation site and detection of reversible enzyme activity of Aa-Aa without S-S bond.

However, electrophoretic mobility shift gave clue for reversible enzyme activity because both of them showed the conformity for the degree of protonation and activity lost under same value of ORP, respectively.

I speculated that protonation and deprotonation of amino acid residues under redox condition may related with reversible enzyme activity. However, it looks likely that the direct protonation of enzyme activity site having histidine as a catalytic core residue might be impossible for reversible enzyme activity. This is because it has long been known that 2-oxo-histidine produced by oxidation of histidine residues is irreversible and histidine restoration system was not discovered (56). Thus, it seems that protonation and deprotonation may be occurred in other amino acid residues related with activity site.

Based on crystal structure of PspA, it was revealed that enzyme activity site containing core catalytic residue, His^{9}, located in deep inside of PspA and the cleft or channel for activity site is covered by lid of entrance comprising C-terminal residues and having flexibility (2). Therefore, it was presumed that the entrance containing lid may protect the enzyme activity site via protonation under the oxidative condition, which means the protonation of lid and entrance results in increasing of molecular weight and loss of flexibility of lid. Consequently, protonation prohibits substrate or ROS from reacting with enzyme activity site.

As lid and entrance contain Arg 155, and Lys 209, the protonation and deprotonation may occur by carbonylation and decarbonylation of Arg 155 and Lys 209 in lid. This is because direct oxidation of proteins by ROS yields highly reactive carbonyl derivatives resulting from oxidation of the side chains of lysine, arginine, proline, and threonine residues (57). Additional

decarbonylation occurs under reduced condition or through activation of the thioredoxin pathway (58).

Considering the ratio of intermolecular disulfide bond of A-B and A-A, almost of A-B composed of 100 % intermolecular disulfide bond under moderately reduced condition (~ -58 mV ORP) whereas 35% of A-A linked by disulfide bond existed. Namely, PspA subunit seemed to be biased to be linked to PspB. Furthermore, the ratio of A-A and A-B in *vivo* was calculated as 36% and 64%, respectively. Although PspB subunit doesn't have PSP activity, PspB subunit could make a dimer with PspA subunit, which suggests that PspB subunit have a role as a client protein to make intermolecular disulfide bond and this disulfide bond presumed to be cleaved with the role of thioredoxin of *H.thermophilus*. Based on thioredoxin (Trx), it has been reported that thiol-disulfide exchanges are usually started by N-terminally located cysteine, which attacks the disulfide bond in client protein due to the low pK_a (59). Although *H.thermophilus* have several thioredoxin genes in genome information, direct correlation with intracellular disulfide bond was not investigated. In this context, transcriptome analysis supported this scheme of reversible cysteine modification, which will be described in 2.3.3.

The results of a fluorescent labelling assay, CPM assay, showed that A-B does not form intermolecular S-S bonds in *E. coli*, a finding that does not conflict with the above information indicating that the intracellular environment of *E. coil* is reduced. In contrast, numerous disulfide bonds were detected in total protein samples from *H. thermophilus*, in addition to the relatively strong band around 24.5 kDa that may be derived from PspA. Although a band of 23.5 kDa corresponding to PspB was faint, A-B may still form an intermolecular disulfide bond in *H. thermophilus*, because PspB is estimated to have a lower molecular number than that of PspA (1) and therefore more difficult to be detected. This speculation does not conflict with the WB data that *H. thermophilus* lysate contained both A-A and A-B dimers with disulfide bonds. The speculation that A-A and A-B may still form an intermolecular disulfide bond in *H. thermophiles* was clarified through the modified western blotting. To avoid the disulfide bond formation during sonification and other experimental process, IAA blocking free thiol was used before and after sonification as described in materials and methods section.

Two species of proteins corresponding to 38.0 kDa of purified A-A and 45.0 kDa of purified A-B were detected from *H.thermphilus*. In contrast, relatively low monomeric A-A was detected from *H.thermophilus.* It was of interest that almost all A-A existed as dimer with disulfide bond *in vivo.* In contrast, A-A existed as dimer with or without disulfide bond *in vitro.*

I speculated that this difference between *in vitro* and *in vivo* might be originated from intracellular environment and proteins such as thioredoxin or protein disulfide bond isomerase (PDI) participating in disulfide bond cleaving and formation. As *H. thermophilus* utilizes the reductive tricarboxylic acid cycle, which is used to fix CO_2 in reducing environments, it seems highly unlikely that the disulfide bond between PspA and PspB would spontaneously form in cells. Therefore, it is more likely that a specific system selectively forms disulfide bonds in thermophiles. *H. thermophilus* has several genes that are predicted to encode protein disulfide isomerases and thioredoxins, which may catalyze the formation of disulfide bonds. However, it remains unclear how disulfide bonds are formed in intracellular environments (53).

1.3 Thermostability

1.3.1 Introduction

Despite considerable research efforts over the last few decades in both scientific and industrial sectors to identify factors that contribute to the thermostability of proteins (60-63), no single or universal factor responsible for protein thermostability has been identified (64-67). However, comparison of homologous proteins between mesophilic and (hyper-) thermophilic organisms, and the mutagenic screening for thermostable proteins have revealed that electrostatic surface interactions, hydrogen bonding, compact protein packing, intrinsic secondary structure propensity and disulfide bond formation all contribute to thermostability (61, 68-71).

The formation of intracellular disulfide bonds is considered to be extremely rare because of the reducing environment of the cytoplasm (17, 72, 73). However, crystal structural analyses have revealed that several intracellular proteins from thermophilic organisms contain disulfide bonds within or between subunits that contribute to thermostability (66, 72, 74). In addition, thermophilic microorganisms, particularly hyperthermophiles, are reported to have a higher ratio of intercellular disulfide bonds compared to mesophiles (53, 74). For this reason, a number of researchers have attempted to create thermostable proteins for industrial applications by artificially introducing disulfide bonds (22, 75-77). However, the disulfide bond found in crystal structures or those that have been introduced manually are limited to intrasubunit bonds or those between two identical subunits.

Although PspA and PspB share 35% amino acid sequence identity and contain a conserved catalytic domain of the histidine phosphatase superfamily, only the PspA subunit shows substantial PSP activity (1, 2). Even if homodimer iPSP1 (A-A) and heterodimer iPSP2 (A-B) linked by intermolecular disulfide bond were detected in *H.thermophilus*, homodimers of PspBs have not been detected. In the previous section, analysis of modified western blotting revealed that A-A and A-B was linked by intermolecular disulfide bond *in vitro* and *vivo*. I therefore hypothesized that these intermolecular disulfide bonds maybe linked to the thermostability of A-A

and A-B. To confirm this hypothesis, here, the contribution of intermolecular bond for the thermostability of A-A and A-B was then examined.

1.3.2 Materials and Methods

Construction of Plasmids for Site-directed Mutants.

For heterologous expression, plasmids were constructed as described in below. The genes encoding the PspA and PspB subunits of *H. thermophilus* TK-6 (IAM 12695, DSM 6534) were cloned into the expression vectors pCDFDuet-1 and pET21c (Novagen, Darmstadt, Germany), as describe in materials and method section chapter 1.2.2. The constructed plasmids were then mutated to express C198S or C198A mutant for PspA subunit and C197S or C197A mutants PspB subunits, in which the 198th and 197th cysteine residues were converted to serine and alanine, respectively. Site-directed mutagenesis was performed by following the instruction of the Prime STAR mutagenesis blast kit protocol (TaKaRa Bio, Otsu, Japan) and the sequence was checked by using DNA sequencer (3130xg/Genetic Analyzer, Hitachi).

Heterologous Expression and Purification.

A-A, A-B, As-As, and As-Bs were expressed in *E. coli* BL21-Codon Plus (DE3)-RIL and then purified according to the materials and methods section of chapter in 1.2.2.

Reductive and Non-reductive SDS-PAGE.

With a minor modification of previous section 1.2.2, Reductive and non-reductive SDS-PAGE were conducted using a 5% stacking gel and 10% separating gel with or without DTT in the loading buffer, respectively. Samples to be analyzed by reductive SDS-PAGE were mixed with loading buffer (4 mM DTT, final concentration) and incubated at 95°C for 10 min prior to separation. After SDS-PAGE, the separated proteins were stained with CBB, and Image J software was used to quantify the band intensity of stained proteins.

Quantification

The protein amount from SDS-PAGE results were quantified by Image J software as a densitometry values with arbitrary units as such in previous section 1.2.2.

Protein Assay

Protein concentrations were measured using the Bradford protein assay (Bio-Rad) with bovine serum albumin as the standard as described in previous section 1.2.2.

Enzyme Assays

PSP activity was assayed by measuring the production of inorganic phosphate, as described previously with minor modifications (1, 28). The reaction mixture contained 200 mM HEPES-NaOH (pH 8.0 at room temperature), 10 mM L-phosphoserine, 1.0 mM EDTA (pH 8.0), and enzyme solution (total volume =50 μl). The reaction mixture was incubated for 7 min at 70 °C. The reaction was stopped by placing the tube in ice-cold water, followed by the addition of 450μL ferrous sulfate solution (0.008 g of $FeSO_4 \cdot 7H_2O$ in 1 mL of 7.5 mM H_2SO_4) and 37.5 μL ammonium molybdate solution (0.066 g of $(NH_4)_6Mo_7O_{24} \cdot 4H_2O$ in 1 mL of 3.75 M H_2SO_4). After precipitated proteins were removed by centrifugation at 10,000 × *g* for 15min, the inorganic phosphate concentration was determined by measuring the absorbance at 660 nm. KH_2PO_4 solution was used for calibration. One unit of PSP activity was defined as the amount of enzyme producing 1 μmol of inorganic phosphate per min.

Thermostability Analysis

One mL of 20 mM Tris-HCl (pH 8.0) with 1 mM EDTA containing 400 μg of purified proteins were incubated at 70, 75, 80, 85, and 90°C for 10 min, and were then placed into ice-water. After 30 min, the precipitants were removed by centrifugation at 20,000×g for 30 min. Ten μL of the supernatants were subjected to SDS-PAGE analysis to confirm the residual proteins in the soluble fraction. Additionally, the supernatents diluted 20 times were subjected to enzyme assays to measure the residual enzyme activity per volume of the heterodimeric A-B. On the other hand, the supernatants diluted to 40 μg/mL were subjected to enzyme assays to measure the residual enzyme activity (U/mg) of the homodimeric A-A.

1.3.3 Results

Construction of Mutant Proteins.

As described in Material and Method in this section, the mutants of As-As, Aa-Aa, As-Bs, and Aa-Ba were constructed to confirm the thermostability by intermolecular disulfide bonds between the PspA and PspB subunits. C198 of PspA and C197 of PspB were changed to serine or alanine. This is because alanine replacements of the disulfide-bonded cysteine residues in some soluble proteins such as bovine pancreatic trypsin inhibitor and lysozyme allow the formation of structures virtually to be identical to those of the native proteins (78).

The wild-type and mutant proteins were heterologously expressed using the same procedure in *Escherichia coli*. The elution patterns of the mutants during the purification by column chromatography exhibited similar profiles as the respective wild-type proteins, suggesting that the overall structure was not changed by the mutations. Additional analysis of Far UV CD(circular dichroism) spectra, which will be described in **Fig. 1-14**, showed that wild-types and their mutants had almost similar CD spectroscopic properties from 200nm to 250nm, indicating the identical structure between them. The homogeneity of the purified proteins was also confirmed by SDS-PAGE and CBB staining (data not shown).

Intermolecular Disulfide bond Enhanced the thermostability of homodimeric A-A

To confirm the function of the intermolecular disulfide bond identified between the PspA and PspA subunits, the thermostability of purified wild type, mutant A-A enzyme, and wild type treated with reductant, DTT, was analyzed. As an analytical method for thermalstability, remained protein solubility via reduced or non-reduced SDS-PAGE and remaining enzyme activity were performed after heat-treatment at designed temperature as described in Materials and Methods. Here, thermostability was defined as the ability of the protein to maintain solubility after heat treatment to clarify this phenomenon.

Thermal stability by Proteins-Proteins association based on intermolecular disulfide bond

As mentioned, co-precipitation of A-A with or without S-S bond was detected. Note that A-A with S-S bond (38 kDa) was homodimeric A-A linked by S-S bond and A-A without S-S bond (24 kDa) was homodimeric A-A without S-S bond. As A-A without S-S bond precipitated together with A-A with S-S bond at relatively high temperature. Protein-protein association between them was expected. In order to investigate whether protein-protein association existed or not, each of A-A with or without S-S bond was separated by treated with reductant,DTT, or oxidant, H_2O_2, and then residual enzyme activities of them were measured. In addition, the analysis for residual enzyme activity and remaining solubility at boiling temperature was also performed with an aim to check the strength of speculated protein-protein association at extremely high temperature. Lastly, the effect of NaCl was investigated since NaCl was one of candidates for influencing protein-protein electrostatic interaction. This is because sodium binding alters the electrostatic potential of protein (79). In addition electrostatic interaction stands for protein-protein association (80).

Therefore, the major role for the thermostability of wild type A-A composing two types of protein was from A-A with intermolecular disulfide bond. Moreover, intermolecular disulfide bond enhanced the thermostability of A-A with S-S bond.

Effect of sodium chloride on thermal stability of A-A

In order to find the clues for protein-protein association, I investigated the thermal stability of A-A at sodium chloride concentrations from 0 to 0.5M, respectively.

On the other hand, residual enzyme activity gradually increased from 0 mM to 250 mM NaCl after heat-treatment at 100 °C). In contrast, residual enzyme activity of A-A with 500 mM NaCl decreased more than that of A-A without NaCl, indicating sodium chloride influenced on thermal stability of A-A.

Intermolecular Disulfide Bond Enhanced the Thermostability of Heterodimeric Protein.

To confirm the function of the intermolecular disulfide bond between the PspA and PspB subunits, the thermostability of purified, electrophoretically homogeneous wild-type and mutant

A-B enzymes was analyzed. A-B was targeted in this experiment as nearly all of the purified A-B heterodimers had intermolecular disulfide bonds. In contrast, as I mentioned in chapter 1.2.3, A-A was composed of 35% of A-A dimer with S-S bond and 65% of A-A dimer without S-S bond (Fig. 1-2). Because the PspB subunit does not have clear enzymatic activity but both PspA and PspB subunits are required for the existence of A-B, thermostability was defined as the ability of both the subunits to maintain solubility after heat treatment (If PspB precipitated, PspA may still be able to stay in the soluble fraction as A-A but it is not the result of thermostability as A-B but that as A-A).

When purified A-B was incubated at 90°C, approximately 30% of the PspA and PspB subunits remained in the soluble fraction (**Fig. 1-8**A, B, E and F). In contrast, only 3% of PspA and almost no PspB retained the solubility when As-Bs, which cannot form an intermolecular disulfide bond, was heat-treated at 90°C (**Fig. 1-8**C, D, E and F). The ratio of residual soluble PspA and B subunits from As-Bs was similar to that of A-B incubated with DTT (**Fig. 1-8**E and F), suggesting that the observed difference in thermostability between A-B and As-Bs is attributable to the presence of an intermolecular disulfide bond.

As can be detected in **Fig. 1-8**C-F, the Bs from As-Bs precipitated at lower temperature than As, whereas the wild-type A-B was precipitated at almost the same conditions (**Fig. 1-8**A-D). In the case of As-Bs, 55% and 100% of PspB subunits were precipitated at 75 and 80°C, respectively, whereas only 21% and 55% of PspA subunits were precipitated at respective temperatures (**Fig. 1-8**E and F). It indicates that the thermostability of As-Bs can be defined as the ratio of residual soluble PspB subunit as mentioned remained solubility of after heat-treatment. Residual PSP activity (**Fig. 1-8**G) showed a similar tendency with the ratio of residual soluble PspA rather than that of PspB; In case of A-B, almost all the activity and both subunits were retained after incubation at 80°C. On the other hand, in case of As-Bs, about 50% of PspA subunit and PSP activity was retained while almost all the PspB subunit was disappeared from the supernatant after incubation at 80°C.

Therefore, I concluded that the intermolecular disulfide bond of the heterodimer enhanced thermostability of the whole protein, but especially of PspB subunit.

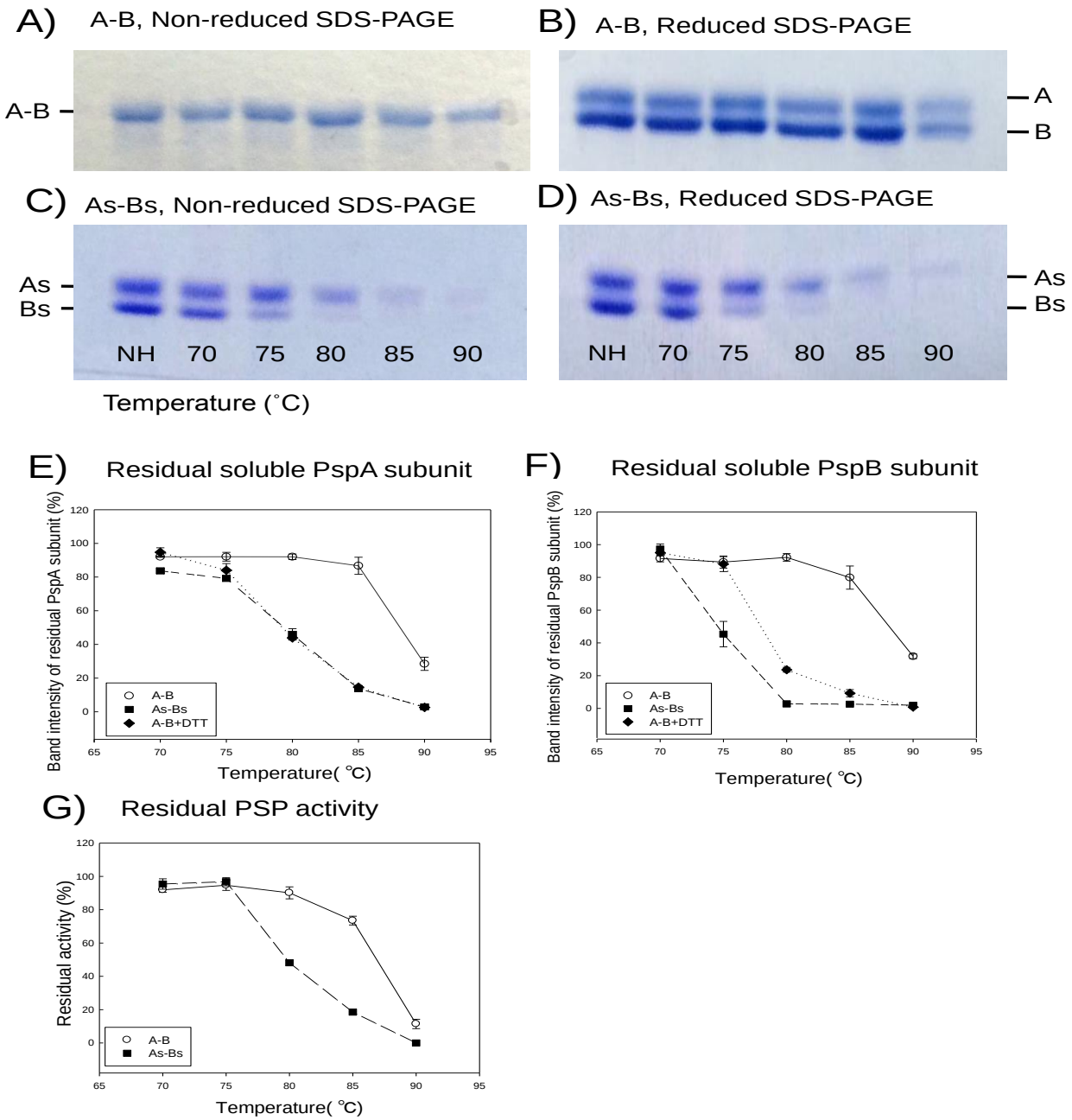

Fig. 1-8 Thermostability of A-B and a mutated form (As-Bs) that cannot form an intermolecular disulfide bond. SDS-PAGE analysis of A-B under non-reducing (A) or reducing (B) conditions. SDS-PAGE analysis of As-Bs under non-reducing (C) or reducing (D) conditions. The same volume of samples corresponding to 4 μg of protein before heat -treatment were applied to 10% SDS-PAGE gels after heat -treatment at the designated temperatures for 10 min and removal of the precipitant. NH: non-heat treated. The ratio of PspA (E) and PspB (F) remaining in the soluble phase was quantified from the band intensities using Image J software with non-heat treated samples as 100%. A-B+DTT indicate that the sample was heat -treated at the designated temperatures with DTT. (G) Residual activity per volume of samples after heat -treatment at designed temperatures was measured at 70°C. Band intensity or activity from the non-heat treated sample was defined as 100%.

Conservation of cysteine residues able to form Intermolecular Disulfide Bonds

The distribution of cysteine residues with the potential to form intermolecular disulfide bonds on heterodimer was examined among species of the order Aquificales with sequenced genomes.

Aquificales, the ancestor of PspA and PspB, divided into PspA and PspB after the family Desulfurobacteriaceae arose, but before the division of Aquificaceae and Hydrogenothermaceae (1). Therefore, Multiple sequence alignments of iPSP homologs from these three families using the CLUSTALW program (81) was performed (Fig. 1-9).

The cysteine residues that correspond to C198 and C197 of *H. thermophilus* PspA and PspB, respectively, were conserved in all homologs from Aquificaceae, except one of the two PspAs (ZP_02179977) from Hydrogenivirga, but not in those from Hydrogenothermaceae or Desulfurobacteriaceae (Table 1-4). The PspA of Hydrogenivirga without the cysteine residue was acquired by lateral gene transfer from Hydrogenothermaceae (1) In contrast, another PspA of Hydrogenivirga (ZP_02178481), which was acquired by vertical inheritance, conserved the cysteine residues. Therefore, Hydrogenivirga's iPSP2 (A-B) can also form intermolecular disulfide bond.

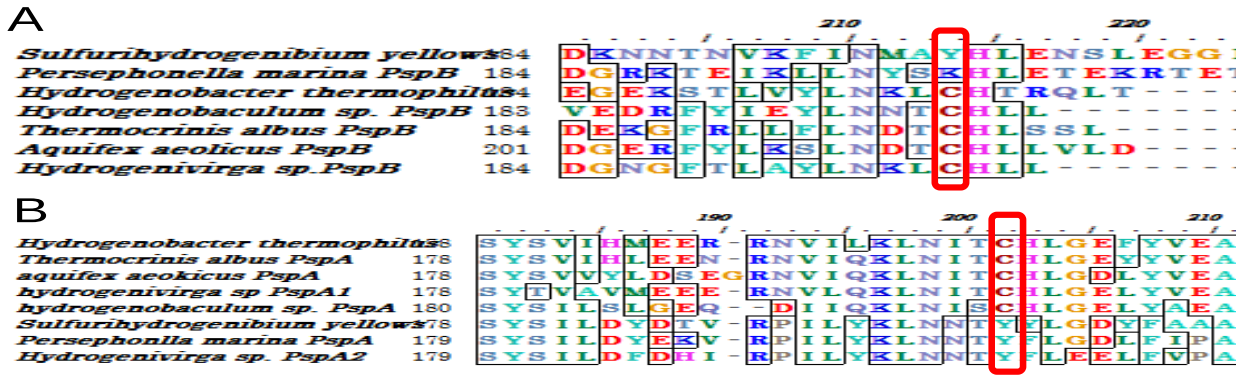

Fig. 1-9 Multiple-sequence alignment of iPSPs homologous and conserved cysteine residues using CLUSTALW.

(A) Residues corresponding to cysteine 198 of PspA subunit via Multiple-sequence alignment using phylogenetic tree of *H.thermophilus.* (B) Residues corresponding to cysteine 197 of PspB subunit via Multiple-sequence alignment using phylogenetic tree of *H.thermophilus*

Table 1-4 Growth temperature range and optimal temperature of selected members of *Aquificaceae*, *Hydrogenothermaceae*, and *Desulfurobacteriaceae*

Family	Organisms	PspA		PspB		Growth Temp. (℃)	Optimal growth Temp. (℃)	Ref
		Accession No.	Residue corresponds to C198	Accession No.	Residue corresponds to C197			
Aquificaceae	*Hydrogenobacter thermophiles*	YP_003431771	C	YP_003431851	C	50 ~ 78	70	(1)
	Thermocrinis albus	YP_003473638	C	YP_003472871	C	55 ~ 89	80	(5)
	Aquifex aeolicus	NP_214366	C	NP_214196	C	~ 95	89	(6, 7)
	Hydrogenivirga sp.	ZP_02178481 ZP_02179977	C Y	WP_008286172	C	60 ~ 87	70	(9)
	Hydrogenobaculum sp	YP_002121633	C	YP_002122276	C	30 ~ 70	55	(9)
Hydrogenothermaceae	*Sulfurihydrogenibium yellowstonense*	WP_007545446	Y	WP_007547062	Y	55 ~ 75	70	(11)
	Persephonella marina	YP_002730136	Y	YP_002730941	K	55 ~80	73	(13)
Desulfurobacteriaceae	*Desulfurobacterium thermolithotrophum*	YP_004280974	G	—	—	40 ~ 75	70	(15)
	Thermovibrio ammonifican	YP_004151946	G	—	—	60 ~ 80	75	(16)

1.3.4 Discussion

Intermolecular Disulfide Bond Enhanced the Thermostability of Heterodimeric Protein.

The soluble forms of both heterologously expressed and purified iPSP1, a homodimer of PspA (A-A), and iPSP2, a heterodimer of PspA and PspB (A-B), were shown to be connected by a disulfide bond formed between both 198th cysteine residues of PspA and between the 198th and 197th cysteine residues of PspA and PspB, respectively *in vitro*. In addition, A-A and A-B linked by intermolecular disulfide bond was also existed *in vivo*.

Nearly 100% of A-B dimers were connected by a disulfide bond. Comparison of the thermostability between wild-type A-B, A-B under reducing conditions, and As-Bs clearly showed that the disulfide bonds was indispensable for thermostability of A-B. These findings are consistent with studies reporting that tight interfacial connections between subunits mediated by hydrogen bonding (82), hydrophobic interactions (83), or disulfide bonds (84) increase protein thermostability.

In addition, disulfide bonds can make substantial contributions to the stability of proteins, a mainly influence on the decrease of conformational chain entropy of the denatured protein (85). After the thermostability by intramolecular disulfide bond that found from nature, many attempts have been made to increase protein stability by intramolecular disulfide bonds that artificially introduced in proteins, however, the reports are limited to intramolecular disulfide bonds (21). In addition, the importance of interactions between subunits for increasing multimeric protein thermostability has already been reported (86), however, these studies were limited to homodimeric proteins and were not usual like as the thermostability by intramolecular disulfide bond (87, 88). To our knowledge, the findings presented here are the first example of a proteins that contains an intermolecular disulfide bond between heteromeric subunits that contributes to thermostability.

Interestingly, PspB subunits that were not connected to PspA by a disulfide bond, Bs of As-Bs, were precipitated at lower temperature than PspA, whereas both subunits as part of the A-B heterodimer with an intermolecular disulfide bond were precipitated under the same conditions in this study (**Fig. 1-8**B and D).

As described, the PspB subunit in As-Bs without S-S bond lost solubility over 70 °C. This observation likely indicates that attachment to PspA is required for PspB to exist in the soluble fraction. Furthermore, based on the following observations from the past study by Ciba *et al* (1) and this studies: 1) PspB does not remain in the soluble fraction when expressed without PspA in *E. coli* ; 2) the elution pattern of A-A and A-B from a hydrophobic Butyl Toyopearl column, suggests that the surface of PspB has higher hydrophobicity than that of PspA; and 3) the surface charge of modeled PspB structure calculated by PyMOL was 0.0, whereas that of PspA was -4.0, suggesting that the surface electron charge of PspB is very low (data not shown) (3).

My speculation concerning this point is as follows: PspA and PspB can stably form heterodimers without a disulfide bond at 70 °C or lower since Bs of As-Bs was precipitated over 75 °C, and therefore the intermolecular disulfide bond is not essential below the optimal growth temperature of *H. thermophilus*. However, the intermolecular disulfide bond between PspA and PspB is necessary for the solubility of PspB at 75°C or higher because PspB detached from PspA may immediately precipitate and disappear from the soluble phase over 75°C, suggesting the strong connection of PspB to PspA through the disulfide bond may prevent the precipitation of PspB at 75°C or higher.

I therefore propose that intermolecular disulfide bonds between subunits with low solubility and those with higher solubility can increase the thermostability of heterodimeric proteins. It is noteworthy that the intermolecular disulfide bond between PspA-PspB is essential for the PspB subunit to exist in the soluble fraction at 75°C, which is the upper limit of the optimal growth temperature of *H. thermophilus* (7). Furthermore, the growth of *H. thermophilus* was detected between 75 °C and 80 °C in this study (data not shown). Thus, if

PspB have function *in vivo*, the intermolecular disulfide bond might appear to be physiologically important for this protein to maintain solubility in *H. thermophilus*.

In the present study, I demonstrated that an intermolecular disulfide bond contributes to the thermostability of a heterodimeric protein from a thermophilic bacterium. The disulfide bond not only increases the thermostability of the whole protein, but also specifically increases the solubility of a single subunit at high temperature. This finding provides new insight into the evolution of proteins with high thermostability and is expected to contribute to the development of new strategies for increasing the thermostability of target proteins.

Conservation of cysteine residues able to form Intermolecular Disulfide Bonds

The physiological importance of the intermolecular disulfide bond identified in iPSP1 and iPSP2 is also supported by the strict conservation of the cysteine residues corresponding to the 197th or 198th cysteines among homologs of these proteins in Aquificacea (Table 1-4). Although the cysteine residues are not conserved in PspA or PspB from Hydrogenothermaceae, it is unclear whether PspB subunits from this family are unable to remain in the soluble phase at physiological temperature. In addition, the growth temperature of many members of Hydrogenothermaceae is lower than that of several Aquificaceae species (Table 1-4). We speculate that the evolution of iPSP in Aquificales occurred as follows. When a single iPSP gene was duplicated to generate PspA and PspB in the ancestor of Aquificaceae and Hydrogenothermaceae, both proteins had iPSP activity and were soluble as homo- and hetero-dimers. Subsequently, PspA maintained PSP activity and solubility, whereas PspB lost PSP activity and became less soluble, but may have acquired other functions. During the evolution of PspB, the solubility of this protein might have reduced to the point that B-B became insoluble. However, PspB retained its ability to form heterodimers with PspA, and therefore can exist in soluble form as a heterodimer. Concurrent with the evolution of PspB in Aquificaceae, PspB inherited cysteine residues from an ancestor of Aquificaceae that allowed for the formation of a disulfide bond between PspA and PspB.

Intermolecular Disulfide bond Enhanced the thermostability of homodimeric A-A

Many extracellular globular proteins contain disulfide bonds, which are thought to provide additional stability against environmental heat stress (89). Even if disulfide bonds are relatively rare in intracellular protein due to the strong reduced condition, Intermolecular disulfide bond of PSPs was clarified from *H.thermophilus* in previous section. Although, it has been well known that protein thermostability can be enhanced by intramolecular disulfide bond, protein thermostability by intermolecular disulfide bond was not so usual (74, 87). Therefore, this section had focused on thermal stability analysis with an aim to check the themostability by intermolecular disulfide bond.

As an analysis method for thermostability of homodimer A-A, remaining protein and residual enzyme activity was performed by using non-reducing SDS-PAGE and PSP activity analysis. When A-A, As-As, and A-A + DTT were applied to analysis for thermostability, the remaining proteins at 95 °C were 72%, 13%, and 0%, respectively. Residual enzyme activities of them were 88%, 20%, and 0%, respectively. These results implied that intermolecular disulfide bond was essential for the thermostability of A-A. This is because when this bond was broken either by point mutation or by thiol-reducing agent, the As-As or A-A+DTT were denatured and lost enzyme activity at relatively low temperature. This result was consistent with the previous report of Benezra et al (87, 88), who noted that purified E2A helix-loop-helix proteins spontaneously form homodimers linked by an intermolecular disulfide bond and linked protein shows the increased thermostability. Therefore, it was clarified that an intermolecular disulfide bond was required for the enhance thermostability of wildtype A-A.

Thermal stability by Proteins-Proteins association based on intermolecular disulfide bond

Wild type A-A composed of 35% of A-A with S-S bond and 65% of A-A without S-S bond (Fig. 1-2C). Intermolecular disulfide bond was revealed to be indispensable for the

thermostability of homodimeric A-A involving A-A with and without S-S bond as described above. However, it was of interest that one species of homodimer A-A, 65% of A-A without S-S bond, didn't lost solubility even at higher temperature in the presence of 35% of A-A with S-S bond. Therefore, each of A-A with and without S-S bond was focused through the thermostability analysis.

A-A with and without S-S bond lost some of solubility simultaneously at 100 °C. Namely, two species A-A were co-precipitated after heat-treat at 100 °C for designed time and the ratio of disulfide bond in A-A was proportional before and after heat-treatment. In this connection, although the residual activity of A-A without S-S bond was 87% even at 95 °C in the condition of existing A-A with disulfide bond, A-A without S-S bond started to lose PSP activity at 80 °C and almost all PSP activity disappeared over 90 °C in the absence of A-A with S-S bond. On the other hand , residual enzyme activity of A-A with S-S bond was 96% in the absence of A-A without S-S bond. Therefore, it looks likely that protein-protein association may exist for the thermostability of A-A without S-S bond by connecting to A-A with S-S bond. These results suggests a novel mechanism whereby proteins-proteins association may enhance the thermostability of dimeric protein without S-S bond in the presence of dimeric protein linked by intermolecular disulfide bond.

Although intermolecular disulfide bond was indispensable for the thermostability of A-B and A-A, the degree of stability at higher temperature was different between them as follows. A-A and A-B, remaining protein of A-A and A-B at 90 °C, were approximately 75% and 30%, respectively. Although both A-A and A-B have intermolecular disulfide bond enhancing thermostability, the stability was more strong in A-A than in A-B, suggesting that each PspA and PspB subunits might have different thermal characteristics such as several thermal influence factors involving intermolecular disulfide bond might be need to retain remarkable thermal stability. These thermal characteristics of iPSPs will be focused in next section 1.4.

Effect of sodium chloride on thermal stability of A-A

The analysis of sodium chloride on A-A showed that proper concentration of NaCl enhanced the thermostability of A-A in some degree. It seems that the interaction of sodium with the surface of A-A might enhance the thermostability. Na^+ or Li^+ have been known to influence on the electrostatic interaction (90, 91). Specific interaction between cations and protein thermolysine might be involved in the activation, and their effective is in the order of $Na^+ > K^+ > Li^+$ (92, 93). Therefore, sodium chloride was presumed to influence on electrostatic interaction for homodimeric A-A, suggesting the possibility of thermostability via protein-protein association. However, to verify this hypothesis, another experiment such as measuring electrostatic interaction using capillary electrophoresis (CE) and protein charge ladders seems to be needed.

Although the exact relationship between protein-protein association and protein with disulfide bond has not been clarified, it was revealed that intermolecular disulfide bond had a major role for the enhanced thermostability when the intermolecular disulfide bond and protein-protein interaction was considered.

Conservation of cysteine residues

The physiological importance of the intermolecular disulfide bond identified in iPSP1 and iPSP2 is also supported by the strict conservation of the cysteine residues corresponding to the 197^{th} or 198^{th} cysteines among homologs of these proteins in Aquificacea (Table 1-4). Although the cysteine residues are not conserved in PspA or PspB from Hydrogenothermaceae, it is unclear whether PspB subunits from this family are unable to remain in the soluble phase at physiological temperature. In addition, the growth temperature of many members of Hydrogenothermaceae is lower than that of several Aquificaceae species (Table 1-4). We speculate that the evolution of iPSP in Aquificales occurred as follows. When a single iPSP gene was duplicated to generate PspA and PspB in the ancestor of Aquificaceae and Hydrogenothermaceae, both proteins had iPSP activity and were soluble as

homo- and hetero-dimers. Subsequently, PspA maintained PSP activity and solubility, whereas PspB lost PSP activity and became less soluble, but may have acquired other functions. During the evolution of PspB, the solubility of this protein might have reduced to the point that B-B became insoluble. However, PspB retained its ability to form heterodimers with PspA, and therefore can exist in soluble form as a heterodimer. Concurrent with the evolution of PspB in Aquificaceae, PspB inherited cysteine residues from an ancestor of Aquificaceae that allowed for the formation of a disulfide bond between PspA and PspB. However, the possibility of PspB enzymatic activity in some of Aquificacea may be agreeable.

1.4 Thermal characteristics between A-A and A-B

1.4.1 Introduction

It was revealed that intermolecular disulfide bond enhanced the thermostability of heterodimeric protein in this study for the first time, which suggests that heat weak protein can be thermal stable by linking thermal stable protein via intermolecular disulfide bond.

This was because although the thermostability of both A-A and A-B was enhanced by intermolecular disulfide bond, A-A was more thermal stable than A-B, indicating that PspA subunit might have more thermal stable characteristics than PspB subunit.

Considering protein thermal characteristics, several decades extensive research has carried out to identify and understand the sole factor contributing to the stability of proteins from organisms living under extreme conditions (64). Several reasons have been attributed to the thermal stability as follows. Greater hydrophobicity (94, 95), better packing, deletion or shortening of loops (96), additional networks of hydrogen bonds (97), smaller and less numerous cavities, increased surface area buried upon oligomerization (98), increase hydrogen bonding (99), salt bridge (63, 100), disulfide bond (75, 101, 102), and amino acids composition(103). Amino acids composition and their exchange of some amino acid are believed to be closely connected with protein thermal characteristic (104, 105). Now, it is accepted that there is no single thermodynamic strategy or molecular(106).

Proteins from thermophilic organisms are usually stable and maintain their activities at high temperature; their molecular features have been proposed to contribute toward greater thermostability (103). Therefore, it is of interest to know what kind of molecular features makes iPSPs, especially pspA or pspB subunit from *H.thermophilus*, stable at high temperature. Taken into consideration the thermal influence factor on iPSPs, several candidates were suggested for the molecular features as follows.

First of all, disulfide bond was detected from the iPSPs in *vitro* and *vivo* in Chapter 1-2. Disulfide bridges can be a stabilization factor above 100 ºC and that conformational environment and solvent accessibility are determining factors in the protection of disulfide bridge against destruction (107). This notion was based on the fact that earlier study on *S. solfataricus* 5'- methylthioadenosine phosphorylase expressed *E.coli* forms in correct, destabilizing disulfide bridges (108).

Secondly, amino acid compositional analysis is a classical protein analysis technique. The statistical analysis of the amino acids composition of proteins from thermophiles provided interesting evidences. For example, abundant charged amino acid residues found in thermophiles points towards the crucial stabilizing role of electrostatic interactions (109, 110). Moreover, generalized features of amino acid composition on thermophilic proteins include an in increase in residue hydrophobicity and decrease in uncharged polar residues (64, 111).

Third, Previous chapter 1-2 showed the presence of intermolecular disulfide bond by using non-reducing SDS-PAGE and SDS-PAGE (Fig. 1-2). As the molecular weight of PspA subunit (25kDa) is higher than that of PspB subunit (24kD), It was expected that A-B (49kDa) migrates faster than A-B (50kDa). However, A-A (50kDa) migrated faster than A-B(49kDa) under non-reducing SDS-PAGE. Thus, the compact conformation of thermal influence factors was suspected to affect electrophoretic mobility. The compactness, which can be explained the surface area of a sphere with equal volume to protein, is also thermal influence factor (112).

Therefore, Available thermal influence factors on pspA and pspB increasing iPSPs thermostability were investigated in this chapter since there might be different thermal characteristics between pspA and pspB subunit and also between A-A and A-B.

1.4.2 Materials and Methods

Data for Comparative Analysis

I compiled *pspA* and *pspB* sequence data comprised of DNA sequence data from *Aquificales* consisting of three families: *Aquificaceae, Hydrogenothermoceae*, and *Desulfurobacteriacea.* The phylogenetic analysis of 16s ribosome RNA sequence shows that *H.thermophilu* belongs to the order of *Aquificales* (31). Available *pspA* and *pspB* orthologs, which have over 40% identities against PspA and PspB of *H.thermophilu* by protein BLAST search, were selected as a comparative analysis.

Analysis of amino acid properties

The amino acid composition for the data set was calculated by using the number of amino acids of each type and the total number of residues. It is defined as:

$$Comp_i = n_i \times \frac{100}{N} \quad (1)$$

Where *i* stands for the 20 amino acid residues, n_i is the total number of each residues and *N* is the total number of residues. Each amino acid was assigned to one of three categories: charged residues (Arg, Lys, His, Glu, Asp), polar (uncharged) residues (Ser, Thr, Gln, Asn, Cys), and aromatic residues (Trp, Phe, Tyr) (61, 113). Statistical test (independent sample T-test) was carried out to determine whether two sets of data (PspA and PspB homologous) were significantly different from each other or not after checking normal distribution of each group.

Circular dichroism measurements

CD measurement was performed to compare the secondary structural difference between A-A and A-B using Jasco spectropolarimeter. The raw CD data shown as a millidegrees was converted mean residue ellipticity (MRE) in degrees square centimeter per decimal as follows.

$$\text{MRE} = \frac{\theta \times Mmrw}{10 \times C \times l}, \quad M_{mrw} = \frac{M.W}{n} \qquad (2)$$

Where θ is the ellipticity of CD in millidegresses, $Mmrw$ is the mean residual molecular weight (g/mol), n is the number of amino acid residues, C is the concentration (mg/ml), and l is the path length of the cell. α–helical content was calculated from the mean residue ellipticity (MRE) values at 222nm using the following equation according to Chen *et al*. (114).

$$\% \text{ alpha helix} = \left|\frac{MRE_{222nm} - 2{,}340}{30{,}300}\right| \times 100 \qquad (3)$$

Buffer of purified A-A and A-B was changed to 5mM phosphate buffer (pH 8.0) by using viva spin centrifuged at 8, 000×g for 1 hour. 0.2 ~ 0.3 mg/ml of protein was applied to CD measurement.

Blue Native Gel Electrophoresis

Blue native gel electrophoresis was performed with minor modifications (115). Briefly, 13% separation gel was poured and stored at 4˚C until use. Composition of an acrylamide separation gel was shown as follows. 3 mL of Gel buffer, 1.54 mL of Acrylamide, 0.86 mL of 87% glycerol, 0.6 mL of distilled water, 16μL of 10% APS, and 1.6μL of TEMED. The First cathode buffer (50mM Tricine adjusted pH 7.0 by NaOH, 15mM Bis-Tricine adjusted pH 7.0 by HCl) containing 0.02% (w/v) Coomassie Brilliant Blue G250, Second cathode buffer (50mM Tricine adjusted pH 7.0 by NaOH, 15mM Bis-Tricine adjusted pH 7.0 by HCl), and the anode buffer (50mM Bis-Tricine adjusted pH 7.0 by HCl) were chilled to 4˚C before use.

For BN-PAGE, 2 μL of sample buffer (5% (w/v) of CBB G250, 500mM of 6-amino caproic acid, 100mM of Bis-Trcine adjusted pH 7.0 by HCl, 1mM of PMSF, and 50% glycerol) were added to 18 μL of sample, which was then loaded onto the sample well. Electrophoresis was begun at 100V at 4˚C under the first cathode buffer. After 100min, The

first cathode buffer was changed to the second cathode buffer, and the electrophoresis was continued with voltage at 300V at 4˚C for 1hr. The BN gel was fixed and stained with CBB.

Construction of Plasmids for Site-directed Mutants

The genes encoding the PspA and PspB subunits of *H. thermophilus* TK-6 were cloned into the expression vectors pCDFDuet-1 and pET21c (Novagen, Darmstadt, Germany), respectively as described in chapter 1.2 material and method section. The constructed plasmids were then mutated to express C198S and C197S mutants of the PspA and PspB subunits as described in previously

Heterologous Protein Expression and Purification

A-A, A-B, and the corresponding dimeric proteins formed with the PspA C198S and PspB C197S mutated subunits were expressed in *E. coli* BL21-Codon Plus (DE3)-RIL and then purified using the protocol described in chapter 1.2 materials and methods section

1.4.3 Results

pspA and pspB orthologous for the amino acid composition data

To obtain clues of molecular features for the thermal characteristics of PspA and PspB, both orthologous were selected and subsequently amino acid composition was computed as follows. This was because thermophilic proteins show more molecular features for the thermal characteristics than their mesophilic proteins. Moreover, the different amino acid composition between thermophilic and mesophilic proteins have shown some generalized features of amino acid composition including an increase in residue hydrophobicity, a decrease in uncharged polar residues, an increase in charged residues (116).

Based on 16S ribosomal ribonucleic acid (rRNA) gene sequence comparison, the order *Aquificales* is composed of three families, *Aquificaceae*, *Hydrogenothermoceae* and *Desulfurobacteraceae*. The family *Desulfurobacteriaceae* which are firstly diverged from

common ancestor consists of *Desulfurobacterium,* and *Thermovibrio* (117). The family *Aquificaceae* consists of the genera *Hydrogenobacter, Thermocrinis, Aquifex, Hydrogenivirga, and Hydrogenobaculum,* whereas the family *Hydrogenothermaceae* consists of the genera *Sulfurihydrogenibium,* and *Persephonella* (Fig**.** 1-10). All of the *psp*A and *psp*B orthologous showed over 40% identities against PspA and PspB of *H.thermophilus* through Protein BLAST.

Charged residues (Arg, Lys, His, Glu, Asp) and polar (uncharged) residues (Ser, Thr, Gln, Asn, Cys) showed the normal distribution, whereas aromatic residues (Trp, Phe, Tyr) didn't show the normal distribution, indicating that aromatic residues were not proper to T-test and to carry out compare amino acid composition analysis. Additional T-test for amino acid composition showed that there was difference between PspA and PspB orthologous on charged and polar residues, respectively (data not shown). Therefore, amino acid composition ratio was carried out on the basis of charged and polar residues since they met the necessary condition such as normal distribution and T-test.

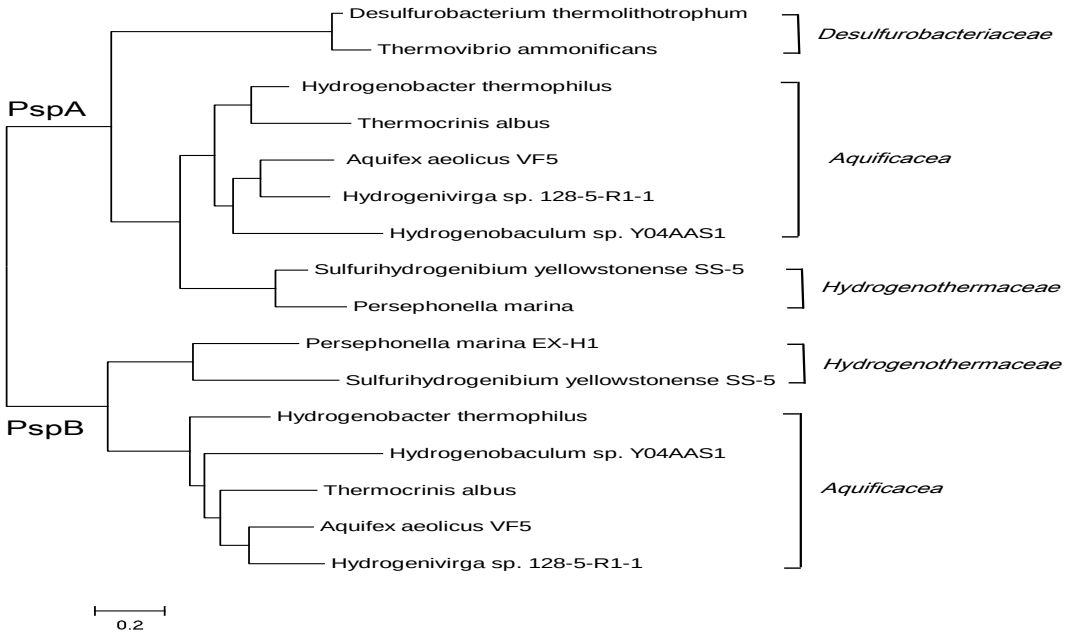

Fig. 1-10 Phylogenetic tree generated using maximum-likelihood analysis showing the position of families within the *Aquificales*. Reproduced using phylogenetic tree from Chiba *et al.* (1)

Amino acid composition in PspA and PspB orthologous

Fig. 1-11 summarized the ratio of each amino acid residues from the homologous of PspA and PspB, which were selected using phylogenetic tree. Subtle difference between PspA and PspB orthologous orthologous was shown in Arg, Lys, His, Ser, and Cys residues. The composition ratio of Ala, Val, Pro, Trp, Tyr, Glu, and Asp was higher in PspA orthologous than in PspB orthologous, whereas the residues having lower composition ratio in PspA were Gly, lle, Leu, Met, Phe, Thr, Gln, and Asn residues. Asn and Gln was known as a thermolabile amino acid due to the its tendency of undergoing deamination at high temperature, thus hyperthermophilic proteins were characteristically reduced in Gln (118). Thr is known as the best residue for interacting with the water surrounding protein structure, the water however would be released at higher temperature, so the hyperthemophilic proteins have very low frequency of Thr compared with mesophilic proteins (64).

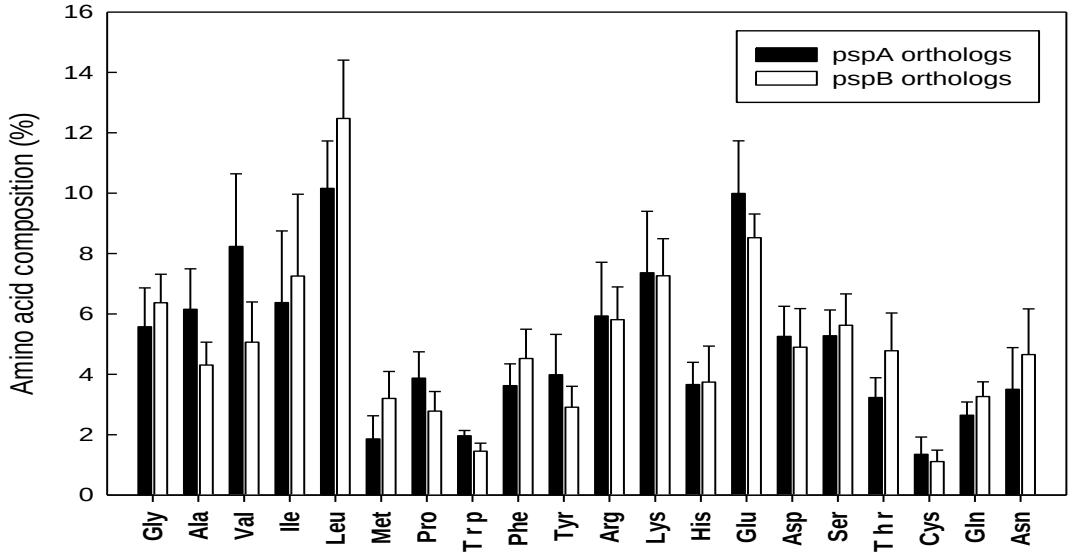

Fig. 1-11 Ratio of amino acid composition from pspA and pspB orthologs. The orthologous of PspA and PspB were selected using phylogenetic tree. Each of amino acid composition ratio was calculated after normal distribution and independent samples T-test.

Aliphatic amino acids such as Val has been known for contributing to the hydrophobic interaction, which is the main force for maintain conformational stability in inner part of protein (119). As can be seen Fig. 1-12, the composition ratio of charged amino acid residues (Arg, Lys, His, Glu, Asp) was higher in PspA orthologous than those in PspB orthologous. The charged amino acid residues would contribute to the electrostatic interaction, which is an important force for maintaining conformational stability in outer part of protein (64, 99, 120). Asp and Glu are only two amino acids with negatively charged side chain. More charged residues are found in hyperthermophilic proteins than in mesophilic proteins (61, 119). Polar, uncharged amino acids (Asn, Gln, Cys, Ser, and Thr) has been known to be readily interact with water (hydrophilic) . PspA orthologous showed smaller ratio of polar amino acid residues than those of pspB orthologous (Fig. 1-12). Ser and Thr are known as the best residues for interacting with waters surrounding protein (121). Since the water interacting with Ser and Thr would be released at higher temperature, the local protein structure around water-binding site could be changed to be unstable enough to evoke protein instability (122, 123). There have been several reports that the uncharged polar residues contents, especially

Ser, Thr, Gln, were much lower in thermophiles than that in mesophiles (61, 64, 119).

Compact conformation

Considering the migration speed of A-A and A-B in non-reducing SDS-PAGE (Fig. 1-3A), A-A (48 kDa) migrates faster than A-B having (47kDa), indicating that different size (volume) and/or charge between them caused a reversed migration. This is because proteins with small M.W. usually migrate faster than protein with large M.W. under Polyacrylamide gel electrophoresis and protein charge also influence on migration.

In order to identify the size difference between A-A and A-B, Blue-Native page was performed. Blue native polyacrylamide gel electrophoresis (BN-PAGE) enable the analysis of native (nondissociated) protein-protein interaction (124). The anionic dye coomassie blue G-250 was added to purified A-A and A-B. G-250 can bind to proteins due to its hydrophobic properties. As the binding of a large number of negatively charged dye molecules to protein makes shift the isoelectric point of the proteins to more negative values, both of A-A and A-B migrate to the anode regardless of their original native charge. Thus, A-A and A-B would be

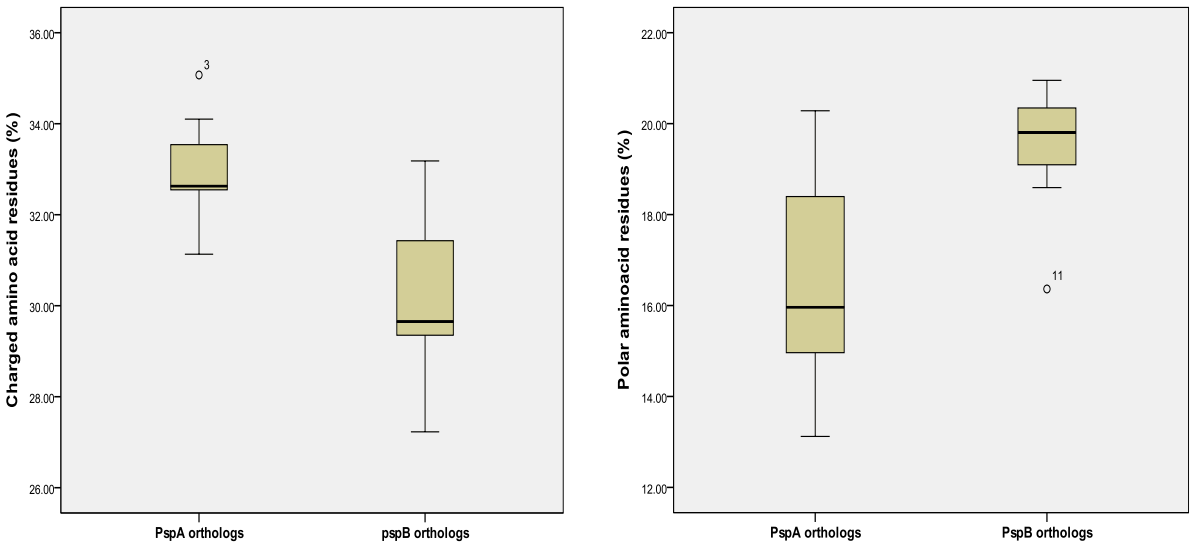

Fig. 1-12 Charged and polar amino acid residues from pspA and pspB orthologs. The ratio of Charged (Arg, Lys, His, Glu, Asp) and Polar (Asn, Gln, Cys, Ser, and Thr) amino acid residues were calculated from Fig. 1-11. Box graph indicated the max, min, and median values.

separated by the difference of M.W. and/or size.

Purified protein A-A migrated faster than A-B and purified As-As also migrated faster than As-Bs under Blue-Native Page (Fig. 1-13), indicating the sized of A-A was smaller than A-B. As described above, the volume and/or charge of protein were candidate factors for reversed migration rate between A-A and A-B. In addition, protein migrating under BN-Page isn't affected by native protein charge. Therefore, the size of A-A was revealed to be smaller than that of A-B since A-A had higher M.W. than A-B, suggesting that the compact conformation of A-A could be also another influence factor for the enhanced thermostability of A-A when compare to A-B.

Protein secondary structural characteristics

α-helix and $\theta_{208}/\ \theta_{222}$ have been known for the stability influence factor (125, 126). The regular secondary structural content of protein, α-helix and β-sheets, can be determined by CD spectra in the far-UV (250 – 200 nm) (127).

The far-UV CD spectra of iPSPs was recorded to investigate the protein structural characteristics as shown in Fig. 1-14**.** The spectra difference between 208nm and 222nm in A-A and A-B was shown, which suggested that A-A and A-B have different structural

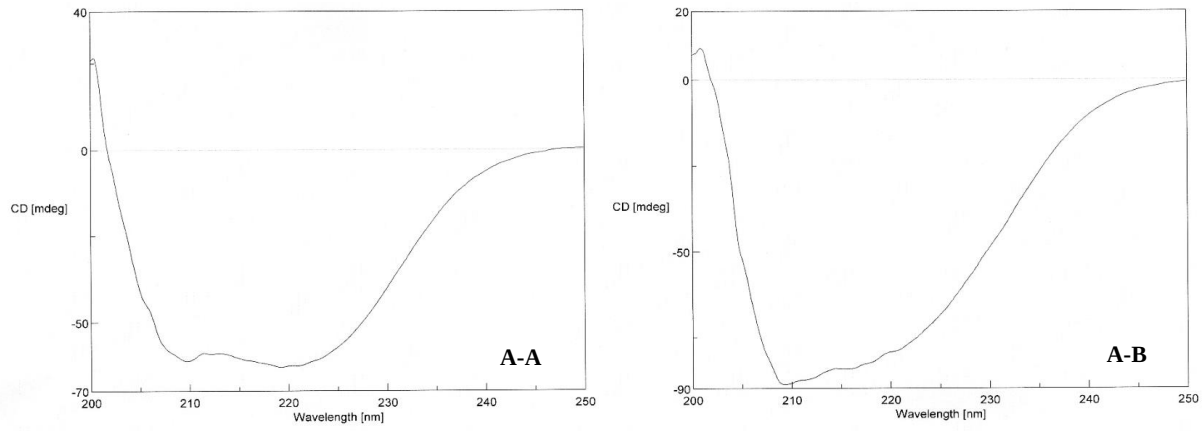

Fig. 1-14 Far UV CD spectra of iPSPs. 200ug/ml of A-A and 300ug/ml of A-B was applied to CD spectro

packing. It has been known that the ratio of $\theta_{208}/\theta_{222}$ is changed according to structural packing of proteins and the values of $\theta_{208}/\theta_{222}$ is varies from 0.8 to 5.0 for the native proteins (128). As can be detected in Table 1-5, the ratio of $\theta_{208}/\theta_{222}$ of A-A and A-B were 0.96 and 1.09, respectively, indicating their structural packing is different. Here, θ indicated ellipticity of CD

The secondary structural content, alpha helix, calculated from the mean residue ellipticity (MRE) values at 222nm using equation of Chen *et al.* method (114) is listed in Table 1-5. A-A showed higher helicity of 29.3% as compared to the A- B of 27.3%, suggesting that A-A has more secondary structural integrity and stability than A-B. Therefore, secondary structural characteristic of A-A also showed more thermostable features than that of A-B.

Table 1-5 CD spectroscopic properties of iPSPs

Annotation	MRE $_{208nm}$	MRE $_{222nm}$	α-helix (%)	$\Theta_{208}/\Theta_{222}$
A-A (A-A)	-6267	-6536	29.3%	0.96
A-B (A-B)	-6442	-5924	27.3%	1.09

1.4.4 Discussions

Amino acid composition in PspA and PspB orthologous. In this section, I compiled *pspA* and *pspB* sequence data to calculate amino acid composition ratio of PspA and PspB orthologous. It has been known that analysis of protein sequences from complete genomes of thermophiles and mesophiles reveals some of factors related to thermostability in proteins (129). Amino acid composition shows several clear differences between proteins from thermophiles and mesophiles and simple statistical tests can be used to identify these differences (61). Although pspA and pspB orthologous were involved in thermopiles, the amino acid sequence composition ratio of pspA and pspB from *H.thermophilus* made me

assumed that different thermal characteristics between pspA and pspB orthologous might be detected through the amino acid composition ratio.

As expected, significant difference was observed in both pspA and pspB orthologs even if both of them are involved in thermophiles. pspA and its orthologous had more charged amino acid residues but less polar amino acid residues than pspB and its orthologous. Additionally, aromatic residues and hydrophobic residues were also higher in pspA orthologous even if both of them didn't satisfy statistical significance (data not shown).

These results were consistent with the result of amino acid composition ratio between thermophiles and mesophiles, which suggested that the observed differences between pspA and pspB orthologous were related to the thermostability features. Therefore, it looks likely that amino acid composition may give more positive effect on the thermostability of pspA than that of pspB.

Structural compact conformation. Along with several sequence, structural factors have been proposed to contribute toward greater stability of thermophilic proteins (64). In relation to structural characteristics, I hypothesized that A-A might have more compact conformation since A-A having 49kDa of M.W migrated faster than A-B having 48kDa of M.W. under non-reducing SDS-PAGE and Native-Page. To confirm the hypothesis, blue native page was conducted. This is because that protein can be migrated not by protein charge but by CBB G250. Namely, proteins can be separated by molecular weight and their size. A-A also migrated faster than A-B under Blue-Native Page. This means that the volume or size of A-B is bigger than A-A. Thus, A-B migrate slower than A-A even if A-B had lower molecular weight. As a result of this, It was suggested that A-A might have structural characteristics of compact conformation as one of thermal influence factors.

Although A-A and A-B mixture was also applied to gel-filtration chromatography , the peaks of A-A and A-B was not separated due to the quantification limit of gel-filtration chromatography.

α-helices of A-A and A-B. The α-helix of A-A (29.3%) was higher than that of A-B (27.3%). It is well known that α-helices have a dipole moment, equivalent to half a positive unit charge at the N-terminus, estimated to be approximately 3.5 D per peptide unit (dipole moment) and β-sheet have 0.5 D, the N-terminal end of the structures corresponding to the positive end of the dipole (130). Although not always explicitly detailed by the authors, an inspection of the reported cases shows that replacements in β-strands would accomplish enhanced thermal stability on stabilizing their stand dipoles (131). From these considerations on secondary structure, it has been suggested that thermophilic proteins have a higher helical content (132). This results were consistent with the result of A-A. Thus, A-A was also expected to be more thermostable than A-B.

As a comparison data, α-helix of A-A was calculated by using X-ray analysis (Crystal structural A-A). α-helix content of A-A, 53.3%, from X-ray analysis was higher than 29.3% from the far-UV CD spectra. Reportedly, the different α-helix value for A-A may be caused by a covalently bonded group (133).

To sum up, although I couldn't investigate all thermal influence factor, it looks likely that PspA subunit have more thermal stable characteristics than PspB subunit. Considering the thermal influence factor, even if intermolecular disulfide bond seemed to be the most important thermal influence factors in iPSPs, association of thermal influence factor was suspected to be the most important for enhancing thermostability of protein.

Chapter 2 Physiology of iPSPs

2.1 *pspA gene* deletion serine auxotroph

2.1.1 Introduction

Hydrogenobacter thermophilus (TK-6) is an obligately chemolithoautotrophic, extremely thermophilic hydrogen-oxidizing bacterium whose optimal growth temperature for autotrophic growth on H_2-O_2-CO_2 is between 70 and 75°C, which was isolated from a hot spring located in Izu, Japan in 1980. Metal-independent phosphoserine phosphatase (iPSPs) identified from *H. thermophilus* had both PspA subunit with PSP activity and PspB subunit without PSP activity (2).

Phosphoserine phosphatase (PSP) is a member of haloacid dehalogenase superfamily, which is utilized to convert phospho-L-serine to L-serine (134). However, as the iPSPs is not the homology of classical PSP and they possess neither mutase activity nor the residues important for the activity, iPSPs was annotated as a novel-type PSPs (1).

Taking the serine biosynthesis pathway into consideration, at least two serine biosynthesis pathways were suggested in *H.thermophilus*, respectively: PSP (de novo serine pathway: PGDH, PSAT and PSP) and SHMT (Fig. 2-1). Based on serine metabolism, SHMT and Tryptophan synthase were found as a candidate for serine catabolic pathway, which was performed using KEGG pathway and homology searching via enzymes involving in serine metabolism (Table 2-1).

Although glycine can be synthesized from serine via reversible SHMT, glycine cleavage system was not detected from *H.thermophilus* due to the lack of homology in previous study (3), suggesting a glycine accumulation or new types of glycine catabolic pathway. However, serine synthesizing from glycine was also possible due to the reversible SHMT. Considering the results of KEGG path way and homology searching, L-

tryptophan was expected as an end of product because of the absence of tryptophan metabolic pathway in *H.thermophilus*, suggesting the tryptophan accumulation.

Which pathway is operated *in vivo*? It was of interest to reveal the serine and glycine catabolic pathway from *H.thermophilus*. To review the overall serine catabolic mechanism, serine is the principal one carbon (1-C) donor for the synthesis of nucleic acid, proteins, vitamins, some amino acids and methylated molecules (135, 136). One-carbon metabolism is a key pathway involved in providing single carbon units for the biosynthesis of purines, thymidylates, serine, and methionine (137). These one carbon units are activated by the carrier molecule tetrahydrofolate (H_4 folate). They are descended from the reactions catalyzed by SHMT, which cleaves serine to produce 5, 10-CH_2-H_4 folate and glycine (138). They can also be made from formate through synthesis of 10-HCO-H_4 folate by the syntheses activity of the C1-tetrahydrofolate synthase enzymes(139) or as 5, 10-CH_2-H_4 folate from glycine cleavage by the glycine decarboxylase complex (GDC) (140).

Furthermore, it has been reported that L-serine metabolism not only provide formyl groups for purine synthesis and methyl groups for pyrimidine synthesis but also an essential role in the development and function of the central nervous system and cancer

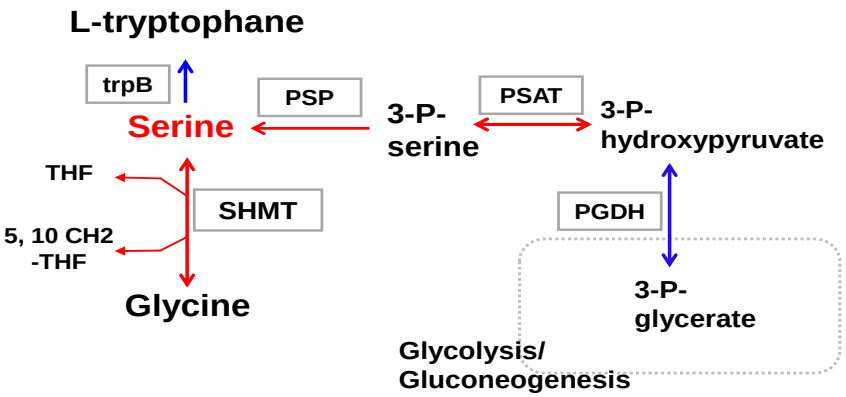

Fig. 2-1 Expected serine metabolic pathway from *H.thermophilus* TK-6. trpB, tryptophane synthase; PSP, phosphoserine phosphatase; PSAT, 3-phosphoserine aminotransferase; PGDH, 3-phosphoglycerate dehydrogenase; SHMT, serine hydroxymethyltransferase; THF, tetrahydrofolate. Red line and blue line indicated that the activity has been detected and the homolog of the enzyme exists. This figure was modified from the general serine anabolic pathway (3).

cells (141, 142), which indicate the possibility of unknown function of L-serine metabolism above iPSPs enzymatic activity.

Therefore, I assumed that *H.thermophilus* involving novel-type iPSPs might have unknown characteristics, which might elucidate the metabolic pathway of *H.thermophilus* and other members such as *Aquificales,* cyanobacteria, and chloroflex with lack an orthologous of classical PSP. With these hypothesis that PspA subunits have unknown

Table 2-1 Enzymes involve in serine metabolism

EC number	Name [Reaction catalyzed]
5.1.1.18	Serine racemase [L-serine ↔ D-serine]
4.3.1.17	L-serine dehydratase [L-serine ↔ Pyruvate + ammonia]
4.2.1.20	Tryptophanesyntase [L-serine + indole 3-glycerol phosphate → L-tryptophan + d-glyceraldehyde 3-phosphate + H_2O]
2.2.2.1	glycine hydroxymethyltransferase (SHMT) [Tetrahydrofolate + L-Serine ↔ 5,10-Methylenetetrahydrofolate + Glycine + H_2O]
2.6.1.45	glyoxylate aminotransferase [L-serine + glyoxylate ↔ Hydroxypyruvate + Glycine]
4.2.1.22	L-serine hydro-lyase, cystathionine beta-synthase [L-serine + L-Hmocystein ↔ L-cystathionine + H_2O]
4.3.1.17	L-serine ammonia-lyase [L-serine ↔ pyruvate + ammonia]
2.7.8.8	L-serine 3-phosphatidyltransferase [CDP-diacylglycerol + L-serine ↔ CMP + phosphatidylserine]
2.6.1.51	L-serine : pyruvate aminotransferase [L-serine + pyruvate ↔ Hydroxypyruvate + L-Alanine]
3.1.3.3	Phosphoserine phosphatase [O-Phospho-L-serine + H_2O → L-Serine + Orthophosphate]

Each reaction was based on KEGG pathway map.

function, I decided to delete the gene of *pspA* to know the property and physiology of PspA subunit.

2.1.2 Materials and methods

Bacterial strain and construction of plasmid for homologous recombination

Primers were designed with product size 1.1 ± 0.1 kbp by using *H.thermophilus* genome information and the binding site of primers was shown in dotted line of the construction scheme of gene deletion (Fig. 2-2). The sequence of primers used to PCR was shown in Table 2-2, and Table 2-3, in which small letter of sequence was denoted as the restriction site. To gain chromosomal DNA, *H. thermophilus* TK-6 was cultivated at 70°C under a gas phase of H_2:O_2:CO_2 (75:10:15, v/v) in a 500-mL vial with an autotrophic medium as shown in Table 1-1 (48), and DNA extraction was followed. PCR was carried out by using Prime STAR HS DNA Polymearase (TaKaRa, Bio, Otsu, Japan) and PCR fragments were clarified by gel electrophoresis.

Purified PCR fragment was inserted into pEX 18 via enzyme restriction and ligation. Plasmids constructed by ligation were transformed into *E.coli.* Following incubation was performed at 37 °C for overnight. Here, *Escherichia coli* strain JM109 was used as cloning host for pEX 18, which was used for disruption of the *pspA* gene by homologous recombination. In case of need, antibiotics were used with the concentration of 25 μg mL^{-1} kanamycine and 100 μg mL^{-1} ampicillin for *E.coli* and 500 μg mL^{-1} kanamycine for *H.thermophilus*

The deleted gene was substituted for marker gene, htk, which was highly thermostable kanamycin nucleotidiyltransferase gene fused with promotor region of *H.thermophilus prod* gene and had 1.3kbp of size. This process was also carried out via enzyme restriction, ligation, and transformation. Transformed marker gene was also clarified by gel electrophoresis.

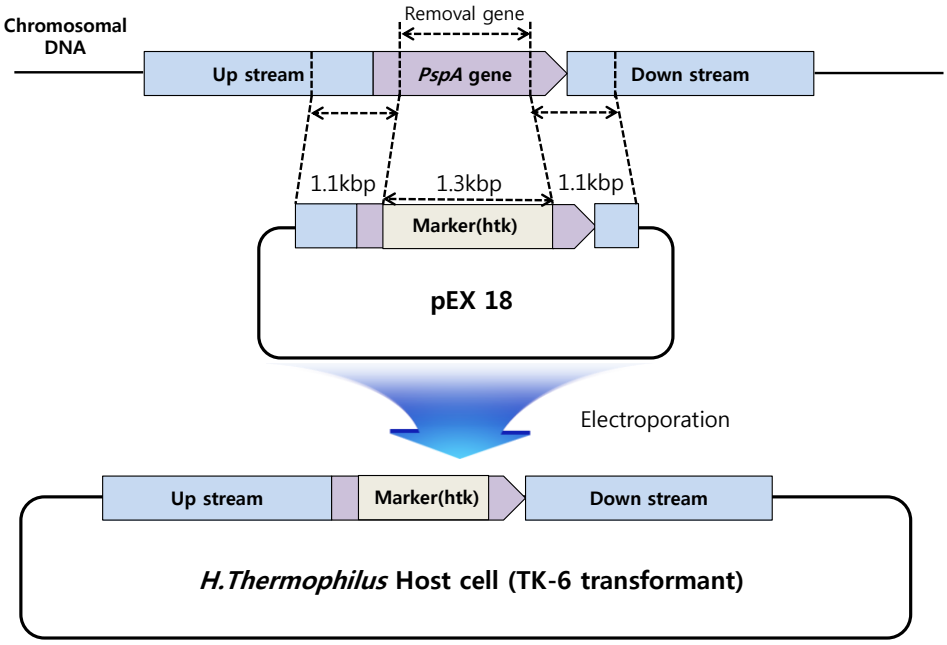

Fig. 2-2 Scheme of *pspA*gene deletion for homologous recombination of *H.thermophilus.*

Table 2-2 Primers used for clone antibiotics resistant marker genes

Primer	Sequence	RE site
htk_kpn_F	5'-AAAGGTACCACATTCGGTGAGAAGCTACAGG-3'	KpnI
htk_kpn_R	5'-AAAGGTACCGGTCATCGTTCAAAATGGTATG -3'	KpnI

Table 2-3 Primers used to construct plasmids for gene disruption.

Disruptant	Primer	Sequence	Marker
ΔPspA	pgma_Up_F_Eco RI	TATGgaattcGTAAGCCTGGAGAG	htk-KpnI
	pgma _Up_R_ Kpn	TGAggtaccAAGAAAAAGACACTGG	
	pgma _Down_F_ Kpn	CAAggtaccTAGCCTGCTTTTTAC	
	pgma _Down_R_ Xbai	TAGtctagaGGAAGCTCTGGGAAG	

Homologous recombination of *H.thermophilus*

H. thermophilus TK-6 was cultivated with an aim to make competent cell at 70°C under a gas phase of H_2:O_2:CO_2 (75:10:15, v/v) in a 100-ml vial with a 10 mL of autotrophic medium. 1.5 mL of *H. thermophilus* was gathered and centrifuged at 20,000 ×g for 3 min when OD_{540nm} was reached 0.5 - 0.8. Cell pellet of *H. thermophilus* was washed by miliQ and repelleted by centrifugation at 20,000 ×g for 3 min. Washed cell was resuspended in 500 μL of 10% glycerol, and centrifugation was followed at 20,000×g for 2min. Supernatant was removed and cell pellet was resuspended by additional 50 μL of 10% glycerol and preserved on ice for using as a competent cell.

Electroporation was performed by using 10 μL of constructed plasmid, prepared competent cell, and 300 μL of autotrophic medium. After the electroporation, subsequent incubation was performed on solid culture, which containing autotrophic medium, 10 μg mL^{-1} of $CuSO_4 \cdot 5H_2O$, 300 μM of L-serine, 500 μg mL^{-1} kanamycine, and GELRITE (Wako Pure Chemical Industries, Osaka, Japan). The plates were settled on a desiccator and incubated at 70°C under a gas phase of H_2:O_2:CO_2 (75:10:15, v/v) for 3 – 7 days and the gas was changed every other day. A colony expressed on a solid medium was transferred into 2mL of liquid autotropic medium containing 300 μM of L-serine, 500 μL^{-1} kanamycine in a test tube with butyl cap and gas phase of H_2:O_2:CO_2 (75:10:15, v/v). The transferred colony was incubated for 2-3 days until the OD_{540nm} was over 0.7. The disrupted gene was confirmed by measuring the DNA sequence, 16s RNA, and the length of PCR-amplified DNA fragments of marker gene (htk) and constructed plasmid

Bacterial growth condition for cell suspension

H. thermophilus TK-6 (IAM 12695, DSMZ 6534) was cultivated at 70°C under a gas phase of H_2:O_2:CO_2 (75:10:15, v/v) and in an inorganic medium as shown in Table 1-1 (48). Cultivation was carried out with an aim to gain cell suspension by using 5L culture bottle containing 1L medium and gas mixtures. The culture bottle was cultivated at the

shaking condition of 150 rpm for 48 hours. Cells were harvested after centrifuged at 6,000 × *g* for 15 min and washed with inorganic medium. Harvested cells were stored at -80ºC until use.

16s rRNA

16s rRNA analysis was performed with an aim to check whether the *H.thermophilus* transformant was polluted by other bacteria or not. *H.thermophilus* and *H.thermophilus* transformant were cultivated at 70°C under a gas phase of H_2:O_2:CO_2 (75:10:15, v/v) in a 500-mL vial with an autotrophic medium. In case of *H.thermophilus* transformant, *pspA* deleted *H.thermophilus*, 300 μM L-serine was added to autotrophic medium. DNA of harvested cells was purified using DNA purification Kit (Wizard Genomic DNA purification Kit, promega). PCR-amplified DNA was followed to amplify the 16s RNA genes using primers of B27F (5'-AGAGTTTGATCCTGGCT-3') and U1492R (5'-ACGGNTACCTTGTTACGACTT-3') (Weisburg et al. 1991). PCR fragment was purified via PCR clean up kit (Wizard SV gel and PCR clean-up sytem, Promega) after checking the 1.4 kbp single band of amplified gene by gel electrophoresis. Sequence of 16s RNA from *H.thermophilus* and *H.thermophilus* transformant was analyzed via 3130xg/Genetic Analyzer (Hitachi).

Growth of *H.thermophilus* mutant under various substrate conditions.

H.thermophilus TK-6 and *H.thermophilus* transformant (*pspA* gene deletion *H.thermophilus*: ΔA), were pre-cultivated at 70°C under a gas phase of H_2:O_2:CO_2 (75:10:15, v/v) for 1 - 2 days using 100 mL of vial containing 10 mL of autotrophic media. In case of ΔA, 300 μM L-serine was added to autotrophic medium. Harvested pre-culture was inoculated into 100 mL of vial containing 10 mL of autotrophic media with or without various amino acids and then incubated at 70°C under a gas phase of H_2:O_2:CO_2 (75:10:15, v/v) condition. OD_{540nm} was measured at regular interval.

Glycine and serine concentration measurement using HPLC

Reverse phase column HPLC was used to measure the concentration of glycine and serine within medium during the growth of *H.thermophilus* and ΔA. Samples were pre-treated according to phenylthiocarbamyl derivatization method and then applied to reverse phase column HPLC (Heinrikson RL and Meredith SC, 1984; Kameya M et al, 2007) as described below. Alanine (0.17 mM) was used as an internal standard.

Samples collected at regular time interval were dried under a vacuum, which was then dissolved in 10 μL of ethanol-water-triethylamine-phenylisothiocyanate (7:1:1:1) and incubated for 10 min at room temperature. Re-drying of phenyl-derivatized samples was carried out under a vacuum, which was mixed with 100 μL of 25 mM $NaPO_4$ (pH 6.5) and applied to a reverse-phase column (Inertsil ODS-3 [4.6 mm by 250 mm]; GL Science, Tokyo, Japan). Here, two kinds of buffer, 25 mM $NaPO_4$ (pH 6.5) and 70% methanol, were used to elute target amino acids. The eluted amino acids were monitored at 254 nm using an L-2400 UV detector (Hitachi, Tokyo, Japan).

ALAS enzyme activity

ALAS synthase (EC 2.3.1.37) activity was measured by the method described by Burnham (143). Three kinds of reaction mixture was prepared as follows. At first, enzyme substrate cocktail by combining 10 mL of 1.0 M glycine, 10 mL of 1.0 M succinate, 10 mL of 0.1 M $MgCl_2$, and 5mL of 1.0 M tris-HCl buffer. Secondly, enzyme control cocktail by combining 10 mL DI water, 10 mL of 1.0 M succinate, 10 mL of 0.1 M $MgCl_2$, and 5mL of 1.0 M tris-HCl buffer. Third, stock cofactor cocktail by combining 10 mL of 0.2M ATP, 8.75 mL of 0.01 M CoA, 6.75 mL of 0.01 M pyridoxal phosphate, and 10 mL of DI water.

Harvested *H.thermophilus* and ΔA were centrifuged at 10,000 × g for 10min. Pelletized cells were re-suspended using 10 mL of 50 mM potassium phosphate buffer (pH 7.0) and centrifuged at 10,000 × g for 10min. After second pelletization of cells, cells were

mixed by 2 mL of 50 mM potassium phosphate buffer (pH 7.0), which then cells were sonificated and preserved as cell-free extract (CFE) until use.

For each assay, enzyme mixtures were incubated at 37 °C for 20 min. Here, enzyme mixture was composed of 480 μL of DI H_2O, 350 μL of Control/Substrate cocktail, and 150 μL of cofactor cocktail. Subsequently, 20 μL of cell extract was added to initiate 2'nd enzyme reaction. After incubation at 70 °C for 20min, 300 μL sample was transferred to a 1.5 mL tube containing 150 μL of 10% trichloroacetic acid.

After centrifugation at 10,000 × g for 5min, 300 μL of each supernatant was conveyed to a glass tube involving 400 μL of 1.0M sodium acetate (pH 4.7). To do blank test, supernatant was substituted for D.W.(distilled water). 35 μL acetylacetone was added to 700 μL sample, which was incubated at 80 ºC for 15min. Following the incubation at room temperature for 5min, 700 μL of modified Ehrlich's reagent was added to sample and mixed. After 10minutes, each of reaction mixtures was measured at 556 nm. Here, Modified Ehrlich's reagent was prepared by 1.0 g of *para*-dimethyl-aminobenzaldehyde to 30mL of glacial acetic acid, 8mL of 60% perchloric acid and diluting to 50 ml with glacial acetic acid.

2.1.3 Discussion

***pspA* gene deletion serine auxotroph.**

H.thermophilus TK-6 is a obligate chemolithoautoroph that assimiliates CO_2 through the reductive tricarboxylic acid cycle (32). L-serine could be produced by PSP using $_L$-O-phosphoserine as a substrate or by SHMT using glycine as a substrate when *H.thermophilus* CFE was analyzed (1). Therefore, I formed a hypothesis that serine might be produced by SHMT using glycine as a substrate when *pspA* gene was deleted from *H.thermophilus*. It is noteworthy that PSP activity was performed not by PspB subunit but by PspA subunit, indicating that serine can not be produced by PspB subunit when *pspA* gene is disrupted.

However, transconjugants for *pspA* gene deletion had failed to grow on autotrophic medium, indicating *pspA* gene was essential in *H.thermophilus* and L-serine produced by SHMT was too small for ΔA to grow. Thus, serine biosynthesis pathway from glycine to serine via SHMT might be agreeable to disregard.

On the other hand, transconjugants for *pspA* gene deletion (ΔA) could grow on the autotrophic medium containing additional L-serine. External L-serine within medium was decrease as ΔA grows. Furthermore, ΔA could grow only in the presence of serine when all amino acids related to serine metabolic pathway were injected to medium. Therefore, *pspA* gene deletion serine auxotroph was clarified from *H.thermophilus.* Furthermore, this result also revealed that obligate chemolitho autotroph can also be changed into mixotroph.

Considering the serine catabolic pathway, the formation of *pspA* gene deletion serine auxotroph would clarify that the pathway of PSP, de novo serine biosynthesis, was the sole major serine anabolic pathway *in vivo.* Serine synthesis starts from the glycolytic intermediate 3-phosphoglycerate (3-PG) and this pathway was annotated as a de novo serine biosynthesis (144)

Serine produced from phosphoserine via PSP could be degraded for L-tryptophan, glycine, and one carbon in *H.thermophilus* (Fig. 2-1). Based on KEGG pathway and homology search via protein BLAST search, *H.thermophilus* didn't have tryptophan metabolism, suggesting that L-tryptophan existed as an end of product.

Therefore, fate of serine could be expected as follows, one carbon metabolism for cleaving serine, glycine catabolic pathway or accumulation, and L-tryptophan accumulation. Firstly, I had focused on the one carbon metabolism as a serine catabolic pathway.

One carbon metabolism not by glycine but by serine in *H.thermophilus*

It has been known that there are totally four pathway for one carbon metabolism (Fig. 2-3A). At first, de novo serine biosynthesis pathway of reaction 9-8, in which serine

produced from PSR (3P-serine) is cleaved two carbon of glycine and one carbon. Here, one carbon of serine feed into one carbon metabolism via THF.

Second, direct carbon fixation of reaction 1-4, which is called Wood-Ljungdahl pathway. Although *H.thermphilus* have formate dehydrogenase genes of reaction 1, it don't have the ATP-dependent formyl THF synthase of reaction 2, which was clarified using KEGG pathway and homology searching of protein BLAST. These results suggested that Wood-Ljungdahl pathway may not exist in *H.thermophilu.* It has been reported that some of *Aquificales* shows the reaction 1-7 sequence missing only the ATP-dependant formyl-THF synthase of reaction 2 (8).

Third, H_4MPT-methanofunran system which converts oxidation state of one-carbon units have been found in both bacterial clades and archaeal but this pathway have based on some hypothesis and several evidences argue against this pathway (8, 145, 146). In addition, homolog of these genes were not found in *H.thermophilus* through KEGG and protein BLAST searching.

Lastly, one carbon unit via glycine cleavage system. The glycine cleavage system is a multienzyme complex that catalyzes the reversible oxidation of glycine to 5,10-methylene THF, ammonia, and CO_2 (147). The complex consists of four proteins: P-protein, H-protein, T-protein, and L-protein (148). However, *H.thermophilus* was absent of glycine cleavage system showing in glycine cycle of reaction 5-7 (Fig. 2-3A). This was because the enzyme activity of glycine cleavage system (GCS) was not detected and lack of L-protein homolog from *H.thermophilus* (3). Among archaea the absence of glycine cleavage system or glycine cycle occurs, the majority of these case are found among methanogens (149). Furthermore, a number of genera of *Aquificales* seem to lack the activity and were insufficient at least one homolog of glycine cleavage system proteins as a results of annotation of KEGG (3).

Enzymatic cleavage of glycine in a glycine cleavage system produces ammonia, carbon dioxide and a carbon unit for the methylation of THF (148, 150). The carbon units need for

one carbon metabolism can be usually produced by de novo serine biosynthesis pathway or glycine cleavage system, in which glycine can be also generated from many sources, including aldol cleavage, glyoxylate, choline, betain, dimethylglycine and sarcosine, through a series of reactions involving demethylation (151). It was noteworthy that recent stable isotope tracer studies in human subjects demonstrate that GCS account for nearly 40% of overall glycine flux and that the 5,10-methylene-THF produced from glycine catabolism makes major contributions to cytoplasmic THF-dependent purine and thymidylate biosynthesis (152).

However, considering the results of *pspA* gene deletion serine auxotroph and the absence of glycine cleavage system in *H.thermophilus*, input to one carbon metabolism within *H.thermophilus* was expected to be just one source "serine"(Fig. 2-3B). Therefore, it was strongly suggested that one carbon metabolism via de novo serine biosynthesis pathway looks like the sole pathway within *H.thermphilus* (Fig. 2-3B). In this context, transcriptome analysis also support this finding, which will be described in next section.

Catabolic pathway for glycine

As glycine cleavage system was not detected in *H.thermophilus*, homology search and enzyme activity test was performed with an aim to find glycine catabolic pathway. All genes related to glycine catabolic pathway of KEGG pathway were applied to protein BLAST search. Although the homolog of ALAS was found in *H.thermophilu* (HT_1352, identity = 34%, query coverage = 92%), the enzyme activity was too low, indicating that glycine catabolic pathway through ALAS might not operate well. Moreover, glycine dehydrogenase activity was also not detected, in which glycine was used as substrate and glyoxylate was produced.

With the hypothesis that glycine may secreted in the condition of glycine accumulation, glycine secretion was investigated. Extracellular glycine concentration was 8.2 μM when TK-6 reached stationary phase. Considering the serine uptake of ΔA over 300 μM of L-serine to grow, relatively very small quantity of glycine was secreted from *H.thermophilus*.

Therefore, the possibility of glycine secretion via accumulation was also decreased. In addition, it looks likely that glycine accumulation within *H.thermophilus* may not occur since *H.thermophilus* didn't show significant growth inhibition under autotrophic medium containing glycine. It is noteworthy that accumulated glycine inhibit the growth of strains (153, 154).

Even if *H.thermophilu* is an obligate chemolithoautotroph, *pspA* gene deletion serine auxotroph was gained in this study and this strain can also assimilate several organic compound such as glyoxylate, acetate, pyruvate, fumarate, and etc. (3, 155). Therefore, it looks like that glycine catabolic pathway might be preserved in *H.thermophilus.* Serine isotope labelling experiment using ΔA is suggested a candidate for verifying glycine catabolic pathway.

Based on the possibility of tryptophan accumulation, it will be described using transcriptome analysis in next section.

LIV system as a serine transporter

The mutual inhibition analysis between serine and designed amino acid had verified that leucine, isoleucine, and valine (LIV) system could also uptake L-serine. When valine or leucine was added to the autotrophic medium containing serine, the growth of ΔA was strongly inhibited. In addition, the homolog of serine transport gene, which was confirmed by homolog search via protein BLAST searching and KEGG pathway, was not found in *H. thermophilus*. These results indicate that L-serine share this LIV system with leucine, isoleucine, and valine.

Considering all serine transporters, three types of serine transporter have been known. At first, a major serine-threonine transport system is an Na^+ coupled symporter (156). Secondly, H^+-coupled symporter induced by leucine (157). A third system, the leucine-isoleucine-valine transport system, which was known as perhaps (158). Although L-serine uptake by LIV system has long been presumed to uptake serine after speculation of Robbins *et al*, there were no clear experimental evidence (157, 159). Robbins *et al.*

deduced that at least part of the L-serine uptake is by the LIV transport system, but it is also possible that L-serine inhibits the activity without itself being transported by this system (158). It seems likely that it might be difficult to measure L-serine uptake rate because they used heterotrophic bacteria such as *E.coli* containing at least two serine transporters. However, *pspA* gene deletion serine auxotroph had an only LIV transporter among amino acid transporters and needed autotrophic medium containing serine to grow. Thus, the fact that L-serine was transported via LIV system was clearly demonstrated. As per our knowledge, this study may be the first clear experimental results for L-serine uptake via LIV system.

NaCl enhanced the initial growth rate of ΔA. It has been known that Na^+ coupled serine symporter uptake serine well (160). As *H.thermophilus* lacks the Na^+ coupled serine symporter homologous, it looks likely difficult to presume the influence on LIV system by NaCl. Further study is need to clarify these phenomena via gene manipulation such as double mutants.

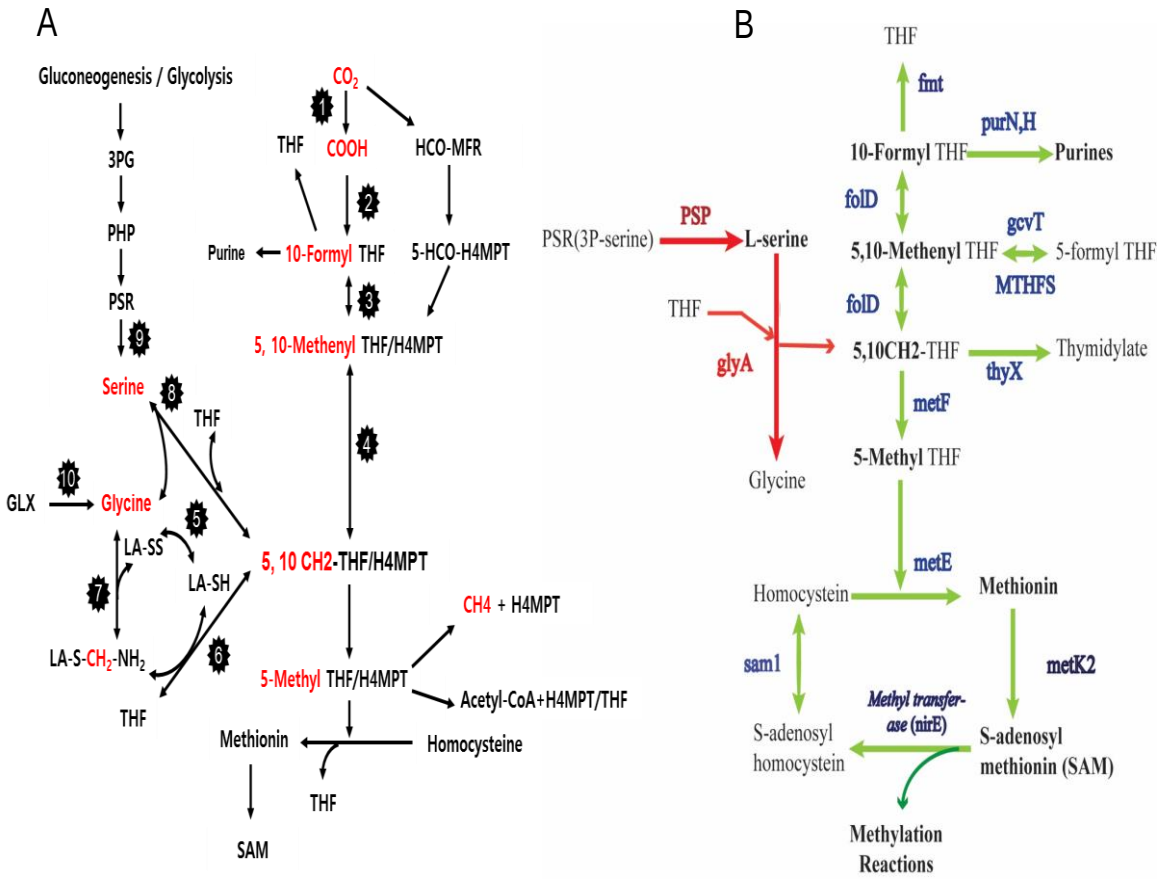

Fig. 2-3 General C1 metabolism and Scheme of C1 metabolism of *H.thermophilus*. (A) summary of one carbon metabolism. Reactions 1-8 represent the route to glycine and serine. In organism that use the Wood-Ljungdahl pathway as the route for carbon-fixation, the direct reduction of CO_2 also end in the synthesis of acetyl-CoA, many organism with absent step employ the preceding parts of the pathway. Reactions 9-8 are subsequently cleaved to supply C_1 metabolism. Reaction 10 constitutes the glyoxylate pathway. (B) Expected C_1 pathway from *H.thermphilus.* Reaction 9-8 of (A) was expected. Genes related to C_1 pathway was confirmed using KEGG pathway and homolog search. Abbreviation: MFR, methanofuran; H_4MPT, tetrahydromethanopterin; THF, tetrahydrofolate; LA, lipoic acid; PSR, phosphoserine; PHP, 3-phosphohydroxypuruvate; 3PG, 3-phosphoglycerate; GLX, glyoxylate; PSP, phosphoserine phosphatase; glyA, SHMT, serine hydroxymethyltransferase; transformylase (fmt), phosphoribosylglycinamide formyltransferase (purN), methylenetetrahydrofolate dehydrogenase (fold), aminomethyltransferase (gcvT), 5-formyltetrahydrofolate cyclo-ligase (MTHFS), thymidylate synthase (thyX), 5,10-methylenetetrahydrofolate reductase (metF), 5-methyltetrahydropteroyltriglutamate (metE), S-adenosylmethionine synthetase (metK), uroporphyrin-III C-methyltransferase (nirE), and S-adenosylhomocysteine hydrolase (sam1). Modified Fig (A) was cited from Rogier *el. al* (8).

2.2 Physiology of PspA

2.2.1 Introduction

Thiols of iPSPs were identified to make intermolecular disulfide bond, which increased the thermostability of homo and heterodimer, and also showed reversible disulfide bond formation in this study. Considering the physiological condition of *H.thermophilus*, the strong reduced condition under the -300 mV (ORP) was expected due to the presence of reductive TCA cycle. It has been also reported that bacterial cytoplasm has been described as a reducing environment with a proposed redox potential value of -220 to -240 mV (161).

As described in previous section lots of intracellular disulfide bonds were detected *in vivo* and disulfide bond of iPSPs formed over -58 mV (ORP) in *vitro* was also detected *in H.thermophilus* from this study (chapter 1.2). Considering *in vivo*, *H.thermophilus* had several genes related with disulfide bond cleavage and formation such as thioredoxin (Trx) and protein disulfide bond isomerase (PDI) (10). It has been known that thioredoxin (Trx) and protein disulfide bond isomerase (PDI) participate in intracellular disulfide bond cleavage and formation process (162). Therefore, I presumed that thiols of iPSPs forming intermolecular disulfide bond might have another function in redox condition. This is because many proteins and enzymes have been known to contain cysteine residues which have a sulfhydryl group in their side chain and the labile proton makes it a chemical hot spot for a wide variety of biochemical interaction such as easily reversible site for oxidation or reduction chemistry (19).

On the other hand, as a serine catabolic pathway, although one carbon metabolism not by glycine but by serine were identified via *pspA* gene deletion serine auxotroph in this study, one carbon flow within *H.thermophilus*, and the possibility of tryptophan accumulation has not been clarified. Thus, with a prospect for the physiology of PspA, transcriptome analysis was performed to check the *pspA* related genes.

2.2.2 Materials and Methods

Culture of *H.thermophilus* TK-6 and *pspA* gene deletion serine auxotroph TK-6.

H.thermophilus TK-6 (WT) and *pspA* gene deletion serine auxotroph *H.themophilus* (ΔA) were used as a bacterial strain. ΔA and WT were cultivated at 70 °C under gas phase of H_2:O_2:CO_2 (75:10:15, v/v) in a 100-mL vial containing autotrophic medium with or without 300 μM L-serine, respectively. The strain, ΔA, was generated as described in chapter 2.1.2 Materials and Methods.

Growth of *H.thermophilus* and ΔA under environment stress conditions.

H.thermophilus TK-6 and ΔA were pre-cultivated under 10 mL of autotrophic medium without or with 300 μM L-serine within 100 mL vial at 70°C for 24 hours, respectively. The pre-cultivated ones were mixed with fresh medium to adjust 0.1 of optical density (OD_{540nm}). With 10mL of designed medium (OD_{540nm} = 0.1), pre-culture was injected to 100 mL of vial and cultivated under anaerobic (N_2:H_2:O_2:CO_2 =10:75:0:15, v/v, NO_3 as electron acceptor), and aerobic condition (H_2:O_2:CO_2 =75:10:15, v/v) at 70 °C, 80 °C, and 85 °C, respectively. Optical density at 540nm was measured at intervals of 3hr.

RNA extractions.

H. thermophilus was grown under 100-mL vial with 10mL of inorganic medium Table 1-1) and gas mixtures of H_2:O_2:CO_2 (75:10:15, v/v), respectively. On the other hand, *pspA* gene deleted *H. thermophilus* was grown under 100-mL vial with 10mL of inorganic medium containing 300 μM of L-serine and gas mixtures of H_2:O_2:CO_2 (75:10:15, v/v).

For wild type and ΔA, 10 mL of the culture was mixed with 10 ml of RNA protect (Quiagen, Hilden, Germany) when the optical density (OD) at 540nm reached approximately 0.38±0.01 for ΔA and 0.43±0.01 for wild type *H.thermophilus* to stabilize total RNA. Cells of ΔA and strain *H.thermophilus* were collected by centrifugation for 10 min. at 3,000 x g.

RNA was extracted from the cell pellet by a hot-phenol method, as described below. The cell pellet was resuspended in 800 µl of 1.0 mg /ml lysozyme (TE pH 8.0). Then, the suspension was mixed with 80 µl of the 10% SDS and incubated at 65^{o}C for one min, which was called lysis sol.

Then, 88 µl of 1M Na- acetate (pH 5.2) and 1 mL of Water Saturated Phenol (pH 7.0) were added to the lysis solution. The mixtures were incubated at 65^{o}C for 7 min. with 7 times of inversion. After incubation, the tubes were centrifuged at 13,000 x g for 10 minutes at 4^{o}C. The upper transparent layer was mixed with 1mL of PCI, phenol/chloroform/isoamylalcohol (25∶24∶1), and centrifuged at 13,000 × g for 10 min at 4°C. The upper layer was then mixed with 1mL of chloroform/isoamylalcohol (24∶1). After centrifugation at 13,000 x g for 5 minutes at 4^{o}C, the upper layer was mixed with a 1/10 volume of 3M Na - acetate (pH 5.2), 1/10 volume of 1 mM EDTA, and 2 folds of cold ethanol. After incubation at -80°C for overnight, the solution was centrifuged at 14,000 x g for 25 min. at 4°C and the supernatant was removed. The pellet was washed twice by 1mL of 80% cold ethanol at 14,000 x g for 5min. The supernatant, ethanol, was removed from the test tube. The pellet dried completely under air condition was resuspended in RNase-free water. The solution was mixed with 10µl of 10×DNase buffer and 10µl of DNase and incubated at 37°C for 1hour with an aim to

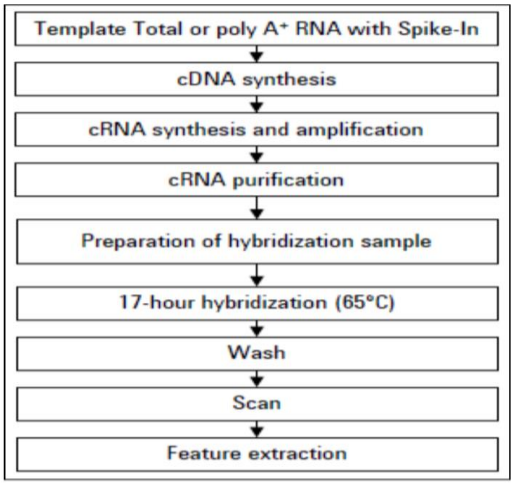

Fig. 2-4 Workflow of *H.thermophilu* and ΔA preparation and array processing

remove DNA.

For cleanup RNA, the sample was purified with an RNeasy Mini kit (Qiagen) according to the manufacturer's instruction. DNase treatment for remove DNA and RNA cleanup was carried out again. Eluted total RNA sample was stored at -80 °C.

DNA contamination, A_{260}/A_{280}, and RNA integrity number were checked. Firstly, PCR amplification was performed to check the DNA contamination. Partial fragment of DNA genome, HT1098 of *H.thermophilus* (forE, 225bp), was amplified by using 0.5μL of the RAN sample as template, *H.thermophilus* chromosome DNA as positive control, and RNase-free waster a negative control. Secondly, A_{260}/A_{280} absorbance was measured to check the contamination by protein or a reagent such as phenol. Lastly, the quality of total RNA was checked before proceeding to Microarray experiment. RIN score for the quality of total RNA was measured by using 2100 Bioanalyzer equipment (Agilent Technologies, Inc.). RNA samples satisfying above 3 condition were applied to Microarray experiment.

Microarray Design, experiments, and data analysis.

The design of microarray with 8 × 15K for *H.thermophilus* was carried out according to manufacturer's instruction (Agilent technology, USA) based on genome sequence. Microarray was organized by one replicate probe set of *H.thermophilus* genes and 10 replicates probe set of reference genes. The information of probe sets was as follows. One replicate probe set with 132,517 probes analyzed all *H.thermophilus* genomes and 10 replicates probe set with 1,057 probes were used as a control probes by measuring 15 genes related to *H.thermophilus* respiration with an aim to clarify no contamination under hybridization. The triplicate RNA samples extracted from wild type, and ΔA were applied for microarray analysis. Total RNA from samples was continuously converted to double-stranded cDNA and cRNA.

Following the conversion of cRNA, Labelling, amplifying, and purifying of cRNA were performed according to the protocol of one-color microarray-based gene expression analysis

(Agilent Technologies). After quantifying the cRNA, 600 ng of cRNA samples applied to hybridization and washing steps according to the protocol of Agilent technology. After washing the microarray slide, it was dried at room temperature for 5 min. Scanning of the microarray slide was carried out by surescan microarray scanner (Agilent Technologies). Agilent Feature Extraction Software 10.7 was used to extract the signal intensities and processing of the data.

Expression data from Agilent Feature Extraction Software 10.7 were normalized by GeneSpring GX version 13.0 software with robust multichip average algorithm (163, 164). The mean signal value of each probe set and their relative fold changes based on the gene expression level of wild type and ΔA were calculated by using software GeneSpring GX version 13.0.

Table 2-4 genes of making reference probes set

	TK-6 tag	Gene		TK-6 tag	Gene		TK-6 tag	Gene
1	HTH1553	*porA*	6	HTH0455	hoxL	11	HTH0154	cyoA
2	HTH1093	*korA*	7	HTH0095	hynL	12	HTH1717	narG
3	HTH1095	*forA*	8	HTH1479	coxA1	13	HTH0150	nirS
4	HTH1013	*hupL1*	9	HTH1486	coxA2	14	HTH0283	norB
5	HTH1005	*hupL2*	10	HTH0944	coxA3	15	HTH0163	nosZ

2.2.3 Discussion

Physiology and transcriptional characteristics of PspA under oxidative stress

Although *H. thermophilus* could grow well under 30% O_2 condition, ΔA couldn't grow under 30% O_2 condition until 40 hours, suggesting that *pspA* gene may be essential genes in higher oxidative stress condition and other genes couldn't substitute for the function of PspA subunit for the aerobic growth of ΔA under 30% O_2 condition.

Considering the PspA function, two kinds of function has been known until now in this study and previous study by Chiba *et al*(3). Firstly, characteristics of reactive thiol forming intermolecular disulfide bond. Secondly, enzymatic activity producing serine and phosphate. Therefore, I focused on the function of thiol forming disulfide bond because thiols has been known well to react with intracellular ROS (165).

As reactive oxygen species (ROS) are toxic at high levels in the cells, cells have developed mechanisms to cope with $O_2^{\cdot -}$ production or ROS, such as conversion to hydrogenperoxide (H_2O_2) by superoxide dismutase(SOD) (166). H_2O_2 can then be removed through enzymatic reactions and thiol-systems (glutathi-one peroxidase (Gpx), and thioredoxin) (167). Although PspA subunit had reactive thiol in cys198th, it had not been clarified whether thiol of PspA sufficiently react with ROS or not. Therefore, transcriptome analysis was performed with aim to find the clues for the function of PspA, especially function for thiols and serine, product of PspA, related metabolism by comparing *H.thermophilus* and ΔA.

The singly-color array format of Agilent Technologies was selected for microarray. It has been known that Agilent Technologies (Santa Clara, CA, USA) has developed a miRNA profiling platform that provides both sequence and size discrimination for mature miRNA and this system generates results that are highly correlated with qPCR results for miRNA profiling (168, 169). Transcriptome analysis was monitored using WT and ΔA incubated under 10% O_2 condition.

Based on transcriptome analysis, among detoxifying genes of *H.thermophilu,* superoxide dismutase (*sodC*) and alkyl hydroperoxide reductase (*AhpC*) were upregulated in ΔA (2.2 to 2.3 fold change $P<0.05$) on the 10% O_2 condition. This transcriptome analysis showed that *Ahp C* and *sodC* was upregulated in the presence of ROS, suggesting that both of genes may compensate the lack of ΔA.

Most oxidative thiol modifications forming disulfide bond are reduced by the thioredoxin or glutaredoxin systems (170). It is noteworthy that PspA-PspA was linked by intermolecular disulfide bond and *H.thermophilu* contains not glutaredoxin but thioredoxin. At the core of thioredoxin systems, thioredoxin (Trx) use direct thiol–disulfide exchange reactions to reduce oxidized protein thiols (171). Therefore, expression level of Trx was monitored with the hypothesis that if the total amount of disulfide bond made by PspA subunit was relatively high in *H.thermophilus,* gene expression of Trx might be significantly changed in ΔA because there were no disulfide bond made by PspA. On the other hand, as PspB-PspB linked by disulfide bond was not detected in *H.thermophilus*, it was agreeable to disregard.

As my expectation, the transcriptome of some of thioredoxin (Trx) showed significant down regulation, indicating that the absence of disulfide bond made by PspA markedly affect the expression of Trx gene (trxA1A2B1, -4.5 to -6.6 fold change, $P<0.05$).

To sum up, the results of inhibited growth of ΔA under 20% and 30% O_2 condition, and transcriptome analysis of both detoxifying genes and thioredoxin suggested that PspA might have a meaningful role as a direct or indirect antioxidant via making disulfide bond.

Transport and sulfur related genes

In order to survive, Δn should take in external serine through LIV transporter system proposed in this study (chapter 2.1.3). LIV system, which has been known to uptake valine, isoleucine, leucine, and presumed serine (158, 172) was firstly clarified to uptake serine via experimental results in this study. Additional transcriptional levels of genes related with LIV system between WT and ΔA were also monitored.

It was of interest that Liv K, H, M, G, and F serine transporter showed the same tendency of down-regulation in ΔA. Namely, they didn't up-regulated in ΔA. It can be suspected that ΔA decrease the L-serine uptake rate via Liv system as ΔA may need time to degrade introduced external serine. Thus, it looks likely that Liv system for serine transport may be a low-affinity transporter. Although it was need to measure the transport activity to confirm Liv system for serine uptake as a low-affinity transporter, transcriptome analysis, I think, also supported the possibility of low-affinity of Liv system for serine uptake. In this context, it has been reported that based on high concentration of substrate, downregulation of Iinsulin receptor mechanism occurs when there are elevated levels of the hormone insulin in the blood (173).

To sum up the results of *pspA* serine auxotroph, inhibition test, and transcriptome analysis for serine transport, to my knowledge, this was first clear evidence for serine uptake via LIV system. This is because even though, LIV system for serine uptake had been presumed by Robbins *et al.*(158) and other researchers have cited his presumption, there was no clear evidence until now.

On the other hand, taken into significant fold change consideration in genes between WT and ΔA, the most remarkable fold change was detected from molybdate transport related genes (-23.2 to -55.7 fold changes, $P<0.05$), indicating molybdate uptake was markedly affected in ΔA. Considering the relationship between molybdate and PSP, it looks likely that there might be no direct relationship because PSP is metal independent protein.

Other candidates for significant down-regulation of molybdate related genes might be from external serine or function of thiol. This is because L-serine as an one carbon source, is connected to homocysteine as a sulfur source amino acid within one carbon metabolism and molybdum oxidation state is influenced by redox condition (174) However, when it comes to molybdate uptake, it has been usually known that sulfate (SO_4^{2-}) competitively inhibit MO_4^{2-} uptake, whereas thiosulfate ($S_2O_3^{2-}$) have no inhibitory effect (175). This is because both molybdate and sulfate have similar chemical properties (176).

The expression levels of sulfate related genes were monitored via transcriptome analysis. Interestingly, sulfate adenyl transferase (*sat*) using sulfate as substrate was markedly induced (16.6 fold change, $P<0.05$) whereas sulfate uptake gene (*sulP*) was down-regulated and most of other genes for producing sulfate showed same tendency of down regulation, suggesting that sulfate related genes were also markedly affected in ΔA.

In addition, sulfur metabolic pathway might be assumed to be connected with one carbon metabolism by a homocysteine desulfhydrase (HT_1157) producing sulfide from homocysteine in one carbon metabolism. Although the clues for the significant down-regulation of molybdate uptake genes was presumed, another experiments such as double mutants and enzyme activity detection may need to clarify it. Even if the relationship between molybdate related genes and sulfur related genes was not verified this study, it was revealed that metabolism related sulfate or molybdate markedly affected in ΔA.

Gene expression related to one carbon metabolism

As described in chapter 2.1.4 (Fig. 2-3B), one carbon metabolism not by glycine but by serine was proposed via *pspA* gene deletion serine auxotroph and the absence of glycine cleavage system in *H.thermophilus.* Additional transcriptome analysis for one carbon metabolism was also in line with proposed one carbon metabolism by serine in *H.thermophilus.*

All of expressed genes related to one carbon flow showed the same tendency of down-regulation in ΔA, which was consistent with down-regulation tendency of Liv system genes for serine uptake. Therefore, my previous speculation for low affinity Liv system that ΔA decrease the L-serine uptake rate via Liv system as ΔA may need time to degrade introduced external serine might be agreeable. As described, downregulation of Iinsulin receptor mechanism occurs when there are elevated levels of insulin as a substrate (173). Therefore, as far as I know, it looks likely that one carbon metabolism not by glycine but by serine was revealed for the first time from *H.thermophilus*.

Based on the physiology of *H.thermophilus* TK-6, it has been known to have primitive metabolic features such as reverse TCA cycle (177). I presumed that one carbon metabolism not by glycine but by serine may be also one of primitive metabolic features. This was because a number of genera of *Aquificales* seem to lack the activity and were insufficient at least one homolog of glycine cleavage system proteins as a results of annotation of KEGG (3).

This one carbon flow pathway via de novo serine synthetic pathway from 3-phosphoglycerate to phosphoserine and serine has been studied extensively with respect to cellular proliferation and in particular its involvement in neoplastic cellular transformation with an aim to know how to control tumor cell (178).

As serine hydroxymethyltransferase (SHMT) produces major one carbon units and gycine for the de novo biosynthesis of purines and of one carbon units for the metylation of dUMP to form dTMR, it is a potential target for chemotherapeutic intervention against cancer, although no clinically effective inhibitors of this enzyme are currently available (179). 3-phosphoglycerate dehydrogenase (PGDH) has been recently reported that PGDH suppression does not affect intracellular serine levels and PSP is the rate-limiting enzyme of this pathway (180, 181).

One carbon of L-serine transported via THF seemed to go to two directions. One of them may go to purine through 5,10-CH_2THF, 5,10-Methenyl THF, 10 formyl THF, and Purine. Another pathway may go to biological methylations via 5-Methyl THF. Methionine synthase (metK) in biological methylations is also a potential target for controlling cell proliferation, because inhibition of this enzyme is expected to inhibit nucleotide biosynthesis in cells (179).

Although SHMT, PGDH, and metK have been studied for cell proliferation control, I presumed that PSP may be relatively good candidate for controlling cell proliferation. This is because PSP has been known rate-limiting enzyme in serine synthesis pathway (181) and it was revealed that *pspA* gene was essential in *H.thermophilus* in this study. Therefore, discovery of proper inhibitor for successful inhibition of PSP will give clue for how to

control the cell proliferation. In this context, *H.thermophilus*, A-A (iPSP1), and ΔA will be the best materials for searching how to control cell proliferation.

2.3 Physiology of PspB

2.3.1 Introduction

PspB subunit existed as a heterodimeric protein linking to PspA subunit via intermolecular disulfide bond and the dimeric form of PspB-PspB was not detected from *H.thermophilus* as described in chapter 1.2.3. On the other hand, It had been detected that the higher ratio of heterodimeric iPSP2 existed in *H.thermophilus* than homodimeric iPSP1 from this study (iPSP1 : iPSP2 = 35 % : 65 %), even though PspB subunit didn't have enzyme activity. Additionally, PspA subunit was more inclined to link to PspB subunit than PspA subunit as described. Heterodimeric A-B (PspA-PspB) was suggested to be the first identification of dPGM-related protein forming a heterodimer with subunit displaying distinct catalytic properties (1). Thus, PspB subunit was presumed as a client protein to make disulfide bond due to the presence of reactive thiols. *pspB* homologous was found in the genomes of all *Aquificaceae* and *Hydrogenothermaceae* species and Cys 197 of ht PspB were also found in their homologous. Although PSP activity was not detected from PspB subunit in the previous and this study, the function of PspB subunit was suspected to be important *in vivo*.

In order to find the unknown function of *pspB*, physiology test and transcriptome analysis using *pspB* gene deletion *H.thermophilus* was planned and carried out.

Δ

2.3.2 Materials and methods

Bacterial strain and construction of plasmid for homologous recombination

Primers were designed with product size 1.1 ± 0.1 kbp using *H.thermophilus* genome information and the binding site of primers was shown in dotted line of the construction scheme of gene deletion (Fig. 2-5). The sequence of primers used to PCR was shown in Table 2-5 and Table 2-6, in which small letter of sequence was denoted as the restriction site. To gain chromosomal DNA, *H. thermophilus* TK-6 was cultivated at 70°C under a gas phase of H_2:O_2:CO_2 (75:10:15, v/v) in a 500-mL vial with an autotrophic medium as shown Table 1-1 (48). Subsequently, DNA extract was performed. PCR was carried out by using Prime STAR HS DNA Polymearase (Takara) and PCR fragment was clarified by gel electrophoresis.

Purified PCR fragment was inserted into pEX 18 via enzyme restriction and ligation. Plasmids constructed by ligation were transformed into *E.coli.* Following incubation was performed at 37 °C for overnight. Here, *Escherichia coli* strain JM109 were used as cloning host for pEX 18, which was used for disruption of the *pspA* gene by homologous recombination. In case of need, antibiotics were used with the concentration of 25 μg mL^{-1} kanamycine and 100 μg mL^{-1} ampicillin for *E.coli* and 500 μg mL^{-1} kanamycine for *H.thermophilus*

The position of deleted genes was substituted by marker gene, htk, which was highly thermostable kanamycin nucleotidiyltransferase gene fused with promotor region of *H.thermophilu prod* gene and has 1.3kbp of size. This process was also carried out via enzyme restriction, ligation, and transformation. Transformed marker gene was also clarified by gel electrophoresis.

Homologous recombination of *H.thermophilus*

H. thermophilus TK-6 was cultivated at 70°C under a gas phase of H_2:O_2:CO_2 (75:10:15, v/v) in a 100-ml vial with a 10 mL of autotrophic medium. 1.5 mL of TK-6 was gathered and centrifuged at 20,000 ×g for 3 min when OD_{540nm} was reached 0.5 - 0.8. Cell pellet of TK-6 was washed by miliQ and repelleted by centrifugation at 20,000 ×g for 3min. Washed cell was resuspended in 500 μL of 10% glycerol, subjected to centrifugation at 20,000×g for 2min. Supernatant was removed and cell pellet was resuspended by additional 50 μL of 10% glycerol and preserved on ice for using as a competent cell.

Electroporation was performed by using 10 μL of constructed plasmid, competent cell, and 300 μL of autotrophic medium. Following incubation on solid culture, which containing autotrophic medium, 10 μg mL^{-1} of $CuSO_4 \cdot 5H_2O$, 300 μM of L-serine, 500 μg mL^{-1} kanamycine, and GELRITE (Wako Pure Chemical Industries, Osaka, Japan). The plates were settled on a desiccator and incubated at 70°C under a gas phase of H_2:O_2:CO_2 (75:10:15, v/v) for 3 – 7 days and the gas was changed every day. A colony expressed on a solid medium was transferred into 2mL of liquid autotropic medium containing 500 μL^{-1} kanamycine in a test tube with butyl cap and gas phase of H_2:O_2:CO_2 (75:10:15, v/v). Following incubation was carried out for 2-3 days until the OD_{540nm} was over 0.7.

The disrupted gene was confirmed by measuring 16s RNA, and length of PCR-amplified DNA fragments of marker gene (htk) and constructed plasmid.

Table 2-5 Primers used for clone antibiotics resistant marker genes

Primer	Sequence	RE site
htk_kpn_F	5'-AAAGGTACCACATTCGGTGAGAAGCTACAGG-3'	KpnI
htk_kpn_R	5'-AAAGGTACCGGTCATCGTTCAAAATGGTATG -3'	KpnI

Table 2-6 Primers used to construct plasmids for gene disruption.

Disruptant	Primer	Sequence	Marker
ΔPspB	PspB_Up_F_ SaC I	GCTgagctcGTTTTGCCTACACC	htk-KpnI
	PspB_Up_R_ Kpn I	TAAggtaccTTTGCCACACAAGAC	
	PspB_Down_F_Kpn I	GAGggtaccGCATATCACTTATGG	
	PspB_Down_R_BamH I	AGCggatccTTTACAGAAGAGGAG	

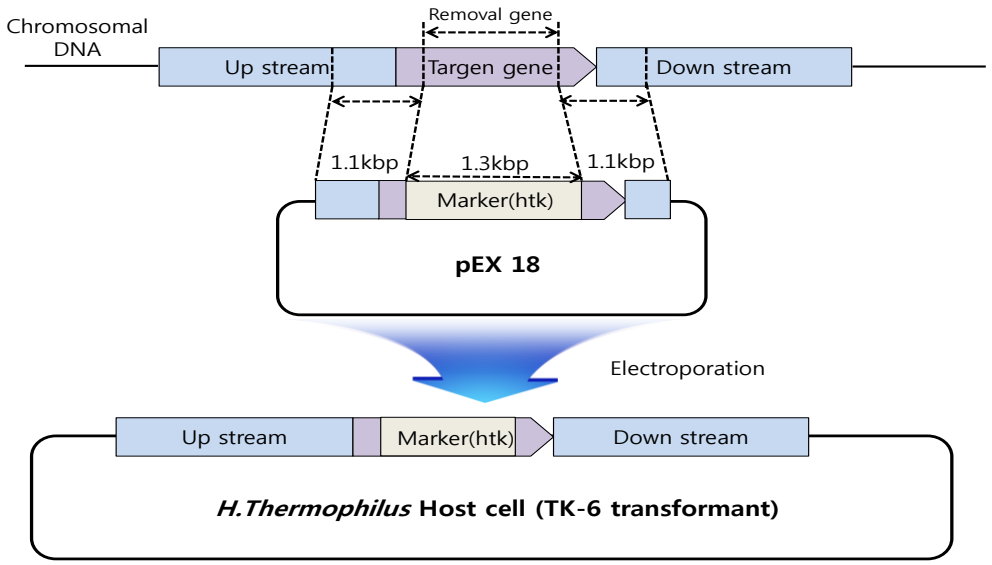

Fig. 2-5 Scheme of *pspB* gene deletion for homologous recombination of *H.thermophilus*.

16s rRNA

16s rRNA was performed with an aim to check whether ΔpsB was polluted or not by other bacteria. TK-6 and TK-6 transformants were cultivated at 70°C under a gas phase of H_2:O_2:CO_2 (75:10:15, v/v) in a 500-mL vial with an autotrophic medium. DNA of harvested cells was purified using DNA purification Kit (Wizard Genomic DNA purification Kit, promega). PCR-amplified DNA was followed to amplify the 16s RNA genes using primers of B27F (5'-AGAGTTTGATCCTGGCT-3') and U1492R (5'-ACGGNTACCTTGTTACGACTT-3') (Weisburg et al. 1991). PCR fragment was purified via PCR clean up kit (Wizard SV gel and PCR clean-up sytem, Promega) after checking the 1.4 kbp single band of amplified gene by gel electrophoresis. Sequence of 16s RNA from TK-6 and TK-6 transformants was analyzed via 3130xg/Genetic Analyzer (Hitachi).

Growth of *H.thermophilus* mutants under different oxidative conditions.

H.thermophilus TK-6 and ΔB were pre-cultivated under 10 mL of autotrophic media within 100 mL vial at 70°C for 24 hours. The pre-culture was mixed with fresh autotrophic medium to adjust 0.1 of optical density (OD_{540nm}). With 10mL of inorganic medium and 0.1 of OD_{540nm}, Adjusted pre-culture was injected to 100 mL of vial and cultivated under anaerobic, micro aerobic, and aerobic condition at 70 °C, 80 °C, and 85 °C, respectively. Optical density at 540nm was measured at three hours intervals.

Transcriptome analysis (RNA extraction).

H. thermophiles TK-6 and *pspB* gene deleted *H. thermophiles* TK-6 was grown under 100-mL vial with 10mL of inorganic medium and gas mixtures of H_2:O_2:CO_2 (75:10:15, v/v), respectively.

For wild types and mutants, 10 mL of the culture was mixed with 10 ml of RNA protect (Quiagen, Hilden, Germany) when the optical density (OD) at 540 nm reached approximately 0.43 ± 0.01 for wild type and ΔB to stabilize total RNA. Cells of strain TK-6

were collected by centrifugation for 10 minutes at 3,000 x g. RNA was extracted from the cell pellet as describe in same method in chapter 2.2.2 by using a hot-phenol method.

DNA contamination, A_{260}/A_{280}, and RNA integrity number was checked. At first, PCR amplification was performed to check the DNA contamination. Partial fragment of DNA genome, HT1098 of TK-6 (forE, 225bp), was amplified by using 0.5μL of the RAN samples as template, TK-6 chromosome DNA as positive control, and RNase-free waster a negative control. Secondly, A_{260}/A_{280} absorbance was measured to check the contamination by protein or a reagent such as phenol. Lastly, the quality of total RNA was checked before proceeding to Microarray experiment. RIN score was measured by using 2100 Bioanalyzer equipment (Agilent Technologies, Inc.). RNA samples satisfying above 3 condition were applied to Microarray experiment.

Microarray Design, experiments, and data analysis.

The design of microarray with 8 × 15K for *H.thermophilus* TK-6 was carried out according to manufacturer's instruction (Agilent technology, USA) based on genome sequence. Microarray was organized by one replicate probe set of *H.thermophilus* TK-6 genes and 10 replicates probe set of reference genes. The information of probe sets was as follows. One replicate probe set with 132,517 probes analyzed all *H.thermophilus* TK-6 genomes and 10 replicates probe set with 1,057 probes was used as a control probes by measuring 15 genes (**Table 2-4**) related to TK-6 respiration with an aim to clarify no contamination under hybridization. The duplicate RNA samples extracted from wild type, and *pspB* gene deletion TK-6 were applied for microarray analysis. Total RNA from samples was continuously converted to double-stranded cDNA and then cRNA. Following the conversion of cRNA, Labelling, amplifying, and purifying of cRNA were performed according to the protocol of one-color microarray-based gene expression analysis (Agilent Technologies). After quantifying the cRNA, 600 ng of cRNA samples applied to hybridization and washing steps following the protocol of Agilent technology. After washing the microarray slide, it was dried at room temperature for 5 minutes.

Scanning of the microarray slide was carried out by surescan microarray scanner (Agilent Technologies). Agilent Feature Extraction Software 10.7 was used to extract the signal intensities and processing of the data.

Expression data from Agilent Feature Extraction Software 10.7 were normalized by GeneSpring GX version 13.0 software with robust multichip average algorithm (163, 164). The mean signal value of each probe set and their relative fold changes based on the gene expression level of wild type were calculated by using software GeneSpring GX version 13.0.

Real-time quantitative PCR analysis.

H. thermophiles TK-6, ΔA, and ΔB were grown under 100-mL vial with 10mL of inorganic medium and gas mixtures of H_2:O_2:CO_2 (75:10:15, v/v), respectively. Here, 300 μM serine was added to inorganic medium for ΔA and another ΔB was also cultured under 30% O_2 conditions. total RNA was extracted as described in material and method of transcriptome analysis and extracted RNA was converted to cDNA as described below.

The RNA samples extracted from cells grown under each of conditions were used for the converting cDNA. Double-stranded (ds)-cDNA synthesis was carried out according to the NimbleGen user's guide for gene expression analysis (Roche NimbleGen). ds-cDNA was synthesized by using a superscript double-stranded cDNA synthesis kit (Invitrogen), which was confirmed by the concentration of cDNA ≥ 100 ng/μl and an A260/A280 ratio ≥1.8 as described previously(182).

RT-QPCR was performed using Thunderbird^R SYBR^R qPCR Mix and LightCycler^R 96 system according to the instruction manual THUNDERBIRD SYBR qPCR Mix 1304 and Roche. For each case, 100 ng of cDNA in triplicates was used for real-time PCR. The sequences of the PCR primer pairs that were used for each gene are as follows: cbiO (forward), tggcgataggctggtagttc; cbiO (reverse), ccgtagaaatgtctctatcttaccg; nkt (forward), acaagcttacctttgcggttt; nkt (reverse), aagctacaaccgcatccttc. porA of *H.thermophilus* was

used as a reference genes; porA (forward), gctggactggtatgcgtgta; porA (reverse), gaaccctcagggctatgga.

In order to calculate relative quantification of genes (cobalt transporter, nickel transporter, and housekeeping genes), calibration of each genes was performed using WT as a standard sample and the relative quantification was carried out using target and housekeeping gene.

2.3.3 Discussion

Physiology of ΔB under heat and oxidative condition

Growth profiles of ΔB that are monitored under heat and oxidative condition confirmed the physiological characteristics of PspB subunit. The lag time of ΔB was more and more increased when compare to that of WT as oxygen concentration goes up from 10% to 30% O_2. In contrast, there were no different the growth rate of between WT and ΔB under anaerobic (denitrification) and micro aerobic (2% O_2) condition. It looked likely that increasing ROS in ΔB relatively inhibit the growth rate of ΔB when the oxygen concentration went up from 10% to 30% O_2 since the absence of reactive thiols of PspB subunit reacting with ROS. However, the inhibition of growth rate for ΔB seemed not so big when compared to other kinds of ROS detoxifying genes of *H.thermophilus* (41) such as peroxidase, alkyl hydroperoxide reductase, rubrerythrin-like protein, which indicated that role of ROS scavenger was weak in PspB. However, these results consistent with my assumption of PspB as a client protein reacting with ROS as describe in section 1.2.4.

Considering the heat-stress response, there were no clear difference between *H.thermophilus* and ΔB under various temperature condition (60 °C, 80 °C, and 85°C, data not shown).

Transcriptome analysis

Gene expression results were also in agreement with the relationship between PspB and intracellular redox condition. Expression profiles of the denitrification and terminal oxidase genes strongly suggested that ΔB had more intracellular oxidative level than WT and ΔA had more intracellular oxidative level than ΔB. This was because, in addition to the oxygen limitation, the presence of respiratory substrates for denitrification such as nitrate and nitrite is required for the expression of denitrification enzymes (183).

The expression level of terminal oxidase, cytochrome c oxidase, was also agreement with Intracellular oxidative levels. As the intracellular oxygen level was increased, relatively high concentration of ROS defecting cytochrome *c* oxidase was seemed to be derived from oxygen. Several publications reported the regulation of intracellular cytochrome *c* oxidase in response to oxygen(184) and ROS production, which could also potentially serve as toxic mediator, had correlation between ROS and cytochrome *c* oxidase (185). Excessive production of ROS may lead to oxidative stress, loss of cell function, and ultimately apoptosis. A balance between oxidant and antioxidant intracellular systems is hence essential for cell function, regulation, and adaptation to diverse growth conditions (186).

On the other hand, it has been also reported that the expression level of cytochrome *c* oxidase is gradually declined with decreasing intracellular oxygen concentration between 200 and 0.5 or 1 μM O_2, but it is rapidly declined below oxygen concentrations of 0.5 or 1 μM O_2 (184). Therefore, intra cellular oxygen levels within ΔB and ΔA might be over the upper limit of intra cellular homeostasis oxygen level, which decrease the expression levels of cytochrome *c* oxidase. It was noteworthy that ΔA could not grow under 30% O_2 condition, indicating higher oxygen level caused ΔA to be repressed.

Considering the expression level of thioredoxin, another characteristic for PspB subunit was also gained from this study. The trioredoxin was significantly repressed in ΔA but was

comparable in ΔB. It was of interest why thioredoxin didn't showed significant change in ΔB. I presumed that two types dimeric A-A might be clue for this phenomenon as follows.

PspA could form dimers by linking PspB and PspA. Here, A-A existed as A-A with intermolecular disulfide bond and A-A without intermolecular disulfide bond (Fig. 1-3). If the A-A without disulfide bond could form disulfide bond within ΔB, A-A without disulfide bond might replace the function of PspB related to redox regulation via forming S-S bond. Hence, gene expression levels of thioredoxn and protein disulfide bond isomerase related with S-S bond cleavage and forming might not be changed. However, considering the ΔA, PspB can't form disulfide bond because B-B couldn't exist in *H,thermophile,* indicating that regulation of thioredoxin genes might be affected within ΔA due to the absence of intermolecular disulfide bond of PSPs. Therefore, the expression of thioredoxin may comparable with WT in ΔB and may down-regulated in ΔA due to the absence of disulfide bond.

Nickel and cobalt accumulation

The accumulation of Nickel and cobalt was presumed under ΔB. This was because hyper significant up-regulation of Nickel and Cobalt uptake genes was detected, inhibition of ΔB was not detected based on the growth rate of ΔB, and relatively high expression levels of Fe-S genes were detected.

Nickel and cobalt are trace elements for a number of prokaryotic enzymes involved in variety of metabolic process (187), essential components of many enzymes, which are required for a Life is dependent on a lots of chemical elements. Although, for instance in metahnogenes, Ni- and Co containing enzymes are essential for energy metabolism and anabolism, the mechanism of nickel and cobalt uptake in many bacteria and most archaea is not known (188). Study on cobalt and nickel genes *in E.coli* reported that cobalt and nickel uptakes *in E.coli* are most needed under anaerobic condition because both of them are valuable in the metabolism of H_2, CO and $–CH_3$ (189). In addition, hydrogenase activity catalyzing the oxidation of molecular hydrogen was required for nickel transporter

(190). This suggest that metabolism of small molecules was might be prerequisite for nickel and cobalt uptake. Although, WT and ΔB was incubated under aerobic condition (H_2:O_2:CO_2 (75:10:15, v/v), gene expression levels of both WT and ΔB was high and previous study reported that WT incubated under 10% O_2 condition showed high hydrogenase activity (191). Therefore, it seemed that culturing under anaerobic condition might not be essential for nickel and cobalt uptake.

What kind of mechanism caused nickel and cobalt transport genes to significantly up-regulated? To elucidate this mechanism, overall data interpretation of ΔB was carried out. At first, PspB subunit don' have PSP activity and another enzyme activity was not detected. Second, PspB was presumed as a client protein having redox sensitive cysteine residue. Third, ΔB showed long lag time under higher 20 and 30% O_2 condition. Lastly, considering the overall transcriptome analysis of ΔB, only 23 genes of total *H.thermophilu* genes showed significant difference and almost 23 genes was related with intracellular redox and nickel and cobalt transport genes, suggesting that intracellular oxygen level might be related with significant up-regulation of nickel and cobalt related genes. To elucidate this speculation, analysis of intracellular oxygen level may be needed in next study. In addition it was also need to check whether PspB subunit influence on intracellular oxygen level directly or indirectly. This was because it looks likely difficult for PspB subunit to influence on intracellular oxygen level directly due to the relatively small quantity in *H.thermophilus.*

To sum up, considering the transcriptome analysis and physiology of PspB, I suggest that proper intracellular oxygen or oxidative condition was required for the cobalt and nickel uptake or accumulation.

Conclusions and prospects

The results of this study is to give insight into how heterodimeric protein can have thermal stability, how to change obligate chemolitho autotroph bacteria into mixotroph bacteria, and what the role of client protein related to natural resource recovery. The investigation of iPSPs, Phosphoserine Phosphatase, from *Hydrogenobacter thermophilus* TK-6 has given another concrete step forward to elucidate the unknown intracellular environment one has been longing for, which was possible due to the advantageous features of *H.thermophilus* such as hyper thermophilic characteristics, obligate chemolithoautotroph, and relatively simple metabolism of evolutionary-ancient bacterium. The results of this study is summarized as follows.

Intermolecular disulfide bond was detected *in vitro* and *in vivo*. Considering intracellular environment, strong reduced condition was expected, which means that it's difficult for thiols of cysteine residues to form intermolecular disulfide bond in reduced condition. However, it was revealed that *H.thermophilus* have lots of intracellular disulfide bond and iPSPs linked by intermolecular disulfide bond *in vivo*. Interestingly, although three kinds of proteins such as A-A, A-B, and monomeric position PspA were detected *in vitro*, only two species of A-A and A-B were detected *in vivo* via modified western blotting using PspA- antibodies, suggesting that some of enzyme may participate in forming and cleaving disulfide bond. It does not conflict with the speculation that thioredoxin and protein disulfide bond isomerase

existing in *H.thermophilus* may take part in cleavage and formation for intermolecular disulfide bond.

I also elucidated that intermolecular disulfide bond enhanced the thermostability of heterodimeric protein for the first time in this study. In addition, intermolecular disulfide bond was also playing a major role enhancing thermal stability by protein-protein interaction. This was because enhanced thermal stability by protein-protein interaction was agreeable to disregard without intermolecular disulfide bond. Therefore, it is of interest to apply this discovery of thermal stability of heterodimeric protein with intermolecular disulfide bond to another commercial advantageous enzyme.

PspA gene was revealed as an essential gene *in H.thermophilus.* Although chemolitho autotroph don't uptake external substrate, *H.thermophilus* with the defection of essential gene had untaken external substrate to survive, indicating that obligate chemolitho autotroph also can be used for genetic engineering strategy. Here, *pspA* gene deletion L-serine auxotroph *H.thermophilus* had clarified that L-serine was transported via LIV system for the first time as far as I know.

One carbon metabolism not by glycine but by serine was also elucidated from this study. Generally, the main source of one carbon is from serine via denovo serine biosynthesis or glycine via glycine cleavage system (151). However, *pspA* gene deletion serine auxotroph and the absence of glycine cleavage system revealed that only one carbon of serine was going into one carbon metabolism within *H.thermophilus.* Additional transcriptome analysis was also consistent with the results of one carbon flow in *H.thermophilus.* In order to regulate cell proliferation, lots of researcher had focused on the inhibition of SHMT and PGDH genes. However, there were no meaningful results until now. I suspected that reversible enzymatic characteristics of SHMT or PGDH might be one of reasons. On the other hand, PSP have irreversible pathway for producing serine and one carbon flow for cell proliferation was started from serine, which suggesting that proper inhibition of PSP might induce the regulation of cell proliferation.

As PspB subunit didn’t have any enzyme activity and couldn’t exist as a dimeric form (PspB-PspB), it was difficult to expect the function of PspB and was still unknown before this study. This study revealed the some part function of PspB that had played roles as a client protein for making disulfide bond (charpter 1) and that had suppressed genes for cobalt and nickel accumulation (chapter 2). The ratio of A-B and A-A was 64% and 36% *in vivo*. Moreover, dimeric formation A-B was more stable than that of A-A in moderate reduced condition, suggesting PspB subunit had played a lots of role to make disulfide bond even if PspB was a client protein. When PspB was deleted from *H.thermophilu,* genes related cobalt and nickel transport genes strongly expressed in *pspB* deleted *H.thermophilus*, suggesting the nickel and cobalt accumulation *in H.thermophilus.* It looks likely that the discovery of this phenomenon, natural resource recovery using bacteria, may give us prospect to apply bacteria to benefit-cost plant system. Furthermore, the presumed mechanism such as intracellular oxygen regulation using reactive thiols or giving signal to some regulators is need to be clarified in interpret this phenomenon, indicating that clarified mechanism will give more insight to understand intracellular environment.

References

1. Chiba Y, Oshima K, Arai H, Ishii M, & Igarashi Y (2012) Discovery and analysis of cofactor-dependent phosphoglycerate mutase homologs as novel phosphoserine phosphatases in Hydrogenobacter thermophilus. *The Journal of biological chemistry* 287(15):11934-11941.

2. Chiba Y*, et al.* (2013) Structural units important for activity of a novel-type phosphoserine phosphatase from Hydrogenobacter thermophilus TK-6 revealed by crystal structure analysis. *The Journal of biological chemistry* 288(16):11448-11458.

3. Chiba Y (2012) Glycine related metabolism of *Hydrogenobacter thermophilus* TK-6. Doctor thesis (Tokyo University).

4. Kawasumi T, Igarashi Y, Kodama T, & Minoda Y (1980) Isolation of Strictly Thermophilic and Obligately Autotrophic Hydrogen Bacteria. *Agricultural and Biological Chemistry* 44(8):1985-1986.

5. Eder W & Huber R (2002) New isolates and physiological properties of the Aquificales and description of Thermocrinis albus sp. nov. *Extremophiles : life under extreme conditions* 6(4):309-318.

6. Deckert G*, et al.* (1998) The complete genome of the hyperthermophilic bacterium Aquifex aeolicus. *Nature* 392(6674):353-358.

7. Kawasumi T, Igarashi Y, Kodama T, & Minoda Y (1984) Hydrogenobacter thermophilus gen. nov., sp. nov., an Extremely Thermophilic, Aerobic, Hydrogen-Oxidizing Bacterium. *International Journal of Systematic Bacteriology* 34(1):5-10.

8. Braakman R & Smith E (2012) The emergence and early evolution of biological carbon-fixation. *PLoS computational biology* 8(4):e1002455.

9. Freedman Z, Zhu C, & Barkay T (2012) Mercury Resistance and Mercuric Reductase Activities and Expression among Chemotrophic Thermophilic Aquificae. *Applied and environmental microbiology* 78(18):6568-6575.

10. Arai H, Kanbe H, Ishii M, & Igarashi Y (2010) Complete genome sequence of the thermophilic, obligately chemolithoautotrophic hydrogen-oxidizing bacterium Hydrogenobacter thermophilus TK-6. *Journal of bacteriology* 192(10):2651-2652.

11. Nakagawa S*, et al.* (2005) Sulfurihydrogenibium yellowstonense sp nov., an extremely thermophilic, facultatively heterotrophic, sulfur-oxidizing bacterium from Yellowstone National Park, and emended descriptions of the genus Sulfurihydrogenibium, Sulfurihydrogenibium subterraneum and Sulfurihydrogenibium azorense. *Int J Syst Evol Micr* 55:2263-2268.

12. Bonjour F & Aragno M (1986) Growth of thermophilic, obligatorily chemolithoautotrophic hydrogen-oxidizing bacteria related to< i> Hydrogenobacter</i> with thiosulfate and elemental sulfur as electron and energy source. *FEMS microbiology letters* 35(1):11-15.

13. Götz D*, et al.* (2002) Persephonella marina gen. nov., sp. nov. and Persephonella guaymasensis sp. nov., two novel, thermophilic, hydrogen-oxidizing microaerophiles from deep-sea hydrothermal vents. *Int J Syst Evol Micr* 52(4):1349-1359.

14. Suzuki M, Cui ZJ, Ishii M, & Igarashi Y (2001) Nitrate respiratory metabolism in an obligately autotrophic hydrogen-oxidizing bacterium, Hydrogenobacter thermophilus TK-6. *Arch. Microbiol.* 175(1):75-78.

15. L'Haridon S*, et al.* (1998) Desulfurobacterium thermolithotrophum gen. nov., sp. nov., a novel autotrophic, sulphur-reducing bacterium isolated from a deep-sea hydrothermal vent. *International Journal of Systematic Bacteriology* 48(3):701-711.

16. Vetriani C, Speck MD, Ellor SV, Lutz RA, & Starovoytov V (2004) Thermovibrio ammonificans sp. nov., a thermophilic, chemolithotrophic, nitrate-ammonifying bacterium from deep-sea hydrothermal vents. *Int J Syst Evol Micr* 54(1):175-181.

17. Gilbert HF (1990) Molecular and cellular aspects of thiol-disulfide exchange. *Advances in enzymology and related areas of molecular biology* 63:69-172.

18. Gilbert HF (1993) Molecular and cellular aspects of thiol-disulfide exchange. *Advances in enzymology and related areas of molecular biology* 63:69-69.

19. Biswas S, Chida AS, & Rahman I (2006) Redox modifications of protein–thiols: Emerging roles in cell signaling. *Biochemical Pharmacology* 71(5):551-564.

20. Yu H & Huang H (2013) Engineering proteins for thermostability through rigidifying flexible sites. *Biotechnology advances*.

21. Chu XY, Tian J, Wu NF, & Fan YL (2010) An intramolecular disulfide bond is required for the thermostability of methyl parathion hydrolase, OPHC2. *Applied microbiology and biotechnology* 88(1):125-131.

22. Takagi H*, et al.* (1990) Enhancement of the thermostability of subtilisin E by introduction of a disulfide bond engineered on the basis of structural comparison with a thermophilic serine protease. *The Journal of biological chemistry* 265(12):6874-6878.

23. Dominici S*, et al.* (1999) Redox modulation of cell surface protein thiols in U937 lymphoma cells: the role of γ-glutamyl transpeptidase-dependent H 2 O 2 production and S-thiolation. *Free Radical Biology and Medicine* 27(5):623-635.

24. Borkenhagen LF & Kennedy EP (1959) The enzymatic exchange of L-serine with O-phospho-L-serine catalyzed by a specific phosphatase. *Journal of Biological Chemistry* 234(4):849-853.

25. Shetty KT (1990) Phosphoserine phosphatase of human brain: partial purification, characterization, regional distribution, and effect of certain modulators including psychoactive drugs. *Neurochemical research* 15(12):1203-1210.

26. Rigden DJ, Bagyan I, Lamani E, Setlow P, & Jedrzejas MJ (2001) A cofactor-dependent phosphoglycerate mutase homolog from Bacillus stearothermophilus is actually a broad specificity phosphatase. *Protein science : a publication of the Protein Society* 10(9):1835-1846.

27. Rigden DJ (2008) The histidine phosphatase superfamily: structure and function. *The Biochemical journal* 409(2):333-348.

28. Kameya M, Arai H, Ishii M, & Igarashi Y (2006) Purification and properties of glutamine synthetase from Hydrogenobacter thermophilus TK-6. *Journal of bioscience and bioengineering* 102(4):311-315.

29. Aragno M (1992) Thermophilic, Aerobic, Hydrogen-Oxidizing (Knallgas) Bacteria. *The Prokaryotes*, eds Balows A, Trüper H, Dworkin M, Harder W, & Schleifer K-H (Springer New York), pp 3917-3933.

30. Burggraf S, Olsen GJ, Stetter KO, & Woese CR (1992) A Phylogenetic Analysis of Aquifex pyrophilus. *Syst Appl Microbiol* 15(3):352-356.

31. Pitulle C*, et al.* (1994) Phylogenetic position of the genus Hydrogenobacter. *Int J Syst Bacteriol* 44(4):620-626.

32. Shiba H, Kawasumi T, Igarashi Y, Kodama T, & Minoda Y (1985) The CO2 assimilation via the reductive tricarboxylic acid cycle in an obligately autotrophic, aerobic hydrogen-oxidizing bacterium, Hydrogenobacter thermophilus. *Arch. Microbiol.* 141(3):198-203.

33. Aoshima M, Ishii M, & Igarashi Y (2004) A novel biotin protein required for reductive carboxylation of 2-oxoglutarate by isocitrate dehydrogenase in Hydrogenobacter thermophilus TK-6. *Molecular microbiology* 51(3):791-798.

34. Aoshima M, Ishii M, & Igarashi Y (2004) A novel enzyme, citryl-CoA synthetase, catalysing the first step of the citrate cleavage reaction in Hydrogenobacter thermophilus TK-6. *Molecular microbiology* 52(3):751-761.

35. Aoshima M, Ishii M, & Igarashi Y (2004) A novel enzyme, citryl-CoA lyase, catalysing the second step of the citrate cleavage reaction in Hydrogenobacter thermophilus TK-6. *Molecular microbiology* 52(3):763-770.

36. Ikeda T*, et al.* (2006) Anabolic five subunit-type pyruvate: ferredoxin oxidoreductase from< i> Hydrogenobacter thermophilus</i> TK-6. *Biochemical and biophysical research communications* 340(1):76-82.

37. Yamamoto M, Arai H, Ishii M, & Igarashi Y (2003) Characterization of two different 2-oxoglutarate: ferredoxin oxidoreductases from< i> Hydrogenobacter thermophilus</i> TK-6. *Biochemical and biophysical research communications* 312(4):1297-1302.

38. Miura A, Kameya M, Arai H, Ishii M, & Igarashi Y (2008) A soluble NADH-dependent fumarate reductase in the reductive tricarboxylic acid cycle of Hydrogenobacter thermophilus TK-6. *Journal of bacteriology* 190(21):7170-7177.

39. Berg IA (2011) Ecological aspects of the distribution of different autotrophic CO2 fixation pathways. *Applied and environmental microbiology* 77(6):1925-1936.

40. Wahlund TM & Tabita FR (1997) The reductive tricarboxylic acid cycle of carbon dioxide assimilation: initial studies and purification of ATP-citrate lyase from the green sulfur bacterium Chlorobium tepidum. *Journal of bacteriology* 179(15):4859-4867.

41. Sato Y*, et al.* (2012) A novel enzymatic system against oxidative stress in the thermophilic hydrogen-oxidizing bacterium Hydrogenobacter thermophilus. *PloS one* 7(4):e34825.

42. Reddie KG & Carroll KS (2008) Expanding the functional diversity of proteins through cysteine oxidation. *Current Opinion in Chemical Biology* 12(6):746-754.

43. Nagahara N (2011) Intermolecular disulfide bond to modulate protein function as a redox-sensing switch. *Amino acids* 41(1):59-72.

44. Branden CI (1999) *Introduction to protein structure* (Garland Science).

45. Fahey RC, Hunt JS, & Windham GC (1977) On the cysteine and cystine content of proteins. *Journal of molecular evolution* 10(2):155-160.

46. Masip L*, et al.* (2004) An engineered pathway for the formation of protein disulfide bonds. *Science* 303(5661):1185-1189.

47. Beeby M*, et al.* (2005) The genomics of disulfide bonding and protein stabilization in thermophiles. *PLoS biology* 3(9):e309.

48. Shiba H, Kawasumi T, Igarashi Y, Kodama T, & Minoda Y (1982) The deficient carbohydrate metabolic pathways and the incomplete tricarboxylic acid cycle in an obligately autotrophic hydrogen-oxidizing bacterium. *Agricultural and Biological Chemistry* 46(9):2341-2345.

49. Laemmli UK (1970) Cleavage of structural proteins during the assembly of the head of bacteriophage T4. *Nature* 227(5259):680-685.

50. Marino SM & Gladyshev VN (2010) Cysteine Function Governs Its Conservation and Degeneration and Restricts Its Utilization on Protein Surfaces. *Journal of molecular biology* 404(5):902-916.

51. Wilkinson B & Gilbert HF (2004) Protein disulfide isomerase. *Biochimica et Biophysica Acta (BBA) - Proteins and Proteomics* 1699(1–2):35-44.

52. Hwang C, Sinskey A, & Lodish H (1992) Oxidized redox state of glutathione in the endoplasmic reticulum. *Science* 257(5076):1496-1502.

53. Mallick P, Boutz DR, Eisenberg D, & Yeates TO (2002) Genomic evidence that the intracellular proteins of archaeal microbes contain disulfide bonds. *Proceedings of the National Academy of Sciences of the United States of America* 99(15):9679-9684.

54. Marino SM & Gladyshev VN (2012) Analysis and functional prediction of reactive cysteine residues. *The Journal of biological chemistry* 287(7):4419-4425.

55. Laurell C-B, Dahlqvist I, & Persson U (1983) The use of thiol-disulphide exchange chromatography for the automated isolation of oil-antitrypsin and other

plasma proteins with reactive thiol groups. *Journal of Chromatography B: Biomedical Sciences and Applications* 278:53-61.

56. Lee J-W & Helmann JD (2006) The PerR transcription factor senses H2O2 by metal-catalysed histidine oxidation. *Nature* 440(7082):363-367.

57. Dalle-Donne I*, et al.* (2006) Protein carbonylation, cellular dysfunction, and disease progression. *J Cell Mol Med* 10(2):389-406.

58. Cattaruzza M & Hecker M (2008) Protein Carbonylation and Decarboylation: A New Twist to the Complex Response of Vascular Cells to Oxidative Stress. *Circulation research* 102(3):273-274.

59. Cremers CM & Jakob U (2013) Oxidant Sensing by Reversible Disulfide Bond Formation. *Journal of Biological Chemistry* 288(37):26489-26496.

60. Imanaka T, Shibazaki M, & Takagi M (1986) A new way of enhancing the thermostability of proteases. *Nature* 324(6098):695-697.

61. Chakravarty S & Varadarajan R (2000) Elucidation of determinants of protein stability through genome sequence analysis. *FEBS letters* 470(1):65-69.

62. Dominy BN, Minoux H, & Brooks CL, 3rd (2004) An electrostatic basis for the stability of thermophilic proteins. *Proteins* 57(1):128-141.

63. Missimer JH*, et al.* (2007) Configurational entropy elucidates the role of salt-bridge networks in protein thermostability. *Protein science : a publication of the Protein Society* 16(7):1349-1359.

64. Kumar S, Tsai CJ, & Nussinov R (2000) Factors enhancing protein thermostability. *Protein engineering* 13(3):179-191.

65. Yano JK & Poulos TL (2003) New understandings of thermostable and peizostable enzymes. *Current opinion in biotechnology* 14(4):360-365.

66. Karlström M, Stokke R, Helene Steen I, Birkeland N-K, & Ladenstein R (2005) Isocitrate Dehydrogenase from the Hyperthermophile Aeropyrum pernix: X-ray Structure Analysis of a Ternary Enzyme–Substrate Complex and Thermal Stability. *Journal of molecular biology* 345(3):559-577.

67. Trivedi S, Gehlot HS, & Rao SR (2006) Protein thermostability in Archaea and Eubacteria. *Genetics and molecular research : GMR* 5(4):816-827.

68. DeDecker BS*, et al.* (1996) The Crystal Structure of a Hyperthermophilic Archaeal TATA-box Binding Protein. *Journal of molecular biology* 264(5):1072-1084.

69. Roca M, Liu H, Messer B, & Warshel A (2007) On the relationship between thermal stability and catalytic power of enzymes. *Biochemistry* 46(51):15076-15088.

70. Basu S & Sen S (2013) Do Homologous Thermophilic–Mesophilic Proteins Exhibit Similar Structures and Dynamics at Optimal Growth Temperatures? A Molecular Dynamics Simulation Study. *Journal of chemical information and modeling* 53(2):423-434.

71. McCully ME, Beck DAC, & Daggett V (2013) Promiscuous contacts and heightened dynamics increase thermostability in an engineered variant of the engrailed homeodomain. *Protein Engineering Design and Selection* 26(1):35-45.

72. Toth EA*, et al.* (2000) The crystal structure of adenylosuccinate lyase from Pyrobaculum aerophilum reveals an intracellular protein with three disulfide bonds. *Journal of molecular biology* 301(2):433-450.

73. Bessette P, Aslund F, Beckwith J, & Georgiou G (1999) Efficient folding of proteins with multiple disulfide bonds in the Escherichia coli cytoplasm. *Proceedings of the National Academy of Sciences of the United States of America* 96:13703 - 13708.

74. Boutz DR, Cascio D, Whitelegge J, Perry LJ, & Yeates TO (2007) Discovery of a thermophilic protein complex stabilized by topologically interlinked chains. *Journal of molecular biology* 368(5):1332-1344.

75. van den Akker F*, et al.* (1997) Crystal structure of heat-labile enterotoxin from Escherichia coli with increased thermostability introduced by an engineered disulfide bond in the A subunit. *Protein science : a publication of the Protein Society* 6(12):2644-2649.

76. Ko JH*, et al.* (1996) Enhancement of thermostability and catalytic efficiency of AprP, an alkaline protease from Pseudomonas sp., by the introduction of a disulfide bond. *Biochemical and biophysical research communications* 221(3):631-635.

77. Liu L*, et al.* (2013) In silico rational design and systems engineering of disulfide bridges in the catalytic domain of an alkaline alpha-amylase from Alkalimonas amylolytica to improve thermostability. *Applied and environmental microbiology*.

78. Davidson FF, Loewen PC, & Khorana HG (1994) Structure and function in rhodopsin: replacement by alanine of cysteine residues 110 and 187, components of a conserved disulfide bond in rhodopsin, affects the light-activated metarhodopsin II state. *Proceedings of the National Academy of Sciences* 91(9):4029-4033.

79. Böckmann RA, Hac A, Heimburg T, & Grubmüller H (2003) Effect of sodium chloride on a lipid bilayer. *Biophysical journal* 85(3):1647-1655.

80. Brady GP & Sharp KA (1997) Entropy in protein folding and in protein-protein interactions. *Curr Opin Struct Biol* 7(2):215-221.

81. Thompson JD, Higgins DG, & Gibson TJ (1994) Improved sensitivity of profile searches through the use of sequence weights and gap excision. *Computer applications in the biosciences : CABIOS* 10(1):19-29.

82. Williams JC*, et al.* (1999) Structural and mutagenesis studies of leishmania triosephosphate isomerase: a point mutation can convert a mesophilic enzyme into a superstable enzyme without losing catalytic power. *Protein engineering* 12(3):243-250.

83. Kirino H*, et al.* (1994) Hydrophobic interaction at the subunit interface contributes to the thermostability of 3-isopropylmalate dehydrogenase from an extreme thermophile, Thermus thermophilus. *European Journal of Biochemistry* 220(1):275-281.

84. Guelorget A*, et al.* (2010) Insights into the hyperthermostability and unusual region-specificity of archaeal Pyrococcus abyssi tRNA m1A57/58 methyltransferase. *Nucleic acids research* 38(18):6206-6218.

85. Zhang T, Bertelsen E, & Alber T (1994) Entropic effects of disulphide bonds on protein stability. *Nature Structural & Molecular Biology* 1(7):434-438.

86. Sørensen HP & Mortensen KK (2005) Soluble expression of recombinant proteins in the cytoplasm of Escherichia coli. *Microbial cell factories* 4(1):1.

87. Hwa K-Y, Subramani B, Shen S-T, & Lee Y-M (2014) An intermolecular disulfide bond is required for thermostability and thermoactivity of β-glycosidase from Thermococcus kodakarensis KOD1. *Applied microbiology and biotechnology* 98(18):7825-7836.

88. Benezra R (1994) An intermolecular disulfide bond stabilizes E2A homodimers and is required for DNA binding at physiological temperatures. *Cell* 79(6):1057-1067.

89. Wetzel R, Perry LJ, Baase WA, & Becktel WJ (1988) Disulfide bonds and thermal stability in T4 lysozyme. *Proceedings of the National Academy of Sciences of the United States of America* 85(2):401-405.

90. Jacobsen T, West K, & Atlung S (1982) Electrostatic interactions during the intercalation of Li in Lix TiS2. *Electrochimica Acta* 27(8):1007-1011.

91. Shields PA & Farrah SR (1983) Influence of salts on electrostatic interactions between poliovirus and membrane filters. *Applied and environmental microbiology* 45(2):526-531.

92. Inouye KI (1992) Effects of salts on thermolysin: activation of hydrolysis and synthesis of N-carbobenzoxy-L-aspartyl-L-phenylalanine methyl ester, and a unique change in the absorption spectrum of thermolysin. *Journal of biochemistry* 112(3):335-340.

93. Inouye K, Lee S, & Tonomura Bi (1996) Effect of amino acid residues at the cleavable site of substrates on the remarkable activation of thermolysin by salts. *Biochem. J* 315:133-138.

94. Schumann J, Bohm G, Schumacher G, Rudolph R, & Jaenicke R (1993) Stabilization of creatinase from Pseudomonas putida by random mutagenesis. *Protein science : a publication of the Protein Society* 2(10):1612-1620.

95. Haney P, Konisky J, Koretke KK, Luthey-Schulten Z, & Wolynes PG (1997) Structural basis for thermostability and identification of potential active site residues for adenylate kinases from the archaeal genus Methanococcus. *Proteins* 28(1):117-130.

96. Russell RJM, Ferguson JMC, Hough DW, Danson MJ, & Taylor GL (1997) The Crystal Structure of Citrate Synthase from the Hyperthermophilic Archaeon Pyrococcus furiosus at 1.9 Å Resolution. *Biochemistry* 36(33):9983-9994.

97. Jaenicke R & Böhm G (1998) The stability of proteins in extreme environments. *Current Opinion in Structural Biology* 8(6):738-748.

98. Wrba A, Schweiger A, Schultes V, Jaenicke R, & Zavodszky P (1990) *Biochemistry* 29:7584.

99. Vogt G & Argos P (1997) Protein thermal stability: hydrogen bonds or internal packing? *Folding & design* 2(4):S40-46.

100. Charbonneau DM & Beauregard M (2013) Role of Key Salt Bridges in Thermostability of G. thermodenitrificans EstGtA2: Distinctive Patterns within the New Bacterial Lipolytic Enzyme Family XV. *PloS one* 8(10):e76675.

101. Xu S*, et al.* (2013) Evidences for the existence of intermolecular disulfide-bonded oligomers in the H3 hemagglutinins expressed in insect cells. *Virus Genes*:1-8.

102. Wiese DA & Sippel TO (1981) Microphotometric analysis of protein-bound thiols and disulfides with an azogenic maleimide. *The journal of histochemistry and cytochemistry : official journal of the Histochemistry Society* 29(7):817-821.

103. Haney PJ*, et al.* (1999) Thermal adaptation analyzed by comparison of protein sequences from mesophilic and extremely thermophilic Methanococcus species. *Proceedings of the National Academy of Sciences* 96(7):3578-3583.

104. Scandurra R, Consalvi V, Chiaraluce R, Politi L, & Engel PC (1998) Protein thermostability in extremophiles. *Biochimie* 80(11):933-941.

105. Diao Y*, et al.* (2008) Using pseudo amino acid composition to predict transmembrane regions in protein: cellular automata and Lempel-Ziv complexity. *Amino acids* 34(1):111-117.

106. Sterpone F & Melchionna S (2012) Thermophilic proteins: insight and perspective from in silico experiments. *Chemical Society reviews* 41(5):1665-1676.

107. Vieille C & Zeikus GJ (2001) Hyperthermophilic enzymes: Sources, uses, and molecular mechanisms for thermostability. *Microbiol Mol Biol R* 65(1):1-+.

108. Cacciapuoti G, Porcelli M, Bertoldo C, De Rosa M, & Zappia V (1994) Purification and characterization of extremely thermophilic and thermostable 5'-methylthioadenosine phosphorylase from the archaeon Sulfolobus solfataricus. Purine nucleoside phosphorylase activity and evidence for intersubunit disulfide bonds. *The Journal of biological chemistry* 269(40):24762-24769.

109. Greaves RB & Warwicker J (2007) Mechanisms for stabilisation and the maintenance of solubility in proteins from thermophiles. *BMC structural biology* 7:18.

110. Karshikoff A & Ladenstein R (2001) Ion pairs and the thermotolerance of proteins from hyperthermophiles: a "traffic rule" for hot roads. *Trends in biochemical sciences* 26(9):550-556.

111. Zhou XX, Wang YB, Pan YJ, & Li WF (2008) Differences in amino acids composition and coupling patterns between mesophilic and thermophilic proteins. *Amino acids* 34(1):25-33.

112. Tsai CJ & Nussinov R (1997) Hydrophobic folding units derived from dissimilar monomer structures and their interactions. *Protein Science* 6(1):24-42.

113. Zhang G (2013) A simple statistical method for discrimination of thermophilic and mesophilic proteins based on amino acid composition. *International journal of bioinformatics research and applications* 9(1):41-52.

114. Chen Y-H, Yang JT, & Martinez HM (1972) Determination of the secondary structures of proteins by circular dichroism and optical rotatory dispersion. *Biochemistry* 11(22):4120-4131.

115. Wittig I, Braun H-P, & Schagger H (2006) Blue native PAGE. *NATURE PROTOCOLS-ELECTRONIC EDITION*- 1(1):418.

116. Fukuchi S & Nishikawa K (2001) Protein surface amino acid compositions distinctively differ between thermophilic and mesophilic bacteria. *Journal of molecular biology* 309(4):835-843.

117. Hugler M, Huber H, Molyneaux SJ, Vetriani C, & Sievert SM (2007) Autotrophic CO2 fixation via the reductive tricarboxylic acid cycle in different lineages within the phylum Aquificae: evidence for two ways of citrate cleavage. *Environmental microbiology* 9(1):81-92.

118. Russell RJ, Gerike U, Danson MJ, Hough DW, & Taylor GL (1998) Structural adaptations of the cold-active citrate synthase from an Antarctic bacterium. *Structure* 6(3):351-361.

119. Pack SP & Yoo YJ (2004) Protein thermostability: structure-based difference of amino acid between thermophilic and mesophilic proteins. *Journal of biotechnology* 111(3):269-277.

120. Dill KA (1990) Dominant forces in protein folding. *Biochemistry* 29(31):7133-7155.

121. Mattos C (2002) Protein–water interactions in a dynamic world. *Trends in biochemical sciences* 27(4):203-208.

122. Denisov VP, Venu K, Peters J, Hörlein HD, & Halle B (1997) Orientational disorder and entropy of water in protein cavities. *The Journal of Physical Chemistry B* 101(45):9380-9389.

123. Nagendra H, Sukumar N, & Vijayan M (1998) Role of water in plasticity, stability, and action of proteins: the crystal structures of lysozyme at very low levels of hydration. *Proteins: Structure, Function, and Bioinformatics* 32(2):229-240.

124. Xie C, Chen P, & Liang S (The Role of Blue Native/SDS PAGE in Depression Research.

125. Eggers DK & Valentine JS (2001) Molecular confinement influences protein structure and enhances thermal protein stability. *Protein Science* 10(2):250-261.

126. Horovitz A, Matthews JM, & Fersht AR (1992) α-Helix stability in proteins: II. Factors that influence stability at an internal position. *Journal of molecular biology* 227(2):560-568.

127. Rabbani G, Ahmad E, Zaidi N, & Khan RH (2011) pH-dependent conformational transitions in conalbumin (ovotransferrin), a metalloproteinase from hen egg white. *Cell biochemistry and biophysics* 61(3):551-560.

128. Rabbani G, Kaur J, Ahmad E, Khan RH, & Jain SK (2014) Structural characteristics of thermostable immunogenic outer membrane protein from Salmonella enterica serovar Typhi. *Applied microbiology and biotechnology* 98(6):2533-2543.

129. Arnold I, Pfeiffer K, Neupert W, Stuart RA, & Schagger H (1998) Yeast mitochondrial F1F0-ATP synthase exists as a dimer: identification of three dimer-specific subunits. *The EMBO journal* 17(24):7170-7178.

130. Hol WG, Halie LM, & Sander C (1981) Dipoles of the alpha-helix and beta-sheet: their role in protein folding. *Nature* 294:532-536.

131. Querol E, Perez-Pons JA, & Mozo-Villarias A (1996) Analysis of protein conformational characteristics related to thermostability. *Protein engineering* 9(3):265-271.

132. Blaber M*, et al.* (1993) Energetic cost and structural consequences of burying a hydroxyl group within the core of a protein determined from Ala .fwdarw. Ser and Val .fwdarw. Thr substitutions in T4 lysozyme. *Biochemistry* 32(42):11363-11373.

133. Matsuo K, Yonehara R, & Gekko K (2004) Secondary-structure analysis of proteins by vacuum-ultraviolet circular dichroism spectroscopy. *Journal of biochemistry* 135(3):405-411.

134. Borkenhagen LF & Kennedy EP (1958) The enzymic equilibration of l-serine with O-phospho-serine. *Biochimica et biophysica acta* 28:222-223.

135. Appling DR (1991) Compartmentation of folate-mediated one-carbon metabolism in eukaryotes. *The FASEB Journal* 5(12):2645-2651.

136. Piper MD, Hong S-P, Ball GE, & Dawes IW (2000) Regulation of the Balance of One-carbon Metabolism inSaccharomyces cerevisiae. *Journal of Biological Chemistry* 275(40):30987-30995.

137. Gelling CL, Piper MD, Hong S-P, Kornfeld GD, & Dawes IW (2004) Identification of a novel one-carbon metabolism regulon in Saccharomyces cerevisiae. *Journal of Biological Chemistry* 279(8):7072-7081.

138. Blakley R (1984) In Blakley RL and Benkovic, SJ (Eds), Folates and Pterins, Vol. 1. (John Wiley & Sons, New York, NY).

139. McKenzie K & Jones EW (1977) Mutants of the formyltetrahydrofolate interconversion pathway of Saccharomyces cerevisiae. *Genetics* 86(1):85-102.

140. Ogur M*, et al.* (1977) " Active" one-carbon generation in Saccharomyces cerevisiae. *Journal of bacteriology* 129(2):926-933.

141. Furuya S*, et al.* (2008) Inactivation of the 3-phosphoglycerate dehydrogenase gene in mice: changes in gene expression and associated regulatory networks resulting from serine deficiency. *Functional & integrative genomics* 8(3):235-249.

142. Yoshida K*, et al.* (2004) Targeted disruption of the mouse 3-phosphoglycerate dehydrogenase gene causes severe neurodevelopmental defects and results in embryonic lethality. *Journal of Biological Chemistry* 279(5):3573-3577.

143. Burnham BF (1970) [14] δ-Aminolevulinic acid synthase (Rhodopseudomonas spheroides). *Methods in enzymology* 17:195-200.

144. Ye J*, et al.* (2012) Pyruvate kinase M2 promotes de novo serine synthesis to sustain mTORC1 activity and cell proliferation. *Proceedings of the National Academy of Sciences* 109(18):6904-6909.

145. Chistoserdova L, Vorholt JA, Thauer RK, & Lidstrom ME (1998) C1 transfer enzymes and coenzymes linking methylotrophic bacteria and methanogenic Archaea. *Science* 281(5373):99-102.

146. Vorholt JA, Chistoserdova L, Stolyar SM, Thauer RK, & Lidstrom ME (1999) Distribution of tetrahydromethanopterin-dependent enzymes in methylotrophic bacteria and phylogeny of methenyl tetrahydromethanopterin cyclohydrolases. *Journal of bacteriology* 181(18):5750-5757.

147. Okamura-Ikeda K, *et al.* (2005) Crystal structure of human T-protein of glycine cleavage system at 2.0 A resolution and its implication for understanding non-ketotic hyperglycinemia. *Journal of molecular biology* 351(5):1146-1159.

148. Kikuchi G (1973) The glycine cleavage system: composition, reaction mechanism, and physiological significance. *Molecular and cellular biochemistry* 1(2):169-187.

149. Maden B (2000) Tetrahydrofolate and tetrahydromethanopterin compared: functionally distinct carriers in C1 metabolism. *Biochem. J* 350:609-629.

150. Vazquez A, Markert EK, & Oltvai ZN (2011) Serine biosynthesis with one carbon catabolism and the glycine cleavage system represents a novel pathway for ATP generation. *PloS one* 6(11):e25881-e25881.

151. Locasale JW (2013) Serine, glycine and one-carbon units: cancer metabolism in full circle. *Nature Reviews Cancer* 13(8):572-583.

152. Lamers Y, Williamson J, Gilbert LR, Stacpoole PW, & Gregory JF (2007) Glycine Turnover and Decarboxylation Rate Quantified in Healthy Men and Women Using Primed, Constant Infusions of [1,2-13C2]Glycine and [2H3]Leucine. *The Journal of Nutrition* 137(12):2647-2652.

153. Hishinuma F, Izaki K, & Takahashi H (1969) Effects of glycine and D-amino acids on growth of various microorganisms. *Agricultural and Biological Chemistry* 33(11):1577-1586.

154. Eisenhut M, Bauwe H, & Hagemann M (2007) Glycine accumulation is toxic for the cyanobacterium Synechocystis sp. strain PCC 6803, but can be compensated by supplementation with magnesium ions. *FEMS microbiology letters* 277(2):232-237.

155. Shiba H, Kawasumi T, Igarashi Y, Kodama T, & Minoda Y (1984) Effect of organic compounds on the growth of an obligately autotrophic hydrogen-oxidizing bacterium, Hydrogenobacter thermophilus TK-6. *Agricultural and biological chemistry* 48(11):2809-2813.

156. Ogawa W, Kayahara T, Tsuda M, Mizushima T, & Tsuchiya T (1997) Isolation and characterization of an Escherichia coli mutant lacking the major serine transporter, and cloning of a serine transporter gene. *Journal of biochemistry* 122(6):1241-1245.

157. Hama H, Shimamoto T, Tsuda M, & Tsuchiya T (1988) Characterization of a novel L-serine transport system in Escherichia coli. *Journal of bacteriology* 170(5):2236-2239.

158. Robbins JC & Oxender DL (1973) Transport Systems for Alanine, Serine, and Glycine in Escherichia coli K-12. *Journal of bacteriology* 116(1):12-18.

159. Velayudhan J, Jones MA, Barrow PA, & Kelly DJ (2004) L-serine catabolism via an oxygen-labile L-serine dehydratase is essential for colonization of the avian gut by Campylobacter jejuni. *Infection and immunity* 72(1):260-268.

160. Ogawa W, Kim YM, Mizushima T, & Tsuchiya T (1998) Cloning and expression of the gene for the Na+-coupled serine transporter from Escherichia coli and characteristics of the transporter. *Journal of bacteriology* 180(24):6749-6752.

161. Wouters MA, Fan SW, & Haworth NL (2010) Disulfides as redox switches: from molecular mechanisms to functional significance. *Antioxidants & redox signaling* 12(1):53-91.

162. Krause G, Lundström J, Barea JL, De La Cuesta CP, & Holmgren A (1991) Mimicking the active site of protein disulfide-isomerase by substitution of proline 34 in Escherichia coli thioredoxin. *Journal of Biological Chemistry* 266(15):9494-9500.

163. Grant RP (2004) *Computational genomics : theory and application* (Horizon Bioscience, Wymondham) pp ix, 305 p.

164. Whitworth GB (2010) An Introduction to Microarray Data Analysis and Visualization. *Method Enzymol* 470:19-50.

165. Lupetti A*, et al.* (2002) Internal thiols and reactive oxygen species in candidacidal activity exerted by an N-terminal peptide of human lactoferrin. *Antimicrobial agents and chemotherapy* 46(6):1634-1639.

166. Wojtovich AP & Foster TH (2014) Optogenetic control of ROS production. *Redox Biology* 2:368-376.

167. Schafer FQ & Buettner GR (2001) Redox environment of the cell as viewed through the redox state of the glutathione disulfide/glutathione couple. *Free Radical Biology and Medicine* 30(11):1191-1212.

168. Ach RA, Wang H, & Curry B (2008) Measuring microRNAs: comparisons of microarray and quantitative PCR measurements, and of different total RNA prep methods. *BMC biotechnology* 8(1):69.

169. Pradervand S*, et al.* (2010) Concordance among digital gene expression, microarrays, and qPCR when measuring differential expression of microRNAs. *BioTechniques* 48(3):219-222.

170. Lu J & Holmgren A (2014) The thioredoxin antioxidant system. *Free Radical Biology and Medicine* 66:75-87.

171. Martin JL (1995) Thioredoxin—a fold for all reasons. *Structure* 3(3):245-250.

172. Ogawa W, Kim Y-M, Mizushima T, & Tsuchiya T (1998) Cloning and Expression of the Gene for the Na+-Coupled Serine Transporter from Escherichia coli and Characteristics of the Transporter. *Journal of bacteriology* 180(24):6749-6752.

173. Sherwood L (2015) *Human physiology: from cells to systems* (Cengage learning).

174. Quincy RB, Houalla M, Proctor A, & Hercules DM (1990) Distribution of molybdenum oxidation states in reduced molybdenum/titania catalysts: correlation with benzene hydrogenation activity. *Journal of Physical Chemistry* 94(4):1520-1526.

175. Elliott BB & Mortenson L (1975) Transport of molybdate by Clostridium pasteurianum. *Journal of bacteriology* 124(3):1295-1301.

176. Dudev T & Lim C (2004) Oxyanion selectivity in sulfate and molybdate transport proteins: an ab initio/CDM study. *Journal of the American Chemical Society* 126(33):10296-10305.

177. Aoshima M, Ishii M, & Igarashi Y (2004) A novel enzyme, citryl-CoA lyase, catalysing the second step of the citrate cleavage reaction in Hydrogenobacter thermophilus TK-6. *Molecular microbiology* 52(3):763-770.

178. Tabatabaie L, Klomp L, Berger R, & de Koning T (2010) L-serine synthesis in the central nervous system: a review on serine deficiency disorders. *Molecular genetics and metabolism* 99(3):256-262.

179. Matthews RG & Drummond JT (1990) Providing one-carbon units for biological methylations: mechanistic studies on serine hydroxymethyltransferase, methylenetetrahydrofolate reductase, and methyltetrahydrofolate-homocysteine methyltransferase. *Chemical Reviews* 90(7):1275-1290.

180. Possemato R*, et al.* (2011) Functional genomics reveal that the serine synthesis pathway is essential in breast cancer. *Nature* 476(7360):346-350.

181. Lund K, Merrill DK, & Guynn RW (1985) The reactions of the phosphorylated pathway of L-serine biosynthesis: thermodynamic relationships in rabbit liver in vivo. *Archives of biochemistry and biophysics* 237(1):186-196.

182. Sakurai K, Arai H, Ishii M, & Igarashi Y (2011) Transcriptome response to different carbon sources in Acetobacter aceti. *Microbiology* 157(3):899-910.

183. Arai H, Igarashi Y, & Kodama T (1995) Expression of the nir and nor genes for denitrification of Pseudomonas aeruginosa requires a novel CRP/FNR-related transcriptional regulator, DNR, in addition to ANR. *FEBS letters* 371(1):73-76.

184. Burke PV, Raitt DC, Allen LA, Kellogg EA, & Poyton RO (1997) Effects of oxygen concentration on the expression of cytochrome c and cytochrome c oxidase genes in yeast. *Journal of Biological Chemistry* 272(23):14705-14712.

185. Cardoso SM, Proença MT, Santos S, Santana I, & Oliveira CR (2004) Cytochrome c oxidase is decreased in Alzheimer's disease platelets. *Neurobiology of Aging* 25(1):105-110.

186. Aruoma OI, Grootveld M, & Bahorun T (2006) Free radicals in biology and medicine: from inflammation to biotechnology. *Biofactors* 27(1-4):1-3.

187. Kobayashi M & Shimizu S (1999) Cobalt proteins. *European Journal of Biochemistry* 261(1):1-9.

188. Rodionov DA, Hebbeln P, Gelfand MS, & Eitinger T (2006) Comparative and functional genomic analysis of prokaryotic nickel and cobalt uptake transporters: evidence for a novel group of ATP-binding cassette transporters. *Journal of bacteriology* 188(1):317-327.

189. Williams JJRFdsaRJP (2001) *The biological chemistry of the elements-The inorganic chemistry of Life-*.

190. Brito B*, et al.* (2010) Rhizobium leguminosarum hupE encodes a nickel transporter required for hydrogenase activity. *Journal of bacteriology* 192(4):925-935.

191. Sato Y*, et al.* (2012) Transcriptome Analyses of Metabolic Enzymes in Thiosulfate- and Hydrogen-Grown Hydrogenobacter thermophilus Cells. *Bioscience, biotechnology, and biochemistry* 76(9):1677-1681.